THE PROCEEDINGS OF
THE PHYSICAL SOCIETY

Section B

VOL. 64, PART 7 1 July 1951 No. 379 B

Modern Problems of Colorimetry

BY W. D. WRIGHT
Imperial College, London

17th Thomas Young Oration, delivered 23rd February 1951

§1. INTRODUCTION

WHEN I was invited to deliver the Thomas Young Oration, my first reaction was to regard the invitation as a challenge to defend the Young–Helmholtz three-components theory of colour vision. Many of you will be aware that this theory has come under fairly heavy attack in the last few years and perhaps the supporters of the theory have not been as outspoken in its defence as they might have been. It seems to me, however, that the subject has had its fill of theories for the time being and I could wish that they were less actively canvassed in the present day. Certainly I do not want to add fuel to the fire at this juncture, for I do not believe we are likely to discover the truth of the matter by speculation from existing data. In due course our physiological friends will be able to tell us just what does happen when light strikes the retina; in the meantime, apart from discouraging the more obvious heresies that get abroad, I am personally well content to let theory alone.

As an alternative subject for this Oration, and in the absence of new experiments on which to report, I felt that it would be appropriate to review the developments that have taken place in colorimetry during the last twenty-five years and to look ahead to the likely problems that may face colorimetrists in the future. Since colorimetry depends on the experimental fact that colours can be matched by the additive mixture of red, green and blue stimuli, the subject is still quite closely related to what Young had to say about colour, and as revision of the standard observer data is under consideration, it may be helpful at this time to survey what has been achieved and what still remains to be accomplished.

Twenty-five years is itself a convenient unit of time to look back on, but in this case it has the added advantage that in 1926 Guild gave an extensive survey of developments in colorimetry at the Optical Convention held in that year. I am particularly happy to base my opening remarks on that report, since it gives me an opportunity to acknowledge the debt I owe to Mr. Guild's papers in the 1920–30 decade. I was, indeed, somewhat embarrassed when I came to re-read his 1926 survey recently, since so much of what he had written I had come to believe were my own original ideas. I can only hope that Mr. Guild will

recognize this assimilation of his views as the tribute which I believe it to be.

My personal obligation to the 1926 Convention does not end there, since as a result of the discussion following Mr. Guild's paper, Professor Martin was able to secure the support of Sir John Parsons and the Medical Research Council for a renewed study of colour vision problems at the Imperial College. While I was the first to benefit from that support, grants have in fact been awarded to a continuous succession of post-graduate students from then until now and I would like to express once again our gratitude to the Medical Research Council for their confidence in our work.

For the benefit of those who are not experts in colorimetry, I should perhaps explain that the aim of colour measurement on the trichromatic system is to specify a stimulus in terms of the visually equivalent mixture of three (usually red, green and blue) stimuli. Such a specification is a physical specification in the sense that it establishes the equivalence between physical stimuli in their capacity to arouse similar visual sensations, but it does not give precise information about the spectral composition of the light; indeed many different spectral compositions may give rise to the same colour sensation. Neither does the specification give any exact information about the sensation, since this will differ according to the state of adaptation and conditions of contrast under which the stimuli are viewed.

A specification with these qualifications might not appear to be of much practical value, but essentially the same principle is involved in other physical measurements. In the case of the balance, for example, an equivalence is established between masses placed in the two scale pans in respect of a certain property—the gravitational pull or weight. The masses may differ in respect of many of their other physical and chemical properties, but they will be equal in that one respect. The analogy may be taken still further, since the establishment of a balance between the forces on the pans gives no information about the magnitude of those forces themselves. If the same operation were carried out on the surface of the moon, for example, a balance would still be obtained, although the forces would be much smaller than in the terrestrial experiment.

I shall be returning to the question of defining colour sensations at the end of this lecture, but in the meantime I hope the distinction is clear between the stimulus quality as defined by the equivalent mixture of three stimuli, and the sensation quality which is a function not only of the stimulus but of the conditions under which the stimulus is seen.

§ 2. PHOTOMETRY

Perhaps one of the most striking features of Guild's survey of colorimetry is that more than half of it was devoted to photometry, but whether we regard colorimetry as an off-shoot of photometry, or photometry as a sub-section of colorimetry, the two are certainly closely related.

In 1926 the international standard luminosity curve was only two years old and Guild naturally discussed the significance of the curve at some length. The curve might be regarded as defining the spectral sensitivity which an observer would have to have if he wished to make standard photometric matches between lights of different colour; on the other hand, the luminosity factor at each wavelength can be used to weight the energy at that wavelength in a beam of light defined by its spectral energy curve and, by summation through the visible

spectrum, to derive a measure of the photometric value of the light. The merits of the latter procedure were less attractive and less in evidence in 1926 than they are today, because of the greater difficulties involved in energy measurements; consequently we find visual methods, and flicker photometry in particular, described by Guild as the standard procedure for heterochromatic photometry.

I think it is true to say that nowadays flicker photometry, as a routine method of photometry, is dead. It still has a use in determinations of the luminosity curve and may, of course, be employed in other special investigations, but improved methods are now available for the photometry of sources whose colour differs from that of the standard source. The latter itself was changed in 1948, the new unit of candle power being defined as $\frac{1}{60}$ cm² of a Planckian radiator at the temperature of solidification of platinum (approx. 2,042° K.). The photometry of sources of similar colour temperature presents no difficulty, since high precision can be obtained with the usual type of photometer head, or with a photocell, and in the absence of any significant colour difference between the two lights to be compared, no special care has to be taken in the selection of the observer or photocell, as the case may be. For the photometry of sources of other colour temperatures, colour filters such as the blue Chance OB9 glass (Harding 1948) can now be used as temperature converters; with these the colour difference is effectively eliminated between the lights being matched, and the correction which has to be applied for the absorption of the filter can be derived by calculation from standard observer data. For more highly coloured sources, or for sources with irregular energy distributions, the Donaldson six-stimulus colorimeter (Donaldson 1947) can be used as a photometer to provide an approximate energy match with the light under test and thus eliminate the observer problem. Alternatively, a photoelectric method may be used in which the spectral sensitivity of the cell is corrected to that of the standard luminosity curve by means of a spectrum and template system. Winch and Machin (1940) have developed a well-known instrument of this type. In the case of colour filters and coloured surfaces, their transmission and reflection factors can be calculated from spectrophotometric measurements with either visual or photoelectric instruments and from standard observer data.

These are now well-established techniques, although in industrial photometry it is often convenient to take advantage of the service provided at the National Physical Laboratory and to use sub-standard lamps calibrated there by methods such as I have just outlined, against which lamps of similar type may be measured by direct comparison. With the virtual disappearance of flicker photometry, the validity of heterochromatic photometry need no longer be judged by correlation with the flicker observation, but rather by whether two sources which have the same candle-power provide illuminations which look equal, or two surfaces which have the same reflection factor appear to have the same lightness, whatever their colour.

That, at least, would seem to me to be the position, yet MacAdam (1950) has recently reported observations which would on this basis make nonsense of heterochromatic photometry. His apparatus consists essentially of two Donaldson trichromatic colorimeters juxtaposed in such a way that the observer sees two large fields side by side, each of which is illuminated by a mixture of red, green and blue matching stimuli. The observer can make colour matches between the two halves of the field or can make photometric matches between

the two fields in the presence of any desired colour difference. The observer uses both eyes, and the adaptation conditions can be controlled by means of fluorescing screens lining the inside of the observing booth.

The results of immediate interest to us concern the photometric comparison of lights of various saturations. When, for example, he matched a saturated and a desaturated red, MacAdam found that the luminances of the two halves of the field, as derived by calculation from the standard luminosity curve and the spectral composition of the two beams, were in the ratio 27 : 47, instead of being equal. Similar discrepancies in the same sense but generally smaller in magnitude were also found for other hues. The observing conditions in this experiment were : 10° field in a dark surround, luminance range 5–80 foot-lamberts.

It is impossible to attribute differences of this order of magnitude to possible errors in the standard luminosity curve. There has recently been some criticism of this curve and some revision may be necessary, but its effect on photometric calculations would be trivial. It may with greater force be urged that the direct comparison of lights of different colour is a difficult and inaccurate procedure, and that the observer may be liable to confuse the vividness of the colour with the luminosity of the light, although MacAdam denied this. It may be worth noting that in tests made some years earlier on the Munsell atlas, coloured surfaces of various chromas were accepted as having the same value or lightness if they had the same reflection factor. Whether or not this disagreement can be attributed to the difference in size of field used in the two cases, the fact remains that we are as interested in large fields as in small.

There is evidently some doubt as to the experimental facts which have to be explained away, and I feel that photometrists should pay enough, but not too much, attention to the correlation between subjective estimates and photometric measurements of lights of widely different colours. Such comparisons are rarely of so vital a nature that high precision is called for and it will always be difficult to eliminate uncertainties due to psychological and adaptation factors. If further tests are to be made on the validity of heterochromatic photometry, and in particular of the luminosity curve and the principle of additivity, then I would suggest that they should be made by photometric matches between light of the same or nearly the same colour but different spectral compositions, for example, by matches between white lights made up from mixtures of various pairs of complementary wavelengths. Equality of luminosity should then be accompanied by reasonably close equality of luminance for an average group of observers, so providing a sufficiently critical test without any uncertainties in the type of visual judgment involved.

§3. STANDARD MIXTURE CURVES

Progress in colour measurement was hampered in 1926 by the absence of adequate data to define the colour matching characteristics of a standard observer. It is well known that the colours of the equal-energy spectrum can be represented in terms of three mixture curves, in which the amounts of defined red, green and blue stimuli required to match each spectral colour are plotted against its wavelength. These curves are of very great theoretical interest, but their technical importance lies in the fact that from such curves we can calculate the amounts of the three stimuli required to match any test stimulus which has been defined by its spectral composition. The calculation is analogous to the

weighting procedure already described for the luminosity curve, except that it has to be done in triplicate.

Prior to 1926 the only important determinations of the colour mixture curves had been by König and Dieterici in Germany and by Abney in this country some thirty years previously, and Guild rightly emphasized the need for a new set of measurements. As a result of investigations carried out during the next few years at the National Physical Laboratory and at the Imperial College, the International Commission on Illumination was in a position by 1931 to adopt a set of curves defining the colour matching characteristics of a standard observer and to establish a reference framework within which a colour could be specified on the trichromatic system.

This system, which is usually identified in this country as the C.I.E. system, appears to have stood the test of twenty years remarkably well, especially when it is realized that the total number of observers who took a complete set of observations in the two investigations totalled only seventeen altogether. Only recently has any suggestion of an error in the data been reported and even this stems not from the colour matching experiments, but from the 1924 luminosity curve with which the colour data had to be incorporated in 1931.

Before, however, being too ready to accept the absence of criticism as a matter for gratification, we ought first to consider the kind of discrepancies that might have been discovered and whether effective tests to discover them have in fact been made. Two things in particular might have occurred: we might have found that a pair of colours which appeared alike were located at different points in the chromaticity chart, or that two colours which looked different were located at the same point in the chart. These possibilities only exist because any given colour sensation can be aroused by a wide variety of light stimuli, but it is doubtful whether anyone has subjected the data to a stringent test of this kind during the past twenty years. If either of these effects had been recorded, then it would have implied one of three things: (*a*) the original colour matching data were in error; (*b*) the data were not sufficiently representative of the average eye; or (*c*) the additivity law of colour equations which is implicit in the process of integration used to calculate the chromaticity coordinates, did not hold.

Although, in theory, a point on the chromaticity chart may correspond to an infinite number of different spectral compositions, in practice any particular red or yellow or green, etc., will be produced with a dye or pigment which has a fairly well-defined type of spectral absorption, especially for bright colours. If we consider different yellow pigments, for example, we find that they all absorb heavily at the blue end of the spectrum and reflect highly at the red end. They differ mainly in the precise values of their high and low reflection factors and in the exact part of the spectrum where the rapid transition from high to low reflection occurs. In these circumstances defects in the colour mixture data would have to be quite gross before they would be revealed by chromaticity distortion among a group of yellow pigments.

In the case of a pair of dyed fabrics which have the same chromaticity but markedly different spectral reflections, at least one of the dyes is usually dichroic; the match between the two fabrics is then extremely sensitive both to the quality of the illumination and to the colour vision of the observer. Again, therefore, any error in the colour data would have to be very large before it produced chromaticity errors comparable with the instability of the colour match.

It follows from these and similar considerations that at least for commercial purposes the ultimate accuracy and internal consistency of the standard observer data may be less critical than might at first be supposed. Even so, examination of both old and new luminosity data (Thomson 1949) suggests that the criticism that the blue and violet end of the spectrum has not been given enough weight may have some substance, but new experiments have been called for by the Illumination Commission to confirm this. The matter has been given some prominence in the United States through the case of two near-white titanium dioxide pigments, one of which has a heavier absorption than the other in the far-violet. Disagreement between the chromaticity differences as calculated from the spectral reflection curves and as measured by visual colour matches was reported, and Judd has shown that closer accord was possible by using new mixture curves derived from a revised luminosity curve with higher blue values (Judd 1949). If this case is to be seen in its proper perspective, however, two points should be noted: the chromaticity differences involved were extremely small although, apparently, of commercial importance; and out of seven observers who made observations, three were in close agreement with the standard observer.

One modification in the standard chromaticity chart has been urged from time to time since 1931, namely a change in coordinates to give a more uniform colour distribution. In the chart as usually drawn, the population of just noticeably different colours is very dense in the blue corner of the diagram and very sparse in the green corner. This is not due to any defect in the data, but arises from the particular choice of coordinates made in 1931 from sound practical considerations. Unfortunately, the amount of information available at that time on colour discrimination was so limited that the question of the spacing of the colours could hardly have affected the choice, and in any case the absence of any agreed system of colour measurement in itself handicapped the recording of colour discrimination data.

Perhaps I might digress for a moment to enlarge on this point. When we are dealing with the spectrum, the position is reasonably clear: we record for various wavelengths λ, the wavelength difference $\Delta\lambda$ that can just be distinguished as a result of the corresponding change in hue; we then plot λ against $\Delta\lambda$ to give the wavelength discrimination curve. This at least gives the impression of having some fundamental significance, by virtue of the simple physical terms in which the stimulus is described. We might, on the other hand, use a mixture of two dyes to dye a series of fabrics, in which the relative concentrations in the mixture were varied systematically from one fabric in the series to the next. Observations could then be made for various concentration ratios c, to discover the smallest change in concentration Δc that could just be detected, and hence we could plot Δc against c to give a concentration discrimination curve.

Observations of this kind can be of great practical value, but they are sometimes used to justify statements to the effect that the eye is more sensitive to differences among near-whites than among any other colours. If such a statement had any visual meaning, it would presumably be that the number of just noticeable steps in a given colour interval defined on some fundamental basis was a maximum for near-white colours. Yet on what fundamental basis can a given colour interval be measured? One possibility, and I think this is the answer most people would give, is by the number of just noticeable steps in the interval, but if we defined

both the interval and the sensitivity in terms of the number of steps, we should have argued in a circle and discovered that the eye was equally sensitive to all colour differences!

I dare not pursue this argument too far for fear of getting in a tangle, but the truth as I see it is that the results of any discrimination experiment have to be expressed in terms of some more or less arbitrary physical coordinates, such as wavelength, concentration, chromaticity, etc., and that the eye may be made to seem more sensitive in one colour region or another, according to the scale that is used.

However that may be, with the introduction of the international system, the way was clear for recording the sensitivity to any type of colour change in any direction through the colour solid. We now know of the serious non-uniformity in the distribution of the colours in the standard chromaticity chart, but we also know that no linear transformation can give an exactly uniform distribution. Two points of view have been expressed, one in favour of substituting for the present chart a linear projection giving an approximately uniform colour population, the other in favour of retaining the obviously non-uniform chart, if only as a precaution against the fallacy of thinking that equal chromaticity differences on some new chart could correspond to equal subjective colour intervals. Perhaps I should add that this question has a direct practical bearing on such matters as the specification of colour tolerances and the assessment of the accuracy of colour reproduction in photography, television, etc.

§4. THE DISSEMINATION OF COLOUR KNOWLEDGE

In 1926, Guild had occasion to comment on the remarkable situation that existed regarding the lack of understanding of the elements of colour physics. Perhaps I may quote as follows: "It is a curious fact", he wrote, "for which I cannot venture an explanation, that phenomena and laws known to the earliest pioneers such as Newton, Maxwell, and others, are still very largely unknown or imperfectly understood even among those engaged in scientific and technical investigations on colour vision. There is no parallel to this in any other branch of experimental science. If every electrician who constructed an ammeter were to attach a perfectly arbitrary scale to the instrument and, instead of troubling to connect its indications with fundamental standards, were to invent a new theory of electricity to account for the peculiarities of his instrument, the position would be not unlike that existing in the science of colour to-day. Such a position would only be excusable were no fundamental basis known by which all methods of measurement could be related. Such a basis as regards colour has long been available in Newton's laws of colour mixture applied to the trichromatic mixture curves of the spectrum."

To some extent the situation to-day has improved. I think, for example, that there is a more widespread appreciation of the importance of knowing the spectral composition of the light reflected from a surface as determined by the quality of the illumination and the nature of the pigmentary absorption in the surface. I should also like to think that the additive nature of the colour mixing which always occurs when any heterogeneous beam is focused on the retina was more widely understood. I believe the Colour Group [of the Physical Society] has made an important contribution to this educational process, not only, and perhaps not primarily, through its meetings and papers, but more

especially through the exhibits which it has organized as part of the Physical Society's Instruments Exhibition, and also through the two Reports which it has published.

Yet we have still hardly touched the fringe of the people who are interested in, and have some concern with, colour. I have only time to give one example, a hoary one, I am afraid, but still a modern problem, of a topic on which enlightenment is still desirable, namely the distinction between the red, yellow and blue colours which are used as primaries in pigment and dye mixture, and the red, green and blue radiations which are used as matching stimuli in additive light mixture. There are several potential sources of confusion here, one of which is the use of red and blue as the names for two of the pigment primaries when they should more correctly be described as magenta and blue-green. Fellows of the Physical Society will, of course, be aware that the function of the red, yellow and blue pigment primaries is to absorb the green, blue and red regions of the spectrum respectively, and that the only essential difference between additive and subtractive mixture is in the means adopted to control the mixture of red, green and blue light. Yet the majority of people would still be prepared to argue, on the basis of their experience with mixing paints, that yellow is one of the three fundamental matching colours and that green is a derived colour from the mixture of yellow and blue. If the Colour Group had nothing else to its credit in, say, fifty years time than the clarification of the relationship between additive and subtractive mixture, I think it could still claim to have justified its existence. But I still think that perhaps the chief hope of an early recognition of the true facts lies in the advent of colour television, since this will make the additive superposition of red, green and blue pictures as much a part of the domestic scene as the proverbial box of paints.

In addition to the need for a better understanding of colour physics in general, there is also the need for a wider exploitation of the C.I.E. system in particular. I will not dwell on the obvious commercial advantages of being able to define a colour by numbers which have an internationally accepted meaning, except to make the comment that very few of the colour cards issued by the paint manufacturer or the dyer include the C.I.E. specification of the goods they are trying to sell. They do not even give their Munsell or Ostwald notations, which can be regarded as acceptable sub-standards of reference, since these atlases have been measured on the C.I.E. system. Even in scientific research, only the most enterprising botanist, biologist or geologist will attempt to classify the colour of his material in scientific terms, and when the physicist is explaining the colours produced by interference or polarization, does he ever give their locus in the chromaticity chart?

If we were merely concerned with cataloguing colours for their aesthetic interest, perhaps the claims of the C.I.E. system would be less insistent, but colour is also, of course, an indicator of definite physical and chemical properties. Colour is often used, for example, to grade the quality of a product—of cotton, vegetable oils, foodstuffs, signal glasses, and so on. I have had interesting discussions with entomologists about the colour of insects, where a quantitative record of the difference in colour between specimens, or a change in colour during the life of a specimen, would have been of great biological interest; in the design of protective goggles in industry, the correct choice of the colour of the goggles may greatly enhance the colour discrimination of the wearer; in the

manufacture of fluorescent lamps, a knowledge of the chromaticity of various phosphors assists in the production of a lamp of maximum efficiency for a given colour; in colour television, the range of reproducible colours can be shown on the chromaticity chart from a knowledge of the chromaticities of the component red, green and blue pictures; in titration, one type of indicator may provide a more sensitive end-point than another, and this can best be determined by a systematic colorimetric (i.e. C.I.E.) analysis in which account is also taken of the data on colour discrimination expressed on the chromaticity chart; by suitable colorimetric calculations, it is possible to determine the theoretical limits to the colourfulness which a coloured surface can have for a given hue and lightness, and this is of great importance in the preparation of new dyes, since it enables the dyemaker to decide which of his dyes are approaching the theoretical limit, and on which he should concentrate his research.

Perhaps the present situation may be summed up by quoting the views expressed by White and Vickerstaff (1945) in their Mercer Lecture addressed to the Society of Dyers and Colourists: "It must be admitted, without dispute, that in the field of colorimetry proper, and particularly in the application of colorimetry to practical problems, the Americans are pre-eminent. In this country we are lagging behind in the application of a very valuable tool for the study of problems encountered in dyeing and colouring, and if this discussion stimulates anyone to take up this subject it will have served its purpose."

§ 5. INSTRUMENTAL DEVELOPMENTS

With the establishment of the C.I.E. standard observer, the whole of colorimetry can in principle be carried through by purely physical measurements, and in the United States the Hardy photoelectric recording spectrophotometer in particular has been used on a very wide scale indeed for a great variety of colour measurements. In 1926, visual instruments alone were feasible and for many years they retained their dominant position in this country. They still have their value, more especially the Donaldson six-stimulus instrument for measurements of the very highest precision, and the Lovibond tintometer for a very wide variety of grading tests, but photoelectric instruments are at last becoming available. A few Hardy spectrophotometers have been imported into this country, and one or two non-recording photoelectric spectrophotometers such as the Hilger and Watts Uvispek instrument, are being manufactured here. One of the most important instrumental developments has been the photoelectric tricolorimeter using a spectrum and template system to correct the photocell sensitivity to be similar to each of the three standard observer spectral distribution curves in turn. Two or three instruments of this type have been described, but that developed by Winch (1946) and manufactured by the General Electric Company seems destined to play a major part in colorimetry.

To suggest that there are no modern instrumental problems would, however, be foolish. We need simpler and cheaper apparatus; there is scope for apparatus more specifically designed for measuring small colour differences and for measuring small areas of colour; with some of the existing equipment a rather indeterminate mixture of the specular and diffuse components of the light reflected from a coloured pattern is measured, while a measuring problem that may become increasingly important concerns fluorescing dyes and pigments.

You will all have seen the fluorescing pigments that have recently become a common feature of the advertisement hoardings, and many of you will also be aware of the use of blue fluorescing dyes in laundering to improve the colour of white articles that have to be washed. Since the usual technique in measuring the spectral reflection curve of a sample is to illuminate the sample with monochromatic light of wavelength λ and to measure the fraction of light reflected, it is evident that if the sample fluoresced under illumination of that wavelength, the light that was measured would be a mixture of the fluorescing component and the reflected component. Since the former will not be of the same wavelength as the latter, an error will be caused if both are counted together as if they were of the same wavelength λ, yet this is what happens in the normal type of recording spectrophotometer. It may prove that the spectrophotometer cannot be used satisfactorily for this type of measurement and that either a visual colorimeter or a photoelectric tricolorimeter will have to be employed. Even here, attention will have to be paid to the standard illuminants at present recommended for colorimetry to see whether their ultra-violet content is sufficiently representative of the type of illumination commonly encountered in practice. The fluorescent lamp may have to be considered as a special case in this connection.

In spite of these particular problems, I think it is true to say that our instrumental needs are largely being met, and that lack of suitable apparatus is no longer a major problem. Paradoxically, now that we are in a position to make colour measurements with purely physical apparatus, the most intricate new problems that are arising are subjective. Disappointment is being expressed that colorimetry, as at present understood, does not claim to define what a colour looks like, and in some cases commercial questions of the utmost urgency hinge for their answer on the possibility of making subjective measurements by which the appearance of a colour can be defined. In the time that remains, I want, therefore, to examine the nature of this type of problem.

§6. SUBJECTIVE COLOUR MEASUREMENTS

At the beginning of this lecture, I emphasized that in trichromatic colorimetry a colour is defined by the equivalent mixture of three reference stimuli. To illustrate the need for, and the limitations of, this type of information in a problem in which we are concerned with the appearance of a colour, I should like to refer to experiments by Holmes (1941) on the colour of light signals. The problem here was to determine how variations in the quality of the light from a signal lamp would affect the recognition of the signal colour, and Holmes constructed a colour mixing lantern with which a small aperture, simulating a light signal, could be illuminated by lights of widely differing colour. He then recorded some 40,000 observations made by a number of subjects, who had the task of recognizing the signals and describing them as one or other of the simple colours red, yellow, green, blue, purple or white. He then plotted contours in the chromaticity chart showing the frequency of recognition of these colours for various conditions of observation, and he discussed the contours in relation to the permissible chromaticity limits for each of the signal colours.

Although the use in this investigation of no more than six colour names implied a quite coarse grading of the colours, a correlation between chromaticity and subjective appearance was in fact established. The observation itself might

almost be described as a kind of memory match in which the subject had the not very difficult task of trying to remember what red, yellow, green, blue, purple and white looked like. In most of the experiments, a fairly orthodox division of the chromaticity chart into six segments was recorded, but for one or two of the conditions under test, an island of yellow was found on the purple side of the chart. This proved to be of special theoretical interest as it confirmed the tendency towards dichromatic vision for small field conditions, an effect that has been the subject of much interesting study during the last few years.

For our present purpose, the interest in Holmes' experiments is not so much in the results as in the three stages of the investigation. His starting point was a light source which was defined colorimetrically; he then made subjective observations on the appearance of the light; he finally deduced colorimetric specifications and tolerances for the colours of signal glasses. Hence although the colorimetric specification did not in itself tell us what the colour looked like, yet it was an essential ingredient in the initial design of the experiment and was also the final end-product for which the investigation was undertaken.

Analogous situations arise in other problems, especially where colour is used for decorative purposes and where the design may be strikingly affected by contrast and adaptation. I should like to illustrate this by discussing, as a final example, the problem of the colour rendering properties of light sources and in particular of the fluorescent lamp, since this is one of the most interesting problems which colorimetrists have yet had to tackle and one of great importance and urgency for lamp manufacturers.

From what has been said earlier, it is evident that the chromaticity of a pattern will vary with the quality of the illumination, since the spectral composition of the light reflected by the pattern is in part a function of the composition of the incident light. The chromaticity shift is in fact quite large when we change from daylight to tungsten light, perhaps surprisingly large in comparison with the small change in appearance which occurs with most patterns other than dichroic colours. This colour constancy is due to the adaptation of the eye which will often compensate very largely for any change in colour of the illumination. We should therefore be led badly astray if we judged the colour rendering characteristics of an illuminant solely from chromaticity data, yet at the present time we have no recognized scientific method of studying the degree of compensation caused by the visual adaptation process, nor of comparing the appearance of colours seen in different illuminations, other than by verbal description.

Until recently, these matters were of academic interest rather than industrial importance, but with the advent of the fluorescent lamp, the lamp manufacturer has been provided with a light source whose energy distribution curve is far more flexible than those of previous types of source, but which nevertheless has some awkward characteristics so far as colour rendering is concerned. It is possible, for example, for a lamp to have the same colour as daylight, but to have a rather different spectral composition. The difference arises chiefly from the presence of the line spectrum of mercury superimposed on the energy distribution of the light from the phosphors in the tube, and also from a lack of a phosphor with a strong energy radiation at the red end of the spectrum. The adaptation of the eye will, so far as we know, be determined by the integrated colour of the light and not by its particular spectral composition, from which it follows that

sources with the same colour but different composition will have different colour rendering properties.

It is not my purpose here to solve the manufacturer's problem for him, but rather to define it. As I see it, it amounts essentially to this: we have two light sources P and Q, and a series of coloured patterns a, b, c, etc.; the chromaticities of the patterns under the two illuminants can be determined either by calculation or by direct measurement with a colorimeter, and can be plotted on two chromaticity charts as a_P, b_P, c_P, and a_Q, b_Q, c_Q, ... The Q chart might be regarded as suffering from some internal strain in comparison with the P chart. but adaptation will normally tend to reduce this strain. There will, in fact, be a series of points a'_P, b'_P, c'_P, . . . in the P chart which, when seen by the P-adapted eye, will have the same appearance as a_Q, b_Q, c_Q . . . when seen by the Q-adapted eye. The residual strain when account has been taken of adaptation, will then be measured by the distances a_P–a'_P, b_P–b'_P, c_P–c'_P, ... The problem is to determine these distances and to assess them relative to the tolerances for colour distortion in a given set of circumstances. (It should be noted that while the distortion will, to a first approximation, be a function of the chromaticities a_P, b_P etc., yet samples having the same chromaticity but different spectral reflection characteristics may yield slightly different distortion values.)

The main observational problem in this analysis is to equate a'_P with a_Q, b'_P with b_Q, etc., since this involves the matching of colours seen under different conditions of adaptation. I referred a moment ago to Holmes' experiments on signal glasses and described the observation as a form of memory matching. A more refined form of memory matching, in which the observer looks first at the patterns under P illumination and then under Q illumination, adapting himself to each in turn, could also be employed here. An alternative technique is to let the left eye be P-adapted and the right eye Q-adapted; a binocular match between the patterns under the two illuminants can then be used to equate a'_P with a_Q, etc. This technique has already proved a powerful tool for the investigation of adaptation phenomena (Wright 1946), and Miss E. G. Tadros has constructed a binocular viewing booth at the Imperial College in an attempt to apply the technique to colour rendering problems and to the measurement of the subjective appearance of colours. If, for example, condition P were adopted as a standard, in which quality of illumination, level of illumination, size of pattern, and so on, were standardized, then the P chromaticity chart could be used as a reference chart against which the appearance of any colour under any other condition of illumination and viewing, could be compared. I have no doubt that unexpected difficulties will appear if attempts are made to record the appearance of colours in a complicated pattern, but these should eventually sort themselves out. Subjective measurements will then be possible, but as I have already emphasized, they will be supplementary to, and not a substitute for, colorimetric measurements.

If I am right in forecasting this twist of events, it will mean that the eye will not, after all, be entirely replaced by the photocell in colorimetry. I should personally be rather pleased about this, even though my recent instrumental interest has been directed to the design of a photoelectric spectrophotometer. I would perhaps have been more hesitant in my emphasis on subjective measurements, if I had not heard recently that at least one colorimetrist who has played a leading part in the development of photoelectric equipment, namely Mr. Winch,

has now got caught up in these binocular matching experiments (Winch and Young 1951). This serves to illustrate the delightful uncertainty of the subject—at one moment you are doing physics, the next physiology, then perhaps psychology, and there is a very good chance that in the end you may get involved in art.

I was rash enough to entitle this lecture "*Modern* Problems in Colorimetry" and my final example has been concerned with colour rendering and colour adaptation. Perhaps it will be fitting, and salutory, to conclude by quoting from Thomas Young's Royal Institution lecture on Vision: "When a considerable part of the field of vision is occupied by coloured light, it appears to the eye either white, or less coloured than it is in reality: so that when a room is illuminated by the yellow light of a candle, or by the red light of a fire, a sheet of writing paper still appears to retain its whiteness"; and a few sentences earlier he explained what was happening under similar circumstances in these words: "The reason ... is probably that the ... retina has lost a part of its sensibility to the light of that colour, with which it has been impressed, and is more strongly affected by the other constituent parts of the white light". That was in 1803. I can only say that the problem is still with us!

REFERENCES

Donaldson, R., 1947, *Proc. Phys. Soc.*, **59**, 554.
Harding, H. G. W., 1948, *J. Sci. Instrum.*, **25**, 333.
Holmes, J. G., 1941, *Trans. Illum. Engng. Soc., Lond.*, **6**, 71.
Judd, D. B., 1949, *J. Opt. Soc. Amer.*, **39**, 945.
MacAdam, D. L., 1950, *J. Opt. Soc. Amer.*, **40**, 945.
Thomson, L. C., 1949, *Proc. Phys. Soc.* B, **62**, 787.
White, G. S. J., and Vickerstaff, T., 1945, *J. Soc. Dy. Col., Bradford*, **61**, 213.
Winch, G. T., 1946, *Trans. Illum. Engng. Soc., Lond.*, **11**, 3.
Winch, G. T., and Machin, C. F., 1940, *Trans. Illum. Engng. Soc., Lond.*, **5**, 93.
Winch, G. T., and Young, B. M., 1951, *G.E.C. J.*, **18**, No. 2.
Wright, W. D., 1946, *Researches on Normal and Defective Colour Vision* (London: Kimpton).

Torque Curves and other Magnetic Properties of Alcomax

By K. Hoselitz and M. McCaig

Permanent Magnet Association, Central Research Laboratory, Sheffield

MS. received 22nd December 1950

ABSTRACT. Using a torque magnetometer, the crystal anisotropy constants of the permanent magnet alloy Alcomax III have been determined. The type of magneto-crystalline energy after rapid cooling is cubic with a positive constant (iron-like); after slow cooling cubic with a negative constant (nickel-like) and after cooling in a magnetic field uniaxial with a positive constant (cobalt-like). The changes in crystal anisotropy are compared with parallel measurements on the hysteresis curve. A direct experiment shows that when the field applied during cooling makes an angle with the crystal axes, the preferred direction is much nearer to a [100] axis than the field direction.

§1. Introduction

Some permanent magnet alloys, known under the names of Alcomax, Ticonal and Alnico V, are magnetically anisotropic after cooling in a magnetic field. The origin of the high coercive force and the mechanism by which it is produced in the material, as well as the cause of the magnetic

anisotropy, present many interesting problems which would best be investigated by experiments on single crystals.

Although single crystals of sufficient size are not at present available, some useful information has already been derived from measurements of the magnetostriction of magnets with columnar crystals (McCaig 1949). These alloys consist essentially of a body-centred cubic phase, and in magnets with columnar crystals all crystallites have one [100] axis parallel to a given direction, and the remaining cube edges are distributed at random in a plane perpendicular to that direction.

Using a torque magnetometer, the magnetic anisotropy for a columnar magnet of Alcomax III has now been studied. From torque measurements the symmetry of the magnetic anisotropy can be found, and constants of magneto-crystalline anisotropy can be derived. The magnitude and type of the magneto-crystalline energy is found to depend on heat treatment, and a relation between the anisotropy constants and other magnetic characteristics which vary with heat treatment has been sought.

The relations between the anisotropy indicated by torque experiments and other magnetic properties appear to be complicated, but certain conclusions can be derived from the experiments, and these are discussed in the light of some theories of high coercive force in magnet materials.

§2. EXPERIMENTAL

The alloy under investigation was Alcomax III, with a composition of 13·45% Ni, 25·3% Co, 2·99% Cu, 7·4% Al, 0·87% Nb, 0·17% Si, the rest Fe. The test pieces were ground to the shape of cylindrical discs with a diameter of 1·0–2·0 cm. and a thickness of about 1 cm. The common crystal axis (columnar axis) was arranged to lie along a disc diameter. The test pieces were suspended in the magnetometer, with the cylinder axis as axis of rotation.

The torque magnetometer was a robust version of the instrument described by Williams (1937). The specimen was fixed to the extreme lower end of a vertical brass axle, and not between the bearings as is more usual. As the torques were large, jewelled bearings were unnecessary; close to the specimen the axle passed through a plain bronze bearing, and about 20 cm. higher through a small ball bearing. The torque was measured by the angle of torsion of a copper–beryllium wire 20 cm. long. Wires of different diameters up to 1·5 mm. could be used.

The magnetic field was produced between the flat cylindrical pole pieces of an electromagnet. The pole gap was about 4·5 cm. and the pole-piece diameter 10 cm. The field strength without a specimen was within the range 7,400–9,000 oersted. As the specimens had a considerable demagnetizing factor, the effective fields were probably about half these values, but were still amply sufficient to produce a high degree of saturation.

§3. THEORETICAL

From the experimental results it will be seen that the torque curves can be explained by the assumption of two types of symmetry of the energy of magnetization, a cubic one and a uniaxial one, where the preferred axis coincides with one of the cube edges.

It is advantageous to express that part of the energy of magnetization which varies with the direction relative to the crystal axes in a formal way, incorporating

both possible types of symmetry. If the direction of magnetization is defined by the direction cosines α_1, α_2 and α_3 of the angles included with the [100], [010] and [001] crystal axes, [100] being the preferred magnetic axis, the magneto-crystalline energy density can be expressed as the energy distribution of a tetragonal crystal lattice:

$$F = C + K_2'(1-\alpha_1^2) + K_4'(1-\alpha_1^2)^2 + K_4(\alpha_1^2\alpha_2^2 + \alpha_2^2\alpha_3^2 + \alpha_3^2\alpha_1^2) + \ldots \quad \ldots\ldots(1)$$

In the absence of any uniaxial symmetry $K_2' = K_4' = 0$, thus

$$F_{\text{cubic}} = C_1 + K_4(\alpha_1^2\alpha_2^2 + \alpha_2^2\alpha_3^2 + \alpha_3^2\alpha_1^2), \quad \ldots\ldots(1\,a)$$

and for the purely uniaxial case $K_4 = 0$

$$F_{\text{uniaxial}} = C_2 + K_2'(1-\alpha_1^2) + K_4'(1-\alpha_1^2)^2 \quad \ldots\ldots(1\,b)$$

where $C_1 + C_2 = C$.

A columnar crystal magnet placed in a field which is sufficient to produce saturation, i.e. to ensure that the magnetization is always in the direction of the applied field, experiences a torque tending to rotate it so that the direction of magnetization is in the position of least energy. If this torque can be measured, as a function of the position of the columnar axis, a torque curve, i.e. a curve showing torque against position of the columnar axis, is obtained.

In order to interpret such an experimental curve in terms of magneto-crystalline energy, the torque curve expected from an assembly of crystals with one common fourfold axis must be calculated assuming that the energy distribution of each crystal can be represented by equation (1). The experimental results have not so far required the inclusion of terms of order higher than the fourth in (1), and hence these will be neglected.

Transforming (1) into spherical polar coordinates by putting $\alpha_1 = \cos\theta$, $\alpha_2 = \sin\theta\cos\phi$, $\alpha_3 = \sin\theta\sin\phi$, we find

$$F = C + (K_4 + K_2')\sin^2\theta + (K_4' - K_4 + K_4\sin^2\phi\cos^2\phi)\sin^4\theta. \quad \ldots\ldots(2)$$

Denoting the angle of magnetization with the columnar axis as θ, a columnar crystal sample can be represented by an assembly in which ϕ takes all values from 0 to 2π. Hence the mean contribution to F from a columnar sample for each value of θ can be expressed by integrating (2) with respect to ϕ from 0 to 2π. This gives

$$F_c = C + (K_4 + K_2')\sin^2\theta + (K_4' - \tfrac{3}{8}K_4)\sin^4\theta. \quad \ldots\ldots(3)$$

The purely cubic part of (3) is

$$F_{c,\,\text{cubic}} = C_1 + K_4(\sin^2\theta - \tfrac{7}{8}\sin^4\theta) \quad \ldots\ldots(3\,a)$$

and the uniaxial part

$$F_{c,\,\text{uniaxial}} = C_2 + K_2'\sin^2\theta + K_4'\sin^4\theta. \quad \ldots\ldots(3\,b)$$

The torque T per unit volume is now given by

$$T = (K_2' + K_4' + K_4/8)\sin 2\theta - \tfrac{1}{2}(K_4' - \tfrac{3}{8}K_4)\sin 4\theta. \quad \ldots\ldots(4)$$

Fom (3) and (4) it can be seen that the values of $K_2' + K_4' + \frac{1}{8}K_4$ and $\frac{1}{2}(K_4' - \frac{3}{8}K_4)$ can be determined from torque experiments or from energy density differences using (J, H) curves for magnetization in different directions, but that it is not possible to obtain three independent expressions to determine K_2', K_4' and K_4.

A measure of the amount of uniaxial distortion of the symmetry of magnetization energy may be obtained by finding the ratio of the coefficient with $\sin 4\theta$ to that with $\sin 2\theta$ in (4):

$$-\frac{\frac{1}{2}(K_4'-7K_4/8)}{K_2'+K_4'+K_4/8}=\frac{7}{2}-\frac{8K_4'+7K_2'}{2(K_2'+K_4'+K_4/8)}.$$

For the cubic case K_2' and K_4' are both zero, and the ratio should be 7/2. Deviations from this value give a measure of the superimposed uniaxial asymmetry.

It is of advantage to express the torque function for the two ideal cases of pure cubic and pure uniaxial energy distribution.

For the cubic case we have

$$T_{\text{cubic}}=K_4(\tfrac{1}{8}\sin 2\theta+\tfrac{7}{16}\sin 4\theta). \qquad \ldots\ldots(4a)$$

The values of maximum and minimum torque and the corresponding values of θ are

θ (°)	24	69	111	156
T	$0{\cdot}53K_4$	$-0{\cdot}34K_4$	$0{\cdot}34K_4$	$-0{\cdot}53K_4$

Inspection of a torque curve of a cubic material makes it immediately obvious whether the constant of magneto-crystalline energy is positive, as in iron, or negative, as in nickel.

For pure uniaxial anisotropy we obtain

$$T_{\text{uniaxial}}=(K_2'+K_4')\sin 2\theta-\tfrac{1}{2}K_4'\sin 4\theta. \qquad \ldots\ldots(4b)$$

The experimental results are not sufficiently accurate to enable the individual values of K_2' and K_4' to be determined accurately but, ignoring the term in $\sin 4\theta$, maximum and minimum values occur for $\theta=45°$, $T=K_2'+K_4'$; $\theta=135°$, $T=-K_2'-K_4'$.

In the preceding calculations it was assumed that the columnar axis is always the preferred magnetic axis in the uniaxial energy distribution. However, one hypothetical arrangement of domain anisotropy deserves to be considered separately.

Suppose that in each domain one of the three cube-edge directions is preferred above the remaining two, but that over the entire assembly of domains in the specimen the choice of preferred axis is completely random, that is, the preferred axis is parallel to the columnar axis in one third of the volume and perpendicular to the columnar axis in two thirds of the volume. Using equation (1), it is possible to calculate the torque for this random distribution of the preferred axis along the three edges. It is only necessary, in the first two terms on the right-hand side of this equation, to replace α_1 in one-third of the volume by α_2 and in another third by α_3, giving $F=C+\frac{2}{3}(K_2'+K_4')+(K_4-\frac{8}{3}K_4')(\alpha_1^2\alpha_2^2+\alpha_2^2\alpha_3^2+\alpha_3^2\alpha_1^2)$ and in polar coordinates

$$F=C+\tfrac{2}{3}(K_2'+K_4')+(K_4-\tfrac{8}{3}K_4')(\sin^2\theta-\tfrac{7}{8}\sin^4\theta) \qquad \ldots\ldots(5)$$

and the torque

$$T=(K_4-\tfrac{8}{3}K_4')(\tfrac{1}{8}\sin 2\theta+\tfrac{7}{16}\sin 4\theta). \qquad \ldots\ldots(6)$$

From this it is seen that for such an arrangement the energy distribution and the torque, as functions of θ, the angle with the columnar axis, are of the same form as for a substance with purely cubic symmetry (equations (3 *a*) and (4 *a*)).

§ 4. RESULTS

Figure 1 shows torque curves obtained for the alloy under investigation after three typical heat treatments: (1) oil quenched from 930° C. without a magnetic field, (2) slowly cooled from 930° C., also without a magnetic field, and (3) cooled in a magnetic field parallel to the columnar axis.

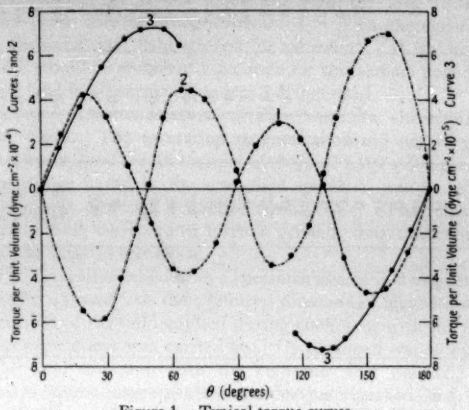

Figure 1. Typical torque curves.
1. Quenched 930° C. 2. Cooled slowly, no field. 3. Cooled in field parallel to columnar axis.

It can be seen at once that three types of torque curves are obtained, depending on the heat treatment. After quenching, the curve resembles that of a material with cubic anisotropy with a positive constant K_4, like iron (curve 1); after slow cooling without a magnetic field (curve 2) the material behaves like nickel with a negative constant K_4, and after cooling in a field (curve 3) the material has a uniaxial anisotropy, like cobalt, the easy axis being the columnar axis, which was parallel to the applied field during cooling. In case (3) the torque is of the order of ten times greater than in the other two cases, and curve 3 is plotted on a smaller scale. Even with the thickest wire which can be accommodated in the torque magnetometer, part of the curve where the torque decreases with increasing angle cannot be obtained, since the specimen is in unstable equilibrium.

It was found that heating to 930° C. eliminates most of the effect of previous heat treatments without changing the crystalline structure, and the magnetic anisotropy can be made successively iron-like, nickel-like and uniaxial in any order time after time. A specimen previously hardened in a field has been found to retain only about 1% of its uniaxial anisotropy after being placed in a furnace at 930° C. for 20 minutes.

In the present work torque curves have been measured for a large number of heat treatments. From these curves the character of the magnetic anisotropy and the magnitude of the constant of the energy expression equation (1), K_4 or $K_2' + K_4'$ have been determined, and the results are shown in the Table. The curves for specimens treated in a field indicate that K_4' is positive, but allow only an approximate estimate of its values (No. 7: $K_4' = 1{\cdot}3 \times 10^5$ erg.cm^{-3}; No. 9: $K_4' = 1{\cdot}8 \times 10^5$ erg.cm^{-3}). Using test pieces from the same alloy, and applying

Table 1

No.	Heat treatment			K_4 (erg.cm^{-3} $\times 10^{-5}$)	$K_2' + K_4'$ (erg.cm^{-3} $\times 10^{-5}$)	β†	E (erg.cm^{-3} $\times 10^{-5}$)	B_r (gauss $\times 10^{-3}$)	H_c (oersted)
	Hardening*	Field	Tempering						
1	20 min. 930° c. Oil-quenched	Nil	Nil	+1·0	—	0	1·3	1·2	5
						90°	1·3	1·4	4
2	Ditto	Nil	48 hr. 590° c.	+0·1	—	0			
						90°			
3	20 min. 930° c. Cooled 9° c/sec.	Nil	Nil	+0·7	—	0	1·3	9·5	24
						90°	1·5	8·5	15
4	20 min. 930° c. Cooled 2·5° c/sec.	Nil	Nil	0·0	—	0	1·2	10·5	89
						90°	1·7	9·9	67
5	20 min. 930° c. Cooled 1·6° c/sec.	Nil	Nil	−1·0	—	0	1·9	9·9	146
						90°	2·1	8·9	147
6	20 min. 1250° c. Cooled 0·9° c/sec.	Nil	Nil	−1·2	—	0	2·5	10·0	188
						90°	2·4	10·0	188
7	Ditto	‖ axis	Nil	—	7·5	0	0·9	14·3	195
						90°	6·2	2·5	100
8	Ditto	Nil	48 hr. 590° c. + 48 hr. 560° c.	−4·2	—	0	4·1	8·3	485
						90°	4·0	8·7	485
9	Ditto	‖ axis	48 hr. 590° c. + 48 hr. 560° c.	—	11·5	0	0·8	13·6	715
						90°	9·9	3·2	295
10	As cast	Nil	Nil	—	—	22·5°	1·8	10·0	163
						67·5°	2·1	9·9	160
11	20 min. 930°c. Cooled 1·25° c/sec.	22·5° to axis	Nil	—	6·0	22·5°	1·0	10·5	73
						67·5°	5·3	1·3	45
12	Ditto	Ditto	48 hr. 590°	—	7·7				

* Cooling speeds quoted are the averages of the rates between 900° and 600° c.
† β is the angle between the direction of measurement and the columnar axis of the test piece.

identical heat treatment, the following magnetic properties have been determined: the saturation magnetization $4\pi J_s$, the remanence $4\pi J_r = B_r$, the coercive force H_c, for $B=0$, and the reversible energy of magnetization between saturation and remanence $E = \int_J^{J_s} H\,dJ$.

The measurement of E was obtained from the area included by the magnetization curve and the straight line $J = J_s$. Thus the experimental value depends on the maximum field applied for saturation. It was considered that the values of E would be sufficiently accurate for comparison purposes, provided the maximum field in all experiments was 3,500 oersted.

The results of the measurements of these magnetic characteristics are also given in the Table. The saturation magnetization did not vary significantly with heat treatment, and for all test pieces $4\pi J_s = 14{,}500 \pm 800$ gauss. The low value of remanence found in the quenched specimen was so remarkable that an anchor ring was cast and quenched from 930° c. The remanence of this was 1,600 gauss and the coercive force 2 oersted, thus confirming the values measured on the original test block.

In order to determine whether in a specimen cooled in a magnetic field which is not parallel to a crystal axis the preferred direction of magnetization coincides with the direction of the field applied during cooling or with the nearest crystal axis a special experiment was carried out. A specimen was so cooled that the angle of the field direction with the columnar axis was 22·5° and torque curves as well as other measurements were subsequently taken (Nos. 10, 11 and 12). The result of this experiment is quite decisive. The preferred direction of magnetization was found to make an angle of less than 5° with the columnar axis, and over 18° with the direction in which the field had been applied. As there were probably a small number of crystals in the specimen which had random orientation and did not conform to the columnar arrangement the preferred direction in each individual crystal must have been very close to a [100] axis. The results of measurements on this magnet are also included in the Table.

§ 5. DISCUSSION

The results of the measurements can be used to give an insight into the mechanisms and processes responsible for the magnetic hardness and anisotropy of Alcomax III and of similar alloys by considering the experimental facts in conjunction with the various existing theories of the magnetization curve.

At the outset of the discussion it may be pointed out that the definition of crystal anisotropy in this work is purely formal. It includes any atomic or larger scale arrangement leading to an energy density distribution within the crystals of the alloy, which has the symmetry expressed by equations (1), (1 *a*), or (1 *b*). For example, if internal stresses or the shape of heterogeneous aggregates within the alloy can become orientated in a direction parallel to particular crystal directions, the resulting anisotropy of the energy of magnetization will be measured as crystal anisotropy, but if they are distributed at random they are not included in the measurement of crystalline anisotropy.

A recognized method of determining the constants of crystal anisotropy is to measure E in different crystallographic directions. For a specimen with uniaxial anisotropy $K_2' + K_4'$ should be equal to the difference in E measured perpendicular and parallel to the preferred axis $(E_\perp - E_\parallel)$. An examination of

the Table shows three cases where comparison of the values of $K_2' + K_4'$ obtained from measurements of torque and of reversible energy is possible. The figures are

Specimen no.	7	9	11
$K_2' + K_4'$ ($\times 10^{-5}$ erg.cm^{-3}) from torque	7·5	11·5	6·0
$K_2' + K_4'$ ($\times 10^{-5}$ erg.cm^{-3}) from $E_\perp - E_\parallel$	5·3	9·1	4·3

The values obtained from the measurements of E are consistently smaller, possibly because the maximum field of 3,500 oersted was insufficient.

For columnar cubic crystals K_4 can, in theory, be determined from $E_\perp - E_\parallel$. An elementary calculation shows that the result gives $E_\perp - E_\parallel = K_4/8$. This difference in reversible energy is too small to allow an estimate of the value of K_4 from our experiments, especially since the measurements of E could not be made with a high degree of precision.

In the absence of any alternative better method we have previously (Hoselitz and McCaig 1949, Hoselitz 1950) attempted to estimate the constant of crystal energy from measurements on polycrystalline specimens with random crystal orientation. For this purpose one can use either the reversible energy of magnetization (Néel 1948) or the approach to saturation (Néel 1945). Both these methods, it was realized, give only an upper limit to K_4, since other influences, including random internal stresses and heterogeneity, contribute to the measured properties. Moreover, in order to determine the constant of magneto-crystalline energy from the reversible energy of a random polycrystalline sample, the type of symmetry and the sign of the constant has to be known. The torque method does not depend on these uncertainties, and hence estimates of the anisotropy constants from torque measurements are more reliable.

In the specimens cooled in a field along the columnar axis (Nos. 7 and 9), and in that resulting in zero anisotropy constant (No. 4), the reversible energy $E_\parallel$ has still considerable positive values. It is concluded that random internal stresses and magnetic heterogeneity are the cause of this residual magnetic energy. The magnitude of these influences should be given by the value of $E = 1{\cdot}5 \times 10^5$ erg.cm^{-3} after heat treatment 4, provided that the alloy was then magnetically isotropic and not composed of an arrangement of domains either with tetragonal anisotropy with $K_4 = \frac{8}{9} K_4'$ or with positive and negative cubic anisotropy whose influences cancelled. In specimens cooled in a field parallel to the columnar axis, the value of $E_\parallel = 0{\cdot}85 \times 10^5$ erg.cm^{-3} due to the random influences cannot be taken as a direct measure of their magnitude.

One question has been decided conclusively. The assumption originally made by the authors that in an alloy treated in a field the preferred direction of domain magnetization lies along the nearest cube edge to that field has appeared to conflict with some results. Hoselitz and McCaig (1949) have pointed out previously that the remanence of an alloy with random crystals after being hardened in a field should be $0{\cdot}83 J_s$, but, in fact, values of over $0{\cdot}9 J_s$ are found. Recently Nesbitt (1950) has published a powder-pattern photograph of a small area of Alnico V treated in a field but afterwards cooled rapidly so that the coercive force is low. The angle between the domain magnetization and field direction is never more than 10° in the plane of the photograph. Allowing for the angle in the third direction, one can assume that greater angles, say 15–20°, may occur. Angles up to 54° with a mean value of 34° would be expected because

the experiment with a columnar sample treated in a field at 22·5° to its columnar axis shows quite conclusively that the preferred direction is very close to this axis. Although this sample contained 0·87% of niobium, the solution is not likely to be connected with this difference. More probably the preferred direction in each crystal is indeed parallel to a crystal axis, but owing to interaction the actual directions of domain magnetization are more nearly parallel, especially after rapid cooling, when the uniaxial part of the energy is not strongly developed. Our sample had been cooled at a more normal speed, so that it had a coercive force of 73 oersted.

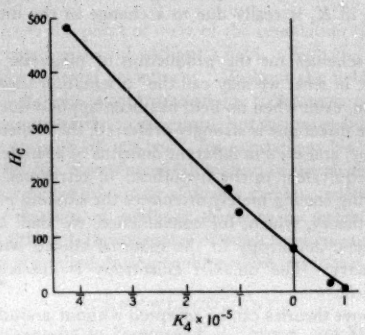

Figure 2.

The variation of coercive force with crystal anisotropy is almost linear, as shown in Figure 2, but there is a coercive force of about 80 oersted when the value of K_4 is zero. As has been mentioned above, it is quite possible that considerable crystal energies still exist, though positive and negative values cancel out for the whole disc, or that a uniaxial energy is superimposed on the cubic domains, with random distribution of the preferred axis and where $K_4 = \frac{8}{3}K_4'$, but if it is assumed that K_4 is really zero throughout the disc we have a convenient means of testing various theories of the coercive force.

According to Néel (1946), if the crystal energy is small the coercive force is given by

$$H_c = \frac{0{\cdot}69vC}{J_s}[1{\cdot}386 + \ln(6{\cdot}8J_s^2/C)^{1/2}],$$

where $C = 3\lambda\sigma/2$, λ is the magnetostriction constant, σ is the mean value of internal strains, and v is the fraction of the whole volume in a state of strain. C can actually be put equal to $3E/2 = 2{\cdot}25 \times 10^5$, and, with J_s equal to 1,125, the value obtained for H_c is $440v$. Thus the experimental value of $H_c = 80$ requires the not unreasonable value of 0·18 for v.

To test whether the single domain theory of Stoner and Wohlfarth (1948) is also capable of accounting for this coercivity we again use the measured value of the reversible energy E, which is about $1{\cdot}5 \times 10^5$. To account for this by a random assembly of single domain 'ellipsoids', each having an energy distribution $F\sin^2\theta$, we put, by averaging over all directions, $E = \frac{2}{3}F$, giving $F = 2{\cdot}25 \times 10^5$. The corresponding coercive force is $H_c = 0{\cdot}96F/J_s$, and, again with J_s equal to 1,125, $H_c = 192$ oersted. Probably not all the energy E should be attributed to

single domain particles since E is not zero parallel to the preferred direction, when no contribution from such particles is expected. It is still, however, impossible to make a final choice between the single domain theory and the strain theory of the coercive force.

The coercive force after different treatments increases with decreasing cooling speed and a further increase results from tempering; Figure 2 shows that the relation between H_c and K_4 is approximately linear. Such a linear relation may arise either from Néel's theory of coercive force due to heterogeneity, or from Stoner and Wolhfarth's theory of single domain particles if, as explained below, the change in K_4 is really due to a change in the uniaxial distortion of these particles.

Two possible schemes for the production of magnetic anisotropy can be proposed. Firstly, in what we may call the 'orientation theory', it is supposed that in each domain, even when no field has been applied during cooling, one of the three cube edge directions is strongly preferred, the choice varying at random throughout the alloy, and even in different domains of a single crystal. Formally such a scheme is equivalent to the hypothesis of tetragonal crystal symmetry. A field applied during cooling merely orientates the existing preferred directions.

In the second theory, which, for convenience, we shall call the 'formation theory', the magnetic anisotropy in the material cooled without a field is of truly cubic symmetry. The uniaxial anisotropy is created, and not merely orientated by the field.

Either of the above theories can be accepted without prejudice to the question of the actual mechanism, such as magneto-elastic deformation or heterogeneous precipitation, which has been proposed as being responsible for the uniaxial energy term.

On the basis of the orientation theory the steep variation of the constant of apparent cubic anisotropy with cooling speed and the linear dependence of the coercive force on that constant in the specimens cooled without a field can easily be explained. Suppose that as the alloy cools through the Curie point range a preferred orientation is developed along a cube edge in each domain, but the distribution of the preferred axis is at random. Slower cooling will allow more time for any process developing this tetragonality, and hence K_2' and K_4' may become larger the slower the cooling speed. This, as can be seen from (5), would result in a more negative constant $K_4 - \frac{9}{8}K_4'$ of the apparent cubic crystal anisotropy. An increase in coercivity with increasing $K_2' + K_4'$ would be expected. Assuming K_4 to be constant, K_4' could be evaluated from the torque experiments, but we have not sufficient experiments for alloys cooled at various speeds in a field to evaluate $K_2' + K_4'$. Experiments on these lines are in progress, but a completely rigorous test of this theory appears to require measurements of the individual values of K_4, K_2' and K_4' on single crystals.

The formation theory would require completely random residual stresses or heterogeneous precipitates to account for the values of H_c and E, and the calculations made above show that these values can be explained without improbable arbitrary assumptions. So rapid a variation of the constant of truly cubic crystal anisotropy is somewhat surprising, but not enough is known about the origin of magneto-crystalline forces to discuss this question of the theory.

On the basis of the orientation theory the ratio J_r/J_s of a columnar magnet cooled slowly without a field and measured along the columnar axis should be

0·33, whilst the formation theory would predict values of J_r/J_s equal to 0·58. The measured values vary from 0·59 to 0·69, which would be more nearly corresponding to the prediction of the formation theory. On the other hand, the orientation theory can account for the exceptionally low remanence of quenched specimens, provided that the further special assumption is made that the initial distribution of preferred directions favours the formation of closed rings of magnetization within the alloy. During slow cooling this system must be supposed to be destroyed by further changes. The explanation of the low remanence given by Bozorth (1947) is not applicable here, since the crystalline energy is not zero.

Next consider, from the point of view of the orientation theory, E for alloys cooled at the same speed with and without a field. With the field $E_\perp - E_\parallel$ gives the magnitude of the uniaxial anisotropy. Without the field E should have a value equal to $\frac{2}{3}(E_\perp - E_\parallel)$ plus a contribution due to whatever cause is responsible for $E_\parallel$. The latter contribution is uncertain, but assuming it is the same in both cases we expect, in units of 10^5 erg.cm^{-3}, for experiment No. 6 a mean E of 4·4 instead of 2·5, and for No. 8 a value of 6·8 instead of the observed 4·0.

Interaction between neighbouring domains creates uncertainties in all these arguments, but the balance of evidence seems to be weighted against a pure orientation theory, although the existence of weak random uniaxial or tetragonal terms when no field is applied during cooling is not improbable.

ACKNOWLEDGMENTS

The authors are grateful to Professor E. C. Stoner and Mr. B. A. Lilley for their interest and for valuable suggestions in connection with the energy and torque expressions for tetragonal crystals, and they thank the Permanent Magnet Association for permission to publish this paper.

REFERENCES

Bozorth, R. M., 1947, *Z. Phys.*, **124,** 519.
Hoselitz, K., 1950, *Research*, **3,** 77.
Hoselitz, K., and McCaig, M., 1949, *Nature, Lond.*, **164,** 581.
McCaig, M., 1949, *Proc. Phys. Soc.* B, **62,** 652.
Néel, L., 1945, *C. R. Acad. Sci., Paris*, **220,** 814; 1946, *Annales de l'Université de Grenoble*, **22,** 299; 1948, *J. Phys. Radium*, **9,** 193.
Nesbitt, E. A., 1950, *J. Appl. Phys.*, **21,** 879.
Stoner, E. C., and Wohlfarth, E. P., 1948, *Phil. Trans. Roy. Soc.* A, **240,** 599.
Williams, H. J., 1937, *Rev. Sci. Instrum.*, **8,** 56.

High-Frequency Discharges: I
Breakdown Mechanism and Similarity Relationship

By F. LLEWELLYN JONES and G. D. MORGAN*
Department of Physics, University College of Swansea

MS. received 14*th November* 1950

ABSTRACT. High-frequency breakdown between wires and coaxial cylinders in air and in hydrogen was investigated over the range of frequencies f from 3·5 Mc/s. to 70 Mc/s. at pressures below 20 mm. Hg. It was found that geometrically similar systems broke down at the same potential provided that both parameters ap and f/p were invariant, a being a linear dimension. Under conditions such that the total amplitude of oscillation of the electron cloud was smaller than the electrode interspace, the electric field at the wire was the controlling factor, and breakdown was found to be independent of the nature of the surface of the cylinder. Consequently, secondary ionization processes did not appear to play an important part as in the case of static discharges. The experiments were in agreement with the view that the high-frequency discharge in air and in hydrogen is determined by primary ionization in the gas and loss of electrons to the walls by diffusion only, provided the electron mean free path is small compared with the linear dimension of the discharge tube, and the collision frequency is very much greater than the oscillation frequency. The significance of the similarity relation is briefly discussed.

§1. SIMILARITY AND HIGH-FREQUENCY DISCHARGES

The original observation of Paschen that the sparking potential V_s in uniform fields is a function only of the number of molecular free paths along the discharge was shown by Townsend (1915) to be part of a general similarity theorem, which applied equally to breakdown in non-uniform fields dependent on ionization by collision. This theorem was later extended by Holm (1924) to include the case when the potentials were determined by space charges as well as by charges on the electrodes, i.e. for the case of finite maintained currents. The similarity principle for static fields has been fully discussed by von Engel and Steenbeck (1934) in relation to the various fundamental collision processes. Under static fields, the application of the similarity principle leads to specific relationships between electron and ion concentrations in one system and those in a similar system, and also between the rates of generation. For example,

$$N_1=(1/k^2)N_2 \quad \text{and} \quad dN_1/dt=(1/k^3)\,dN_2/dt, \qquad \ldots\ldots(1)$$

where N is the concentration and the suffixes apply to the two discharge systems I and II of linear dimensions in the ratio k, and gas pressures p in the ratio $1/k$. These general results are a consequence of the specific nature of breakdown under static conditions, in which the general Townsend relation (Huxley and Bruce 1937)

$$\gamma\left(\exp\int_0^d \alpha\,dx-1\right)=1$$

expresses the fact that the primary, α, and secondary, γ, processes together just replace each electron swept away by the field along a path d. For high-frequency breakdown no such specific criterion is known, but it is generally assumed that

* Now at University College of North Wales, Bangor; formerly Fellow of the University of Wales.

on breakdown the rate of generation of electrons just exceeds the rate of loss. It is convenient to classify H.F. discharges in terms of the parameter f/p, f being the oscillation frequency of the applied electric force. When f exceeds the electron collision frequency $f_c = u/l$, u being the mean electron speed and l its mean free path, the electron suffers a small superimposed oscillatory motion between collisions. Since $u \sim 10^8$ cm/sec. and $l \sim 10^{-2}$ cm. at a pressure of 1 mm. Hg for most gases, then $u/l \sim 10^{10}$ collisions/second, and the assumption of freely oscillating electrons in the discharge involves the use either of microwaves or of very low gas pressures. Thus for frequencies less than 100 Mc/s., and gas pressures greater than 0·1 mm. Hg, more than about 50 electron collisions can take place during half a period when the electric field is in the same direction. Consequently, there are certain analogous features of H.F. and D.C. discharges.

Within certain limits, the r.m.s. high-frequency field in an H.F. discharge is approximately equal to the static field in the corresponding D.C. discharge (Llewellyn Jones 1931, Townsend 1932), and this indicates that the mean electron energies are approximately the same in the two types of discharge under corresponding conditions. Again, the variation of spectral line intensities with changes in the mean energy is the same for both H.F. and D.C. discharges (Townsend and Llewellyn Jones 1931 a, b), and this indicates that the electron energy distribution function is the same for uniform glows in both kinds of discharges within limits. Townsend (1928) applied the same theory of the maintenance of uniform glows to both H.F. and D.C. discharges, in which he regarded the generation of electrons by ionization by collision as balancing the loss due only to diffusion; in the case of finite discharge currents, however, the positive space charge in the gas sets up ambi-polar diffusion. It is thus reasonable to consider that when $f < f_c$ breakdown in H.F. fields occurs in the neighbourhood of the condition when the rate of ionization just balances loss by diffusion, and that the space charge is negligible. Very little generality is lost at this stage in neglecting processes of attachment and recombination. The mean electron energy builds up until the mean rate of loss in inelastic and elastic collisions is balanced by the mean gain from the field, and this determines approximately the form of the distribution function as is the case under weak uniform fields. Herlin and Brown (1948) have applied this view to their calculation of the H.F. ionization coefficient; and it is significant that they found a rapid fall in this coefficient corresponding to the condition $f_c = f$.

The form of the electron energy distribution function under H.F. fields has been investigated theoretically by Margenau (1948), and the function has been applied by Hartman (1948) to estimate the electron concentration in a gas in an infinite space for various values of the field, on the assumption (not applicable to finite discharge tubes) that the only process removing electrons is recombination. When the field attained values comparable with, though smaller than, the observed breakdown field, the function indicated a large increase in the electron concentration. Margenau's distribution function remains unchanged (i.e. u is constant) when the parameters X/p and f/p remain constant, where X is the electrostatic intensity. The first condition is equivalent to Paschen's law for static breakdown.

Consider, for example, high-frequency breakdown between a wire and a coaxial cylinder. When $f < f_c$ the mechanism of electron generation is an α-process in the gas only, and as this occurs in the region of greatest field near

the wire, ionization is controlled by the field X_s there. The mechanism of loss of electrons is, however, due to two factors: (i) diffusion down the concentration gradient from wire to cylinder; and (ii) drift along the electrical gradient from wire to cylinder.

The diffusion flow along the concentration gradient is governed by the factor $K\,dn/dz$, where $K=lu/3$; this therefore depends upon the product ap, where a is a linear dimension such as the radius of the wire, and upon the factor X/p and n. The loss due to the drift motion of the electron cloud depends on the electron mobility, which is a function of X/p (since u depends on X/p).

Under conditions when H.F. breakdown involves only the two processes of ionization by collision by electrons and electron diffusion and drift, the similarity principle can be expressed by the relation

$$V_s=\phi(ap, f/p), \qquad \ldots\ldots(2)$$

which can also be written as $$aX_s=\phi_1(ap, f/p), \qquad \ldots\ldots(2a)$$

since $aX_s=V_s/\ln(b/a)$, and b/a is constant for geometrically similar electrode systems. That this result is quite general, and does not depend upon the form of the distribution function, can be seen from the following simple considerations. The effects of collisional processes in general are dependent upon (i) the energies of the colliding particles, (ii) the form of the scattering, and (iii) the collision frequency. For electrons in elastic collisions with atoms of an ideal gas, scattering is uniform, so that all directions of motion after collision are equally probable. Consequently, the direction of the electric field is of no significance in this action. In a gas of given pressure and composition the number of electrons produced per unit volume per unit time must depend on the number n of electrons per unit volume and on their velocity distribution; and since for a given velocity distribution it is evidently proportional to n it may be written as $nF(u)/l$. Thus at corresponding points in two similar discharge systems the ratio of the two rates of generation is the ratio of the two values of $NF(U)/l$ or of $NpF(U)$, where N is the electron concentration at some specific region, say at the surface in the gas, bounding the region of ionization, and the mean electron velocity of agitation there.

Hence, the rates of generation in similar volumes in the two systems I and II are in the ratio

$$a_1^3(N_1p_1)/(N_2p_2)a_2^3=k^2(N_1/N_2). \qquad \ldots\ldots(3)$$

Since u is the same at corresponding points in the two systems, the result also holds when the cross section varies with the velocity. Under oscillatory fields, the actual path traversed by an electron and the gain of energy from the field, are not determined only by the concentration p of gas atoms, as in the case when the electron drift is uni-directional under static fields; after scattering, the actual path of an electron and the energy gained depend on the frequency of oscillation of the field. The free paths in similar discharges must be such that the electron displacements due to the field are similar in every respect and the energy gain per free path equal. For electrons scattered at the same velocities in the two systems this is only the case if X is constant and if $T(=1/f)$ is proportional to the time of flight $(=l/u)$, i.e. if $f/p=$ constant. In other words, the 'unit of time' in similar high-frequency discharges is the time of flight of the electrons between successive collisions. Under these conditions the velocities at corresponding points, and

therefore α/p and the drift velocity are the same in both systems, as is the case for static fields. Consequently, the similarity conditions become $a_1 = ka_2$, $p_1 = p_2/k$, $f_1/p_1 = f_2/p_2$, and these conditions make V_1 equal to V_2, independently of the form of the distribution function.

It is pertinent to note an important aspect of high-frequency discharges. When there is no external ionization, recombination, or attachment, electron generation is due to ionization by electron collision, and the only loss is due to diffusion. This conclusion is modified under conditions when the oscillation frequency is so low, or the linear dimensions so small in relation to the gas pressure, that the electron cloud is swept as far as the walls by the electric field during each oscillation. High-frequency breakdown represents, therefore, very simple conditions, provided the gas pressure is not so low that wall effects are introduced (Gill and von Engel 1949).

In two similar systems, the rates of loss r_1 and r_2 due to diffusion alone through corresponding areas A_1 and A_2 are in the ratio

$$(A_1 l_1 U_1 \, dN_1/dx_1)/(A_2 l_2 U_2 \, dN_2/dx_2) = (a_1^2 N_1/a_1 p_1)/(a_2^2 N_2/a_2 p_2),$$

that is

$$r_1/r_2 = k^2(N_1/N_2), \qquad \ldots\ldots(4)$$

when the similarity conditions hold so that $a_1 = ka_2$ and $p_1 = p_2/k$. It will be noted that this is the same as the ratio of the rates of ionization given in (3), so that no relation between N_1 and N_2 can be obtained by equating expressions (3) and (4).

The following sections of this paper describe an experimental investigation of the similarity relationships for high-frequency breakdown in air and hydrogen under non-uniform fields (which are most suitable for testing such relationships) over a range of oscillation frequencies from 3·5 to 70 Mc/s. at gas pressures from 0·1 to 20 mm. Hg.

§ 2. APPARATUS

Discharge Tubes

The experiments were carried out using three discharge tubes of the same general design: each tube had nickel electrodes in the form of a coaxial rod and cylinder. The cylinders, 9·5 cm. long, were supported on quartz rods and the whole formed a sliding fit into hard glass envelopes. The inner rod electrode was 22 cm. long, and was supported centrally by mica discs which fitted the envelope tightly, and at one end by a tungsten rod sealed through the end of the envelope. In order to prevent premature breakdown due to corona discharges at sharp points, the edges of the outer cylinders were bevelled, and the ends of the rod electrodes were fitted with metal balls. The diameters ($2a$) of the inner rod electrodes of the three tubes A, B and C were: 0·159, 0·318 and 0·160 cm. respectively and the internal diameters ($2b$) of the outer cylinders 3·945, 3·950 and 2·080 cm. respectively.

Tubes B and C were exactly similar with dimensions in the ratio 2:1. The design of the three tubes was such that both similarity relationships and also the discharge mechanism could be investigated. The tubes were connected to a common vapour trap and the gas system was of hard glass. Mercury vapour was completely excluded from the system. The pumping system consisted of an oil diffusion pump backed by a rotary pump. The hydrogen was generated by electrolysing a saturated solution of recrystallized barium hydroxide using nickel electrodes, and stored over phosphorus pentoxide. The gas pressure in the

discharge tubes was measured by means of a manometer containing Apiezon oil freed from dissolved gases. The error in the measurement of pressure amounted to about 1% at a pressure of 2 mm. Hg (31·2 mm. of oil) and was proportionately less at higher pressures.

The high-frequency potential was applied to the discharge tubes from a resonant circuit loosely coupled to a push-pull oscillator. This ensured almost complete freedom from harmonic frequencies generated in the oscillator, and it was also advantageous for determining the onset and extinction potentials of the discharge.

The high-frequency potentials were measured by means of a small diode rectifier (type VR 78) valve voltmeter (Figure 1). The diode valve and the

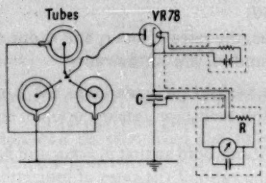

Figure 1. H.F. voltmeter.

reservoir condenser C of 1,000 pF. were fixed centrally between the three discharge tubes with one side connected permanently to each of the outer cylindrical electrodes and earthed. All leads were kept as small as possible, and the apparatus appropriately screened. The rectified voltage across the condenser was measured with a microammeter in series with a high stability resistor R of about 5 megohms: an H.F. by-pass condenser (1,000 pF.) was connected across the meter. The instrument was calibrated at a frequency of 50 c/s. by comparison with a sub-standard dynamometer instrument; the relationship between the applied potential and microammeter current was found to be linear. The errors associated with the voltmeter were estimated to be about 4% at 70 Mc/s. and less than 2% below 50 Mc/s., at the discharge tube electrodes. Measurements of frequency were made using crystal-calibrated wavemeters giving calibration points at 1 Mc/s. intervals throughout the range used. The frequencies at which measurements were made were chosen to be harmonics of 1 Mc/s. so as to obviate interpolation. The relative accuracy of similar settings of the generator frequency made at different times was estimated to be within 0·02% at 5 Mc/s. and closer at higher frequencies. For comparison, data for static breakdown were also obtained.

§ 3. EXPERIMENTAL PROCEDURE

In the present work, the applied voltage was approximately controlled by varying the coupling between the tube resonant circuit and the generator, and fine adjustment was obtained by varying the H.T. supply to the generator; experiments showed that variation of the H.T. supply had no perceptible effect on the generator frequency. When breakdown occurred (as indicated by the appearance of a glow), the potential across the tube decreased suddenly, due to the discharge loading the circuit, and the change was clearly indicated in the valve voltmeter. The maximum voltage attained was taken as the *breakdown potential* V_s.

Some preliminary measurements of breakdown potentials, both H.F. and static, were carried out, using first air, then hydrogen. The first series of measurements with hydrogen was made with the electrodes in the oxidized state caused by exposure to air and heat during construction. After these measurements, the electrodes were de-oxidized, and, together with the glass envelope, degassed, and a second series of measurements in hydrogen made. The initial de-oxidation was made by prolonged heating at 300° C. in an electric furnace surrounding the tubes which contained hydrogen at a pressure of a few millimetres of mercury; the tubes were then evacuated, and the heating continued with the pumps running in order to degas the envelopes and electrodes. Finally, further de-oxidation, to remove any oxide which might have been formed by the evolution of oxygen during the degassing, was accomplished by admitting fresh hydrogen and bombarding the electrodes with positive ions in a hydrogen discharge. This latter treatment was severe and caused sputtering, but it was an efficient method of obtaining a clean metallic surface.

The procedure adopted ensured that about 5 minutes elapsed between consecutive discharges in any one tube, as preliminary measurements had shown in the case of static discharges that the sparking potential was determined to some extent by the interval between successive discharges when this was less than about 1 minute.

§ 4. EXPERIMENTAL RESULTS—MECHANISM OF LOSS

Typical (V_s, p) curves for the two tubes A and B, at frequencies from 5 to 70 Mc/s. are shown for air in Figures 2 and 3, and for hydrogen in Figures 4 and 5. The results for tube C are given in terms of the parameter ap in Figures 6 and 7 which also contain results for tube B for comparison. The general shape of

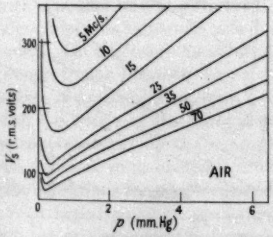

Figure 2. Breakdown potentials for tube A.

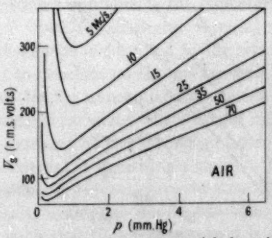

Figure 3. Breakdown potentials for tube B.

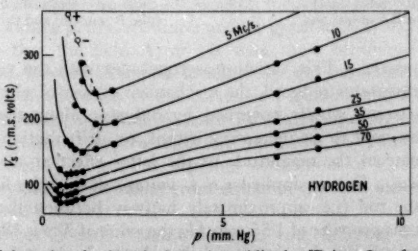

Figure 4. Breakdown in tube A with electrodes oxidized. [Points ●—after de-oxidation.]

the (V_s, p) curves for a radial field is the same as that for H.F. sparking potentials in uniform fields (Rohde 1932). For a given frequency the (V_s, p) curve is concave upwards and exhibits a single minimum at the point (V_{sm}, p_{sm}); as the frequency is increased V_{sm} and p_{sm} decrease. On the other hand, the curves for the lowest frequencies have the same general features except that the value of p_{sm} decreases as the frequency decreases, and tends towards the values for D.C. discharges (points + and − in Figure 4).

Consideration of these curves provides information concerning the discharge mechanism. The variation of the minimum V_s (indicated by the broken line in Figure 4) shows the turning point between the values for high and low frequencies to be at approximately 190 volts and 1·55 mm. Hg pressure, i.e. about the minimum

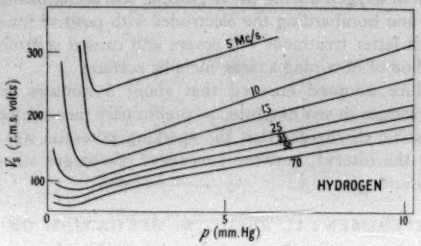

Figure 5. Breakdown in tube B.

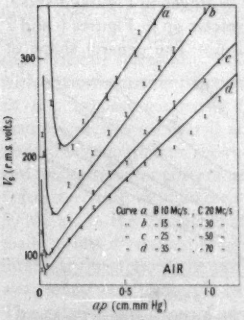

Figure 6. Similarity relationships in air with tube B (curves) and tube C (I).

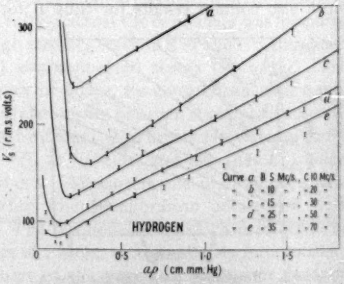

Figure 7. Similarity relationships for hydrogen with tube B (curves) and tube C (I).

of the 10 Mc/s. curve. This variation is consistent with the view that, as the frequency (or pressure) is reduced, the mechanism of loss of electrons from the discharge space is not wholly governed by diffusion along the concentration gradient, but also, and to an increasing extent, by drift motion in the electric field. An estimate of the magnitude of the latter effect at the turning point supports this view. For an applied r.m.s. voltage of 190 the field at a radius of 1 cm. from the rod (i.e. approximately halfway between the electrodes) is 59 v/cm. For a gas pressure of 1·55 mm. Hg the value of X/p is 38 v/cm. mm. Hg, and for this value of X/p the electron drift velocity is about $1{\cdot}5 \times 10^7$ cm/sec.

Hence, the time required for the electrons to pass from the rod to the cylinder is of the same order as the half-period of the field. Under these conditions a large fraction of the electrons generated during one half-cycle may be lost during the same half-cycle by being swept into the electrodes, which is similar to the loss mechanism for D.C. discharges. At even lower frequencies (<1 Mc/s.) the positive ion loss would increase for a similar reason, and the mechanism of the discharge would then be the same as in the D.C. case but with the electrode polarities being alternated.

A similar conclusion follows from rather different considerations. It is well known (Townsend 1915, Huxley and Bruce 1937) that under certain conditions the corona breakdown potential under static fields with a given wire of radius a varies with the cylinder diameter b in such a way as to maintain the field X_s at the wire constant. Thus if V_s and p are known for any given wire, V_s can be calculated for any other cylinder radius, provided that $b>c$, where c is the radius of the small cylindrical volume, coaxial with the wire, within which the discharge is confined. The controlling factor is then the field X_s, at the wire where the electron production occurs, where

$$X_s = V_s/\{a \ln (b/a)\}. \qquad \ldots\ldots(5)$$

Thus, the sparking potentials V_1 and V_2 corresponding to different cylinder radii b_1 and b_2 and the same wire diameter a are given by the relation

$$V_1/V_2 = \ln (b_1/a)/\ln (b_2/a). \qquad \ldots\ldots(6)$$

Neglecting attachment and recombination, in static discharges two mechanisms of electron loss—diffusion along concentration gradient and current drift down the electric field—are always occurring, but the loss due to drift is usually much greater than that due to diffusion. The cylinder only affects the concentration gradient, and this influence only takes place when the discharge extends to the cylinder. On the other hand, when the discharge is confined to the wire, the ion concentration between the cylinder and the surface on the gas bounding the discharge is practically constant (Townsend 1915); consequently, provided the field at the wire and the current are maintained constant, the cylinder has, on this view, no effect on the concentration gradient at the discharge boundary: this is the more so at breakdown when the current is vanishingly small. These are the conditions for which equation (6) holds.

With high-frequency discharges precisely analogous conditions also hold. When the pressure and the frequency are such that the electron cloud is swept to the cylinder during one half-oscillation, then that electrode increases the electron loss. Hence it follows that a greater generation is required to produce breakdown, so that the field X_s at the wire must be increased. The three tubes A, B and C were designed to show up the influence of these various mechanisms. Consideration of the curves in Figures 2 and 3, 4 and 5, shows under what conditions equation (6) holds for high-frequency corona breakdown in air and hydrogen. Typical data are tabulated in Table 1, which gives observed values of V_s for tube A, together with values of V_s for tube C (same wire, smaller cylinder) calculated from equation (2), and also the values of V_s actually measured with that tube.

With the tubes A and C (same diameter rod, different diameter cylinder) we find that (6) holds for the higher frequencies. At the highest frequency

of 70 Mc/s. and for pressures 3·0 mm. Hg, the discharge was confined to the wire, so that the only loss mechanism was that of electron diffusion from the outer surface in the gas bounding the discharge. For lower frequencies, or for lower pressures, on the other hand, equation (6) did not hold, since tube C broke down when X_s was greater than the value required by tube A (larger cylinder), at the same pressure; typical results are those for air at 20 Mc/s., also given in Table 1. This result indicated the influence of an additional loss mechanism, when the discharge extended to the cylinder; i.e. the oscillations of the electron cloud filled the electrode interspace.

Table 1. The Corona Relationship at High Frequency

Hydrogen, 70 Mc/s.

p (mm. Hg)	16·4	13·8	9·4	5·5	3·7	1·7
V_s (tube A, obs.)	212	194	169	140	122	90
V_s (tube C, calc.)*	169	155	135	112	97	72
V_s (tube C, obs.)*	171	156	137	113	99	78

* These figures show that equation (6) holds nearly down to 3·7 mm. Hg pressure.

Hydrogen, 15 Mc/s.

p (mm. Hg)	13·8	10·6	8·9	7·5	5·7	4·2
V_s (tube A, obs.)	342	302	280	257	226	202
V_s (tube C, calc.)*	272	240	223	205	180	161
V_s (tube C, obs.)*	270	246	228	210	195	187

* Owing to the reduced frequency, divergence is now apparent at pressures higher than 3·7 mm. Hg.

Air, 70 Mc/s.

p (mm. Hg)	6·5	5·2	4·0	3·0	2·2	1·15
V_s (tube A, obs.)	218	196	167	147	128	101
V_s (tube C, calc.)*	174	157	134	118	102	81
V_s (tube C, obs.)*	177	161	150	129	119	108

Air, 20 Mc/s.

p (mm. Hg)	5·84	5·06	4·00	2·5	1·5
V_s (tube A, obs.)	337	308	269	212	175
V_s (tube C, calc.)*	270	246	215	170	140
V_s (tube C, obs.)*	285	265	245	212	214

* The corona relation (6) does not hold so well for air as for hydrogen, the divergence being somewhat larger with reduction of frequency and pressure.

This is all in accordance with the principles discussed above. The drift amplitude of the electron cloud is greater at lower frequencies; hence at lower frequencies the loss by drift in the field is the main loss, and this is very dependent upon the position of the cylinder wall. The loss is greater for the smaller cylinder, hence X_s must be greater for that tube to break down. The fact that equation (6) was found to hold much better for hydrogen than for air can be accounted for by the higher electron drift velocity in air for these values of X/p.

The effect on V_s, X_s and aX_s of varying the diameter of the outer cylinder, but keeping the rod diameter constant, is seen by comparing the values for tubes A and C in Table 1 and also in Table 3. Reducing the size of the cylinder

from 4 cm. in tube A to 2 cm. in tube C *decreases* V but *increases* the field X_s at the rod. Thus, for this range of pressures and frequencies, the breakdown field at the rod, for a fixed frequency and gas pressure, is not determined solely by the radius of the rod, but is also dependent upon the size of the cylinder.

For corona discharges from isolated wires, or when the cylinder is remote so that the discharge is determined only by the field at the wire, equation (6) shows that it is possible to calculate the breakdown field for any diameter wire, from the data obtained with the present tubes.

The variation of the sparking potential with the field frequency for fixed values of the gas pressure is shown in Figure 8, which refers to tube A. It is seen

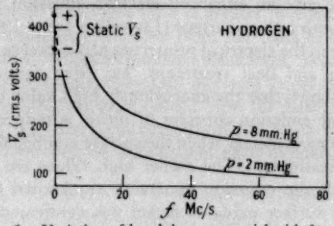

Figure 8. Variation of breakdown potential with frequency.

that as the frequency is increased from zero the diminution of V_s is rapid at first and then much less. For the higher frequencies the value of V_s tends to a constant value, and in all probability rises again at still higher frequencies, as shown by the experiments of Hale (1948) for conditions such that the field frequency was greater than the collisional frequency of the electrons.

Experiments were also carried out to show the influence, if any, of processes of electron production other than the α-process in the gas.

It is well known that for static sparking at low pressure the breakdown potential depends on the nature of the cathode surface (Llewellyn Jones and Henderson 1939). If the oscillation frequency of an applied E.M.F. is so low that an electron avalanche or the positive ions can cross the tube and strike the walls or an electrode during a half-cycle, then it is to be expected that the discharge will depend upon those surfaces. For higher frequencies, on the other hand, motion of positive ions can be ignored, and ionization becomes merely a gas process; under these conditions the nature of the wall or electrode surface has little effect on the sparking potential. These conclusions were first tested with the present tubes by using the electrodes first in an oxidized state and then in a de-oxidized state, after severe heat treatment and positive ion bombardment in a hydrogen discharge, as the electron emission properties, whether due to impact of positive ions or of radiation, would be very different in the two cases.

Consider the minimum sparking potential for static discharges in hydrogen when the rod electrodes were cathodes, given in Table 2.

Table 2

	Rod cathode		Cylinder cathode	
	Oxidized	Clean	Oxidized	Clean
Tube A	324 v.	275 v.	368 v.	360 v.
Tube B	335 v.	283 v.	359 v.	356 v.

It is seen that when the rods were cathodes the effect of oxidation was to increase the minimum sparking potential by about 17%, but in the case where the rod electrodes were anodes the values of the minimum sparking potential were found to be the same to about 2% before and after oxidation.

This reduction of sparking potential on de-oxidation when the rods were cathodes can be explained on the assumption that a surface film of electro-negative oxygen atoms was removed and replaced by electro-positive hydrogen. Thus the effective work function of the electrode surface was reduced (de Boer 1935) and the sparking potential decreased. It should be noted that here we are dealing with surface oxide films of molecular thicknesses, and not thick oxide layers which are known to give an enhanced electron emission and a lower sparking potential than that with a clean surface (Llewellyn Jones 1949).

A similar change in the electrical properties of a nickel surface, when subjected to severe degassing and heat treatment, has been found by other workers. Wahlin (1942) has shown that the anomalously high value of about 1,400 for the Dushman thermionic emission constant of nickel is reduced to a value of from 30 to 70, as found for most metals, when the surface is subjected to severe degassing and rigorous heat treatment. The earlier high values are accredited to surface impurities, to which the emission constants are known to be very sensitive. The stability of the surface oxide of nickel was confirmed by the constancy of the values of the minimum sparking potential when the outer cylinders were cathodes. In these cases the values of the minimum sparking potential before and after de-oxidation were the same within 2%, showing that the de-oxidation treatment of the cylinders was not completely effective. Although the cylinder surfaces were subjected to the initial de-oxidation process of prolonged heating at 300° c., the second and more severe treatment of bombardment by high energy protons did not take place at these surfaces, since the electric field strength there was so small that the positive ions merely drifted to the surface which consequently did not undergo severe bombardment. Hence the static measurements showed that the electrical properties of the rod electrodes were altered by the de-oxidation process, and that the static discharge was sensitive to those changes.

Measurements of breakdown potentials in hydrogen in high-frequency fields were made both before and after the electrodes had been degassed and de-oxidized. The results are given in Figure 4 by the continuous (V_s, p) curves for selected frequencies: these curves are drawn through the plotted measured values obtained using tube A with the electrodes oxidized. The values obtained after de-oxidation are shown by the circles, and it is seen that they lie along the smooth curves. These results are typical. It is therefore concluded that the nature of the electrode surface played a negligible part in breakdown in high-frequency fields when the electron mean free path was much smaller than the radius of the cylinder, and when the oscillation frequency was such that electrons could not travel across the tube during one half-cycle.

The fact that the H.F. breakdown potentials were found to be independent of the nature of the electrode surface was consistent with the general theory and also with the measurements of Herlin and Brown (1948) on breakdown in microwave fields. Their measurements confirm their theoretical values of breakdown potential which were made on the assumption of the negligible emission of electrons from surfaces enclosing the discharge space. They

assumed that breakdown was dependent upon electron generation by the collisional process under the influence of the field and electron loss by diffusion to the walls followed by recombination there. Breakdown was considered to occur when the rate of generation of electrons was just sufficient to replace the loss: if other processes of generation occurred, such as emission from the walls or electrodes, then that effect would be magnified by multiplication in the field.

Comparison of the experimental results for high-frequency and static discharges show that high-frequency discharges differ from the static type in that secondary ionization effects at the electrodes are not essential. It should, however, be noted that under some conditions, notably when the gas pressure is so low that the electron mean free path is greater than the linear dimension of the discharge space, secondary emission from the walls or electrodes is a major factor in the process. High-frequency discharges occurring under these conditions have been investigated by Gill and von Engel (1949). In this case electrons may gain sufficient energy (about 90 v. for glass) during a half-period of the field to cause secondary emission from the walls which is the electron generation process controlling the subsequent glow discharge in the gas.

§ 5. SIMILARITY RELATIONSHIPS

Consider, for example, certain specific values (r.m.s.) of V_s for hydrogen in the three tubes, for different values of the parameter ap, where a is the radius of the rod in centimetres, and p the gas pressure in millimetres of mercury at an oscillation frequency of 50 Mc/s. These are given in Table 3.

Table 3

	Frequency 50 Mc/s.						Frequency 25 Mc/s.	
	Tube A		Tube B		Tube C		Tube B	
ap	V_s	aX_s	V_s	aX_s	V_s	aX_s	V_s	aX_s
1·61	268	83·5	189	75	215	84	220	87
1·10	220	68·4	155	61·5	184	71·6	180	71·5
0·75	187	58·3	131	52	152	59·4	154	61
0·44	155	48·2	108	43	132	51·3	130	51·5
0·17	112	34·8	80	32	99	38·6	102	40·3

Comparison of the figures at 50 Mc/s. for the two geometrically similar tubes B and C shows that, for each value of ap, the breakdown potential is about 20% greater for tube C. Further, the values of the parameter aX_s at the rods for these tubes show a difference of about the same magnitude. Thus the discharge characteristics, at this particular frequency, are not in accordance with the static similarity relationship.

For oscillating fields, however, there are theoretical reasons given in § 1 why the parameter f/p as well as ap should be taken into account. Thus, for the same value of ap, the breakdown potentials for tube C at 50 Mc/s. at any pressure p should be compared with those for the geometrically similar tube B at pressure $p/2$, not at 50 Mc/s. but at 25 Mc/s. in order to maintain f/p the same. These values are also given in Table 3, from which it can be seen that the sets of values of V_s show good agreement to within the 3% spread of the measured values. The same result holds for any other pair of frequencies in the range 5 to 70 Mc/s.

The complete data for various pairs of frequencies are best expressed graphically in the general (V_s, ap) diagram for hydrogen for these frequencies (Figure 7). The continuous curves refer to tube B and the values indicated

by the symbol I to the measurements for tube C. The extent of the I indicates the spread of the measured values. It is seen that, in general, the plotted values for tube C coincide with the curves for tube B. The poorest agreement is for the highest and lowest values of ap relating to the highest frequencies (70 Mc/s. and 35 Mc/s.), in which case the difference in the values of aX_s for the two tubes is in some cases as high as 5%, due to the increasing inaccuracy of voltage measurement with increasing frequency. Similar conclusions follow from a consideration of the curves in Figure 6 for air. The results therefore confirm the similarity relations (2) and (2a) for H.F. breakdown.

It is now interesting to see how this similarity relationship applied in the case of tubes which were not geometrically similar. The tubes A and B were not geometrically similar because the rod (the more important electrode) of B was twice the diameter of that of A, while the cylinders had the same diameter. aX_s was plotted as a function of ap for various values of f for these two tubes, and typical results are given in Figure 9 for the pairs of frequencies 5–10 Mc/s.,

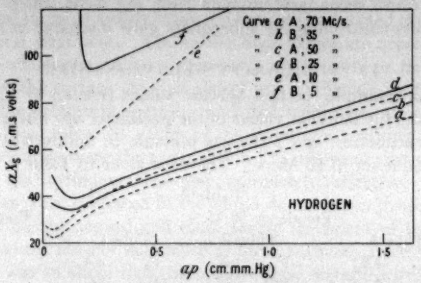

Figure 9. Influence of geometrical dissimilarity.

25–50 Mc/s., and 35–70 Mc/s. If the similarity relationship still held in this case even though the tubes were not exactly similar, the pair of curves a and b should coalesce, and the pairs (c and d) and (e and f) should also coalesce. On the contrary, it will be seen that the relation of aX_s to ap and to f/p was sensitive to departures from geometrical similarity even when it was the cylinder (the less important electrode) which was concerned.

The results show the strong dependence of aX_s on the parameters ap and f/p, and these experiments thus confirm the general theory of the high-frequency discharge outlined in § 1. A consequence of this result, which is of practical interest in high-frequency engineering, is that it is now possible to calculate from the data of Figures 2 and 4 the breakdown potentials in air and in hydrogen for similar coaxial electrode systems at other gas pressures and oscillation frequencies. It should be noted that this result holds whether the discharge extends to the cylinder or not: it thus differs from that of the previous section which was only valid when the discharge was confined to the wire.

§ 6. CONCLUSIONS

1. For geometrically similar electrode systems the breakdown potential is the same, provided both the parameters ap and f/p are invariant. Consequently, breakdown potentials can now be calculated for similar coaxial electrode systems for all other pressures and oscillation frequencies within the limits discussed.

2. For pressures and frequencies such that the discharge does not extend to the cylinder, breakdown is independent of the nature of the cylinder surface. Under these conditions secondary ionization processes do not play as important a part as in static breakdown.

3. The static corona property, viz. when the discharge is confined to the wire the electric field there is the controlling factor, holds also for high-frequency breakdown.

4. The experiments are in general agreement with the view that the high-frequency discharge in air and hydrogen is determined by primary ionization in the gas and loss of electrons to the walls by diffusion only, provided that the electron mean free path is small compared with the linear dimension of the discharge space and that the collision frequency is greater than the oscillation frequency.

ACKNOWLEDGMENTS

We wish to thank the Council of the University of Wales for the award of a Fellowship to one of us (G. D. M.) during 1947–49 to undertake this work. We also wish to express our gratitude to Mr. G. C. Williams, of this Department, for help with the measurements and for interesting discussion.

REFERENCES

DE BOER, J. H., 1935, *Electron Emission and Adsorption Phenomena* (Cambridge : University Press), Chap. VI.

VON ENGEL, A., and STEENBECK, M., 1934, *Elektrische Gasentladungen*, Vol. II (Berlin : Springer), p. 95.

GILL, E. B. W., and VON ENGEL, A., 1949, *Proc. Roy. Soc.* A, **197**, 107.

HALE, D. H., 1948, *Phys. Rev.*, **73**, 1046.

HARTMAN, L., 1948, *Phys. Rev.*, **73**, 316.

HERLIN, M. A., and BROWN, S. C., 1948, *Phys. Rev.*, **74**, 291, 902.

HOLM, R., 1924, *Phys. Z.*, **25**, 497.

HUXLEY, L. G. H., and BRUCE, J. H., 1937, *Phil. Mag.*, **23**, 1096.

LLEWELLYN JONES, F., 1931, *Phil. Mag.*, **11**, 163; 1949, *Proc. Phys. Soc.* B, **62**, 366.

LLEWELLYN JONES, F., and HENDERSON, J. H., 1939, *Phil. Mag.*, **28**, 185.

MARGENAU, H., 1948, *Phys. Rev.*, **73**, 326.

ROHDE, L., 1932, *Ann. Phys., Lpz.*, **12**, 569.

TOWNSEND, J. S., 1915, *Electricity in Gases* (Oxford : Clarendon Press), Chap. X; 1928, *C.R. Acad. Sci., Paris*, **186**, 55; 1932, *Phil. Mag.*, **13**, 745.

TOWNSEND, J. S., and LLEWELLYN JONES, F., 1931 a, *Phil. Mag.*, **11**, 679; 1931 b, *Ibid.*, **12**, 815.

WAHLIN, H. B., 1942, *Phys. Rev.*, **61** 509.

High Frequency Discharges: II—Similarity Relationship for Minimum Maintenance Potentials

By F. LLEWELLYN JONES and G. D. MORGAN*
Physics Department, University College of Swansea

MS. received 14*th November* 1950

ABSTRACT. The same similarity relationship which applies to breakdown applies also to the maintenance of H.F. currents, but the dependence of the minimum maintenance potential upon the parameters ap and f/p (linear dimension a, pressure p, frequency f) is not so well defined, an effect due to discharge instability.

§1. SIMILARITY CONDITION FOR MAINTAINED HIGH-FREQUENCY CURRENTS

When a finite high-frequency current passes through a gas the resultant space charge modifies the electric intensity so that the resultant field X is determined both by the space charge and by the potentials on the electrodes. The mean electron energies in any region of the discharge are determined by the ratio X/p in that region, where p is the gas pressure, and the rate of generation of electrons at any given gas pressure is determined by X/p and by p. The space charge field modifies the electron loss by setting up ambipolar diffusion, reducing the diffusion coefficient of the electrons from $k(=lu/3)$, where l is the mean free path, to $k(W_2/W_1)$, where W_2 and W_1 are the mobilities of positive ions and electrons respectively. W_2/W_1 and u are functions of X/p, consequently, the rate of loss of electrons is determined by the factors X/p and p.

Similar maintained discharges can be defined as discharges which give the same current I at the same potential V in two systems I and II which are geometrically similar in that the linear dimensions in system I are k times those of system II, and the gas pressure in system I is $1/k$ of that in system II. It is clear, therefore, that a condition for similar discharges to occur is that the parameter X/p shall be the same in corresponding regions in the two systems. This is quite a possible condition in high-frequency discharges, and it is therefore interesting to investigate whether a similarity relationship such as $V=\phi(X/p, f/p)$, of the kind which has been established for high-frequency breakdown potentials (Llewellyn Jones and Morgan 1951, to be referred to as I) applies also to high-frequency maintenance potentials.

Measurements of the high-frequency current in a discharge offer considerable difficulty, and earlier measurements (Townsend and Donaldson 1928, Townsend and Nethercot 1929, Townsend and Llewellyn Jones 1931 a, b) have been made with oscillation frequencies of the order of 10 Mc/s. or less. The difficulty of measuring accurately oscillatory discharge currents at very much higher frequencies makes it interesting to test the validity of a similarity relationship for maintenance potentials, the measurement of which does not offer such difficulty.

When breakdown occurs the voltage V_s across the oscillatory circuit which supplies potentials to the discharge tube suddenly falls, and this is due to the loading of the circuit by the discharge. As the oscillatory power is decreased,

* Now at University College of North Wales, Bangor; formerly Fellow of the University of Wales.

the voltage across the electrodes also decreases until a certain minimum maintenance value V_m is reached. As the oscillatory power is decreased further the potential across the discharge tube then increases, until finally the extinction potential V_e is reached. As the current is decreased from the value corresponding to the minimum maintenance potential V_m the space charge is also decreased; consequently, the loss of electrons due to ambi-polar diffusion is then increased, and this loss has to be made good by increasing the rate of generation by increasing the field. When the rate of loss exceeds the rate of generation the discharge ceases. Before the question of the similarity relationship for high-frequency maintenance potentials can be investigated it is necessary first to find the relation between the various discharge maintenance potentials and the source of the E.M.F., as only those potentials which are independent of the source can be regarded as characteristic of the discharge. However, it is not clear that the difference between the minimum maintenance and extinction potentials has always been sufficiently recognized, and this is all the more important when comparing the values for the extinction potential obtained by different observers. It was necessary, therefore, to investigate this point experimentally.

§ 2. MAINTENANCE AND EXTINCTION POTENTIALS

The discharge tubes and the experimental arrangements were the same as those used in work on high-frequency breakdown in hydrogen (I). The glow discharge which was produced after breakdown was, in general, uniformly distributed along the rod within the cylinder; but at the lower field frequencies the discharge was usually localized near the centre of the cylinder, and was unstable when near extinction. The variation of the extinction potential V_e with gas pressure, for a fixed frequency, was found to be of the same general form as shown by the (V_s, p) curves. However, the values of V_e were much less than the corresponding values of V_s; e.g. for tube B (paper I) at a frequency of 70 Mc/s. and gas pressure of 7·45 mm. Hg the sparking potential was 142 volts peak, the minimum maintenance potential 80 volts and the extinction potential 90 volts. The difference between V_s and V_e was most noticeable at the lower pressures.

In the case of the higher field frequencies the minimum value of V_e was not attained, even at the lowest pressure of 0·1 mm. Hg, an effect which could be explained by the influence of the positive space charge in the gas in reducing the lateral diffusional loss of electrons. The plotted (V_e, p) points were not found to lie on a smooth curve, as in the case of the breakdown values (I). This result was considered to indicate that the extinction voltages were dependent upon the properties of the electrical circuits, and in particular upon the arbitrarily set degree of coupling between the tuned circuit and the oscillator. This point, therefore, required investigation.

The determination of the value of the source impedance for any particular combination of the various factors is complex. However, the effect of the variation of the source impedance was demonstrated by the following experiments.

(i) The coupled circuit was tuned to resonate at the oscillator frequency in the absence of a discharge. Measurements of V_s, V_m, and V_e were made with different values of carbon resistors shunted, in turn, across the coupled circuit. The values of the potentials are given for comparison in arbitrary units in Table 1 (the valve voltmeter readings are in μa.), and relate to tube B containing hydrogen at a pressure of 3·7 mm. Hg, with a field frequency of 25 Mc/s.

Table 1

Shunt (ohms)	∞	20,000	10,000	5,600
V_s (arbitrary units)	38·5	38·6	38·5	38·6
V_e (arbitrary units)	25	24·5	23·5	23·0
V_m (arbitrary units)	22·4	22·3	22·3	22·4

Thus the minimum maintenance potentials and the breakdown potentials were independent of the degree of damping of the tuned circuit. The extinction potential, however, was dependent upon the circuit impedance, and varied by about 8% under the above conditions.

(ii) Table 2 shows the results of measurements with different degrees of coupling between the oscillator and tuned circuit coils. These measurements are for 35 Mc/s. with tube B at a gas pressure of 4·6 mm. Hg of hydrogen.

Table 2

Distance apart of coils (cm.)	12·5	15·0	20·0
V_e (arbitrary units)	24·5	25·6	26·3
V_m (arbitrary units)	21·8	21·8	21·9

These results show that the extinction potential depended on the circuit conditions, but that the minimum maintenance potential was characteristic of the discharge only.

(iii) Table 3 shows the effect of de-tuning the coupled circuit. The measurements were carried out under the same conditions as those of Table 2, and with the coupling corresponding to a distance of 15 cm. between the coils.

Table 3

Circuit tuned to resonance (% response)	100	67	40
V_e (arbitrary units)	25·6	24·9	22·5
V_m (arbitrary units)	21·8	21·8	21·8

These experiments also showed that the minimum maintenance potential was independent of the source impedance whereas the extinction potential depended upon the circuit conditions.

§ 3. THEORY OF OBSERVED DISCHARGE CHARACTERISTICS

The above experimental results may be explained by considering the (I, V) characteristics of the H.F. discharge to be of the form A, B, C, D, shown in Figure 1.

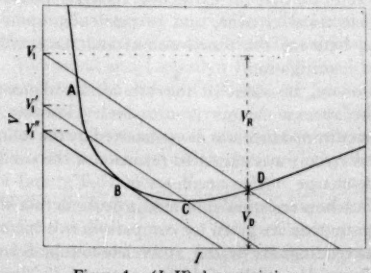

Figure 1. (I, V) characteristic.

Consider the simple network of a pure resistance R in series with the discharge and a potential V_1 applied across it. The effect of R is then represented by a load line V_1D of slope determined by the value of R. Under these conditions the stable state of the discharge is given by the point D, where the load line and characteristic intersect. The total applied potential V_1 is then divided, as V_R and V_D, where V_R is the potential across the resistance R, and V_D that across the discharge. As the applied voltage is varied from V_1' to V_1'', say, the load line of R is moved parallel to itself, and the point of stability moves along the curve from C to B as shown. It should be noted that for the experiments at high frequency it was the voltage V_D across the discharge which was measured, and not the overall applied voltage V_1 as is usual in examining direct current discharges.

Consider the variation of V_D with the power applied to the discharge, as deduced from Figure 1. After breakdown occurs the discharge conditions settle and V_D moves along the curve to a point of stability represented by C. As the output of the oscillator is increased V_1 is increased, and the point of stability moves from C to D. Thus the voltage V_D between the electrodes increases, and so does the current. When the power applied is reduced, the stable point moves back towards C and the measured voltage indicates a minimum value V_m. Further decrease of the oscillator output causes an increase in V_D, and a decrease in current, and the point of stability then moves towards B. At B, where the load line is tangential to the discharge characteristic, any further decrease of V_1 causes the extinction of the discharge V_e. These variations are in agreement with those found experimentally. The effect of a different source impedance (corresponding to a load line of different slope) can be seen from the diagram. The value of the least maintenance voltage V_m (point C) remains as before, but the extinction voltage V_e is different. Thus V_m is characteristic of the discharge, whereas V_e is dependent upon the electrical circuit properties. Along the portion of the curve C to D, the maintenance voltage increases with current, as in Townsend's experimentally determined equation (Hayman 1929) $V=X(x+a)-bI/f$. As the current is reduced beyond C towards B and A the maintenance voltage rises. For this portion of the characteristic the current density in the glow is reduced to such an extent that the positive space charge is insufficient to keep the diffusional loss of electrons to a low level. Hence an increase in the electric field strength with an increase in the rate of ionization is necessary to make up for the increased loss.

§4. SIMILARITY RELATIONSHIPS FOR MAINTAINED HIGH-FREQUENCY DISCHARGES

The above results showed that the significant discharge parameter was the minimum maintenance potential V_m, and it is now interesting to investigate whether a similarity relationship applies to this factor. To do this, V_m was measured for hydrogen for two geometrically similar tubes B and C, over a range of gas pressures from 0·1 to 10 mm. Hg, and over a range of oscillation frequencies from 10 to 70 Mc/s. The results are expressed by a set of (V_m, ap) curves for various values of f (Figure 2). It will be seen that, on the whole, there is support for the view that the similarity relationship applies to maintained currents. On the other hand, the agreement is certainly not as good as was the case for breakdown (I) for which the agreement was clear cut, i.e. the breakdown potentials were sensitive to variation for both geometrical and frequency factors.

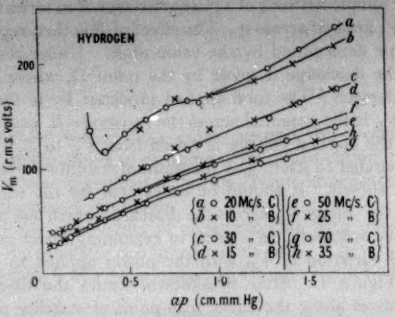

Figure 2. Similarity relationships for minimum maintenance high-frequency potentials.

There are various reasons, however, which would account for this in the case of the maintained currents. As indicated in § 2, at the lower oscillation frequencies the discharge was, in general, not in the form of a uniform glow along the wire, but consisted of localized asymmetric glows at different points on the wire; these occurred usually near the centre of the cylinder. Further, the glows were unstable on the wire, and tended to move about as the power in the discharge was altered. In fact, at times it was not at all clear whether the glow was actually static and uniform, or was moving about very rapidly, and appearing to merge into a continuous glow. When the glows decreased in number or size, or even disappeared, the voltmeter reading showed corresponding falls, but it was not easy to determine the exact value of V_m. On the other hand, at the higher frequencies, the discharge appeared steady and stable, and V_m could be measured accurately.

§ 5. CONCLUSIONS

The extinction potential of the glow discharge is not solely a property of the discharge, but is dependent upon the impedance of the high-frequency potential source. On the other hand, the minimum maintenance potential, at any given gas pressure is independent of the impedance of the source of high-frequency potential, and is a characteristic of the discharge.

The experiments give general support for the view that the same similarity relationship which applies to breakdown also applies to the maintenance of H.F. current. However, the dependence of the minimum maintenance potential upon the parameters ap and f/p is not so well defined as is the case for the breakdown potential, and this appears to be due to effects such as discharge instability.

REFERENCES

HAYMAN, R. L., 1929, *Phil. Mag.*, **7**, 586.
LLEWELLYN JONES, F., and MORGAN, G. D., 1951, *Proc. Phys. Soc.* B, **64**, 560.
TOWNSEND, J. S., and DONALDSON, R. H., 1928, *Phil. Mag.*, **5**, 178.
TOWNSEND, J. S., and NETHERCOT, W., 1929, *Phil. Mag.*, **7**, 600.
TOWNSEND, J. S., and LLEWELLYN JONES, F., 1931a, *Phil. Mag.*, **11**, 679; 1931b, *Ibid.*, **12**, 815.

On Resonance Damping at Injection in Betatrons and Synchrotrons

By S. E. BARDEN

Research Department, Metropolitan-Vickers Electrical Co. Ltd., Manchester

Communicated by D. Gabor; MS. received 1st November 1950, and in amended form 28th February 1951

ABSTRACT. It is shown that under special conditions of injection, damping of electron oscillations can occur in 'imperfect' cyclic accelerators, i.e. those with an azimuthally inhomogeneous electromagnetic field, in the presence of resonance between their different periodic motions. This mechanism is invoked to explain the successful injection of electrons in most betatrons and synchrotrons. The necessary coupling inhomogeneity to induce resonance damping at injection can be created by the large currents circulating during this period in the acceleration cycle.

§1. INTRODUCTION

THE possibility of particle orbits becoming unstable in cyclic accelerators in the presence of resonance between the various frequencies of the oscillations to which they are subjected, was first pointed out by Dennison and Berlin (1946), and Sewell, Henrich and Vale (1947), and treated analytically by Courant (1949). Recently, however, evidence has been published (Davis and Langmuir 1949, Jones *et al.* 1950), of the fact that such resonance between the radial and vertical oscillations and the circular motion of the particles in the accelerator can, with suitable control of the azimuthal field variation, give rise to a damping, which may be called 'resonance damping', of the 'free' oscillations (Kerst and Serber 1941). It is the purpose of this paper to provide the analysis to support these experimental facts, and to derive explicitly the conditions under which one can expect such damping to occur.

It is also shown that, in the presence of azimuthal irregularities created by the large currents circulating at injection, resonance damping of radial oscillations can take place if the field index n has an average value $\langle n \rangle_{av}$ sufficiently near 3/4. It is suggested that such resonance damping could be a contributory cause of the successful operation of a large number of betatrons and synchrotrons; quantitative results are given to show that such damping is of the right order of magnitude to allow particles to miss the injector structure during their initial revolutions, for cases both of external and internal injection.

§2. THE EQUATIONS OF MOTION

Assume that the magnetic field $\mathbf{H}$ is symmetrical about the median ($z=0$) plane, and curl $\mathbf{H}=0$; div $\mathbf{H}=0$.

Write $\rho=\Delta r/r_i$ where Δr represents the radial displacement of the particle from its instantaneous circle of radius r_i; let z represent the vertical displacement of the particle from the median plane, and let ϕ be the azimuthal variable.

Consider the axial component $H_z(r,\phi)$ of the magnetic field to be given at any point in the median plane by the series

$$H_z(r,\phi)=H_0\{1+h_0-[\langle n\rangle_{av}-h_1(\phi)]\rho+O(\rho^2)+\ldots\}, \quad \ldots\ldots(1)$$

where $h_0(\phi)$, $h_1(\phi)$ are functions giving the magnitude, phase and azimuthal distribution of the 'error' fields with respect to the homogeneous component H_0

at radius $r=r_1$, and n is a constant, called the field index, satisfying the relations (Kerst and Serber 1941)

$$H_z(r,\phi)=H_0(\phi)[r/r_1]^{-n} \quad 0<n<1. \qquad \ldots\ldots(2)$$

$H_0(\phi)$ represents the magnitude of the *total* magnetic field at radius $r=r_1$ in the median plane, so that $H_0(\phi)=H_0\{1+h_0(\phi)\}$.

If we neglect the growth of the magnetic field with time, using the principle of adiabaticity to make our results completely general, and terms of second and higher orders in the dependent variables, the equations of motion of particles performing radial and vertical oscillations in an azimuthally inhomogeneous magnetic field $H_z(r,\phi)$ given by equation (1) can be written respectively

$$\frac{d^2\rho}{d\phi^2}+[1-\langle n\rangle_{\mathrm{av}}+2h_0(\phi)+h_1(\phi)]\rho=-h_0(\phi), \qquad \ldots\ldots(3)$$

$$\frac{d^2z}{d\phi^2}+[\langle n\rangle_{\mathrm{av}}+2\langle n\rangle_{\mathrm{av}}\rho(\phi)-h_1(\phi)]z=0. \qquad \ldots\ldots(4)$$

In general, azimuthal irregularities in the magnitude of the magnetic field are caused by quadrature fields, due to hysteresis effects (resulting in the presence of remanent magnetism), and eddy currents in the iron cores of ferromagnetic accelerators, and by mechanical errors in the magnet structure. These defects can give rise to 'error' fields consisting either of an azimuthally variable field index n, or of azimuthal variations in the magnitude of the axial component of magnetic field at a given radius, or of both.

Error fields due only to $n=n(\phi)$ give $h_1(\phi)\neq 0$, $h_0(\phi)=0$. If the magnitude of the magnetic field varies azimuthally at radius r_1, then $h_0(\phi)\neq 0$, and we have, as a consequence of (1) and (2):

$$h_1(\phi)=\left[r\frac{\partial}{\partial r}h_0(r,\phi)\right]_{r=r_1}=-nh_0(\phi), \qquad \ldots\ldots(5)$$

where $h_0(r,\phi)=h_0(\phi)[r/r_1]^{-n}$.

In the particular case of cyclic accelerators of the betatron and synchrotron type, the effects of such inhomogeneities are usually largest during the interval immediately following the injection of the particles (usually electrons). We shall therefore confine ourselves in this paper to a treatment of this particular interval in the cycle of acceleration.

Equation (3) has a particular integral which has been shown (Bohm and Foldy 1946) to indicate the presence of 'forced' oscillations. These can be shown, to the first order, not to affect directly the resonance between the 'free' radial oscillations and the orbital motion of the electrons described by (3) for special values of $\langle n\rangle_{\mathrm{av}}$. We shall therefore suppress $h_0(\phi)$ where it occurs on the right-hand side of this equation. It should, however, be noted that the presence of 'forced' radial oscillations can lead to resonance with the 'free' vertical oscillations as indicated by the term $2\langle n\rangle_{\mathrm{av}}\rho(\phi)z$ in equation (4).

Since any inhomogeneity can be represented by a Fourier series, we shall assume, in order to simplify the analysis, that it is a circular function of azimuth, with a period $1/l$ times that of the orbital motion, and a phase angle γ_l relative to the azimuthal situation of the injector, $\phi=0$. We write therefore:

$$h_1(\phi)=\mp\alpha_l\cos(l\phi+\gamma_l), \qquad \ldots\ldots(6a)$$

$$2\langle n\rangle_{\mathrm{av}}\rho(\phi) \quad \text{or} \quad (2-n)h_0(\phi)=-\alpha_l\cos(l\phi+\gamma_l). \qquad \ldots\ldots(6b)$$

The upper sign on the right-hand side of (6 *a*) gives the expression for substitution into equation (3), the lower sign that for substitution into equation (4).

With this convention, substitution of equation (6) into equations (4) and (3) can be shown to result in an equation of the form

$$\frac{d^2\zeta}{d\chi^2}+(a-2q\cos 2\chi)\zeta=0^* \qquad \ldots\ldots(7)$$

where we have written $l\phi+\gamma_l=2\chi$, and ζ represents either z or ρ.

In the case of the radial equation (3) we then have

$$a=4(1-\langle n\rangle_{\mathrm{av}})/l^2; \qquad q=2\alpha_l/l^2, \qquad \ldots\ldots(7\,a)$$

while for the vertical equation (4),

$$a=4\langle n\rangle_{\mathrm{av}}/l^2; \qquad q=2\alpha_l/l^2. \qquad \ldots\ldots(7\,b)$$

§ 3. THE GENERAL SOLUTION

It will be noted that equation (7) is the usual form for the generalized Mathieu equation. Solutions to this equation are stable (periodic or non-periodic, and bounded) or, in the general case, unstable ($\rho\to\infty$, $\chi\to\infty$) depending on the relative magnitude of the parameters a and q. In particular if $a=1^2, 2^2, 3^2, 4^2, \ldots$, the solutions of (7) are stable only if $q=0$, i.e. if the magnetic field is azimuthally homogeneous. If the parameter $q>0$, and a is sufficiently near one of the above integral values, the electrons must perform oscillations that are essentially unstable. These are cases of resonance between the various periodic motions of the particles. For values of the field index n obeying the inequality (2), the following cases are of importance.

When $a=1$, $l=1$, it follows from (7 *a*) that $\langle n\rangle_{\mathrm{av}}=3/4$. This is the important case of resonance between the fundamental of the electron orbital motion, and the 'free' radial oscillations, the frequency of the latter being then exactly one half that of the former. Other less important cases of resonance occur when $a=4$, $l=1$ and $a=1$, $l=2$ when $\langle n\rangle_{\mathrm{av}}$ has the value zero.

In the case of 'free' vertical oscillations, we have $l=1, 2, 3, \ldots$, for cases of resonance with the fundamental and higher harmonics of the orbital motion of the electron, and $l=m(1-\langle n\rangle_{\mathrm{av}})^{1/2}$ for the case of resonance between the 'free' vertical and 'free' radial oscillations. In the first case we see from (7 *b*) that the most important resonance from the practical point of view occurs when $\langle n\rangle_{\mathrm{av}}=1/4$, ($a=1$, $l=1$). Other less important cases of resonance occur when $\langle n\rangle_{\mathrm{av}}=1$, ($a=1$, $l=2$; $a=2^2$, $l=1$). In the second case, important values of $\langle n\rangle_{\mathrm{av}}$ giving resonance, follow from equation (7 *b*), viz.

$$a=\frac{4\langle n\rangle_{\mathrm{av}}}{m^2(1-\langle n\rangle_{\mathrm{av}})}=1, 2^2, 3^2, 4^2, \ldots; \qquad m=1, 2, 3, \ldots$$

i.e. $\langle n\rangle_{\mathrm{av}}=0{\cdot}20, 0{\cdot}50, 0{\cdot}70, 0{\cdot}80, \ldots$ $\begin{cases} a=1, m=1, 2, 3, 4, \ldots \\ m=1, a=1, 4, 9, 16, \ldots. \end{cases}$

In most practical cases, $q\ll 1$. It can be shown that for $a=2^2, 3^2, 4^2, \ldots$, resonance instability can only occur if this parameter does not depart from these values by more than terms of the order of magnitude of q^2. Also the presence of oscillation frequencies $m(1-\langle n\rangle_{\mathrm{av}})^{1/2}$, $m\geqslant 2$ require terms of second and

* Since this work was completed a solution of (7), for $a\simeq 1$, by Langmuir and Davis has been brought to the author's notice. An entirely different analytical procedure has been used; it is available in detail in a privately distributed report entitled: "Injection of electrons into a betatron". However, the results were not applied to conditions imposed by the circulating space charge at injection.

higher orders in ρ. In the case of $a \simeq 1$, however, resonance can occur even if this parameter has a value differing from unity by terms of the order of magnitude of q. To the first order in the parameter q, therefore, only those cases of resonance will be considered for which $a \simeq 1$. In addition we shall confine ourselves to important practical cases arising when $l = 1$.

In the region $a \simeq 1$, the general solution of (7) can be written (Whittaker and Watson 1950) in the form

$$\zeta = Ae^{\mu\chi}\sin(\chi - \sigma) + Be^{-\mu\chi}\sin(\chi + \sigma), \qquad \ldots\ldots(8)$$

where $\zeta \ll 1$, A and B are arbitrary constants of the order of ζ, and terms of the order of q^2 are neglected. The constants μ and σ are related to each other and to a and q by means of the relations

$$\mu = \tfrac{1}{2}[q^2 - (a-1)^2]^{1/2} \neq 0; \quad 2\sigma = \cos^{-1}[(1-a)/q] = \sin^{-1}[-2\mu/q]. \quad \ldots\ldots(9)$$

§ 4. DISCUSSION OF THE GENERAL SOLUTION

It is obvious from (8) that in the general case $A \neq B \neq 0$ the solutions ζ are unbounded if μ is real, i.e. if $q^2 > (1-a)^2$. The solution is, however, stable if μ is imaginary, i.e. if $q^2 < (1-a)^2$. The boundary between the stable and unstable regions is thus given by the equations $q^2 = (a-1)^2$ or $\pm q = (a-1)$. The stability chart is plotted in Figure 1 for the important case $a \simeq 1$, $l = 1$. The ordinate scale is given in terms of $\langle n \rangle_{av}$ satisfying this relation in equations (7*a*) and (7*b*) respectively (denoted by n_I and n_{II}).

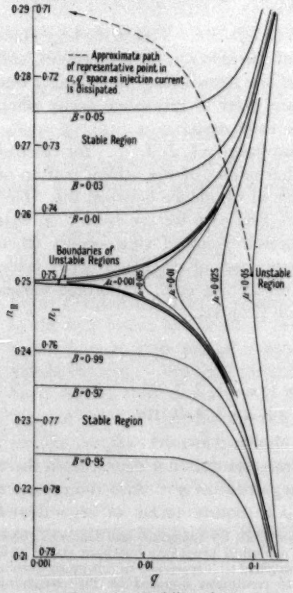

Figure 1. Stability chart.

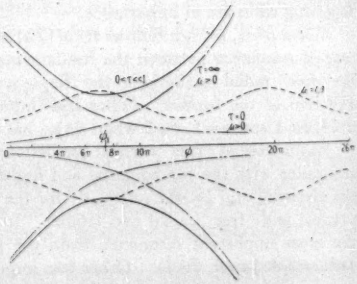

Figure 2. Modulation envelopes.

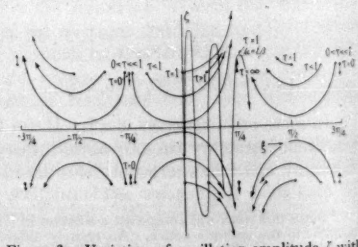

Figure 3. Variation of oscillation amplitude ζ with its phase ξ relative to the coupling inhomogeneity.

An electron injected under initial conditions requiring $A \neq B \neq 0$, will, in a field characterized by parameters a and q giving a point just inside the stable region (i.e. μ imaginary), perform oscillations whose amplitude is periodically modulated. Thus, if we assume $A = B \neq 0$, we have, writing $\mu = i\beta$,

$$\zeta = A[(e^{i\beta\chi} + e^{-i\beta\chi}) \sin\chi \cos\sigma - (e^{i\beta\chi} - e^{-i\beta\chi}) \cos\chi \sin\sigma],$$

giving
$$\zeta = \sqrt{2}A[\cos 2\beta\chi + \cos 2\sigma]^{1/2} \sin(\chi - \xi) \qquad \ldots\ldots(10)$$

where
$$\xi = \tan^{-1}(\tan\beta\chi \tan\sigma); \qquad \beta^2 = \tfrac{1}{4}[(a-1)^2 - q^2]. \qquad \ldots\ldots(11)$$

The ratio of maximum to minimum oscillation amplitude is then given by the ratio $[(\cos 2\sigma + 1)/(\cos 2\sigma - 1)]^{1/2} = [(1 - a + q)/(1 - a - q)]^{1/2}$. The effective phase difference ξ of the 'free' oscillations relative to the inhomogeneity, will slowly increase according to (11) while the amplitude is modulated to (10). The graph of ζ against ξ is given in Figure 3, indicating qualitatively the slow precession of phase against the relatively fast changes in ζ.

If (a, q) lies in the stable region of Figure 1 and the inequality $q^2 \ll 2a(a-1)$ is satisfied, however, the solution ζ of (7) can be written

$$\zeta = Ace_\nu(\chi, q) + Bse_\nu(\chi, q),$$

where A and B are arbitrary constants and $ce_\nu(\chi, q)$ and $se_\nu(\chi, q)$ are Mathieu functions, of fractional order given by $\nu = a^{1/2}$.

When the point (a, q) lies in the unstable region of Figure 1, so that μ is real, the oscillation amplitude will be exponentially modulated; its phase ξ in general, will precess relatively slowly at first, then more rapidly, and finally more slowly as it approaches the value $+\pi/4$ (when $a = 1$) relative to the inhomogeneity. When the phase is precessing most rapidly, the value of ζ reaches a minimum. As ξ tends to $+\pi/4$, the amplitude ζ, already increasing, will build up very rapidly.* The occurrence of phase precession is prevented only when $\tau = 0, \infty$. Figure 3 also includes curves for cases when μ is a real quantity, showing qualitatively the features described above for $a = 1$, and various values of τ, where

$$\tau = A/B. \qquad \ldots\ldots(12)$$

In Figure 2 the variation of ζ with ϕ is shown qualitatively for the different conditions treated.

Suppose we have for our initial conditions $\zeta = \zeta'$; $d\zeta/d\phi = \eta$; $\chi = \gamma_1/2$; $\phi = 0$. Then the general relation between ζ' and η will be

$$[2\eta/\zeta'] \simeq \frac{A \exp \tfrac{1}{2}\mu\gamma_1 \cos(\tfrac{1}{2}\gamma_1 + |\sigma|) + B \exp -\tfrac{1}{2}\mu\gamma_1 \cos(\tfrac{1}{2}\gamma_1 - |\sigma|)}{A \exp \tfrac{1}{2}\mu\gamma_1 \sin(\tfrac{1}{2}\gamma_1 + |\sigma|) + B \exp -\tfrac{1}{2}\mu\gamma_1 \sin(\tfrac{1}{2}\gamma_1 - |\sigma|)}$$

as $\mu \ll 1$. If $a = 1$, we have $|\sigma| = \pi/4$, from (9); using (12) we obtain

$$[2\eta/\zeta'] \simeq \frac{\tau \exp \tfrac{1}{2}\mu\gamma_1 \cos(\tfrac{1}{2}\gamma_1 + \tfrac{1}{4}\pi) + \exp -\tfrac{1}{2}\mu\gamma_1 \cos(\tfrac{1}{2}\gamma_1 - \tfrac{1}{4}\pi)}{\tau \exp \tfrac{1}{2}\mu\gamma_1 \sin(\tfrac{1}{2}\gamma_1 + \tfrac{1}{4}\pi) + \exp -\tfrac{1}{2}\mu\gamma_1 \sin(\tfrac{1}{2}\gamma_1 - \tfrac{1}{4}\pi)}. \qquad \ldots\ldots(13)$$

Hence in the limiting cases $\tau \to 0$, $\tau \to \infty$, we have:

$$[2\eta/\zeta']_{\tau \to 0} \simeq \cot(\tfrac{1}{2}\gamma_1 - \tfrac{1}{4}\pi) \quad \ldots(14\,a); \qquad [2\eta/\zeta']_{\tau \to \infty} \simeq \cot(\tfrac{1}{2}\gamma_1 + \tfrac{1}{4}\pi). \quad \ldots(14\,b)$$

These conditions are plotted in Figure 4 (where ζ_1 is written for ζ'), which shows also equation (13) for $\tau \gg 1$ and $0 < \tau \ll 1$.

* It is clear that the existence of such a fixed azimuth at which the oscillation amplitude builds up exponentially, makes it feasible to use a resonance mechanism to extract the electrons or the gamma-beam from accelerators of this type. Experiments based on such mechanism are in progress. Its main advantage over other extraction methods lies in the comparatively small external perturbation that should be necessary to induce resonance divergence.

It is obvious from (8) that when $\tau=0$, the oscillations described by the function $\zeta(\phi)$ are exponentially damped. Thus (14 *a*) gives the conditions of injection under which oscillations undergo resonance damping, the phase difference between the damped 'free' oscillations and the coupling inhomogeneity being $\xi=\sigma=-\pi/4$ (Figure 3). If a is not precisely unity, $|\sigma|$ will differ from $\pi/4$, being determined by equation (9).

It follows from (14 *a*) that there will be a series of values of ζ' to each of which corresponds a certain angle (given approximately by η) for a given inhomogeneity. An electron injected under such conditions will perform oscillations that are exponentially damped with time, at a rate depending on the strength of the coupling term q, and the proximity of the parameter a to unity, i.e. the proximity of $\langle n\rangle_{\text{av}}$ to the value 3/4 when $\zeta=\rho$, and of $\langle n\rangle_{\text{av}}$ to the value 1/4 when $\zeta=z$ (Figure 1).

In the more general case $\tau\neq 0$, the electron will oscillate with exponentially modulated amplitudes when μ is real. If $\tau\geqslant 1$, the amplitude will increase from the instant of injection, but if $\tau<1$, the amplitude will reach a minimum before subsequently diverging. It is clear, therefore, that if $0\leqslant\tau\ll 1$, electrons will be injected within a small but finite range of ζ', and consequently a small but finite range of angles, with an exponentially damped oscillation amplitude that takes a long time, relative to the period of orbital motion at injection, eventually to diverge.

Two special cases are of importance, namely, $\gamma_1=\pm\pi/2$. Equation (13) then becomes

$$|2\eta/\zeta'|_{0<\mu\ll 1}\simeq\frac{1}{\tau}e^{-\tau\mu/2}\sim\frac{1}{\tau}\gg 1;\quad 0\leqslant\tau\ll 1 \qquad \text{.....(15 a)}$$

$$\ll 1;\quad \tau\gg 1 \qquad \text{.....(16 a)}$$

and

$$|2\eta/\zeta'|_{0<\mu\ll 1}\simeq|-\tau e^{-\mu\pi/2}|\sim\tau\ll 1;\quad 0\leqslant\tau\ll 1 \qquad \text{.....(15 b)}$$

$$\gg 1;\quad \tau\gg 1 \qquad \text{.....(16 b)}$$

respectively.

Equations (15 *a*) and (16 *b*) result in initial conditions relatively difficult to obtain in practice if the presence of free oscillations of comparatively large amplitude at injection is required. Equations (15 *b*) and (16 *a*), however, describe initial conditions which result in the presence of large amplitude 'free' oscillations at injection whose maxima occur at, or near, the injector azimuth.

The conditions ideal for resonance damping are therefore prescribed by (15 *b*), i.e. $\gamma_1=-\pi/2$, $0<\tau\ll 1$.

From Figure 4 it is clear that the conditions at injection necessary to give effective resonance damping do not change substantially with changes in τ.

The rate at which the minimum oscillation amplitude is approached depends on the magnitude of μ. It occurs at azimuth ϕ_1, defined by

$$1/\tau=e^{2\pi\mu N}\quad\text{or}\quad 2\pi\mu N=-\ln\tau,\quad\text{where}\quad\phi_1=2\pi N. \qquad \text{.....(17)}$$

Equation (17) is plotted in Figure 5, and in the family A of curves in Figure 6.

§ 5. RESONANCE DAMPING OF VERTICAL OSCILLATIONS

In the case of vertical oscillations $\zeta=z$, and $\zeta'=z'$. Here, z' is a fixed constant representing the height of the injector above the median plane, and η is the angle of injection measured relative to the plane, parallel to the median plane, which contains the injector. The important resonance occurs when $a=1$, $l=1$, i.e. $\langle n\rangle_{\text{av}}=1/4$ (see equation (7 *b*)). As mentioned earlier in this paper, resonance

damping of vertical oscillations under these conditions has been shown (Jones *et al.* 1950) to play a vital role in the successful injection of electrons into a 300 MeV. non-ferromagnetic synchrotron. The injector was situated at a height above the median plane; for the necessary coupling a first harmonic inhomogeneity in the form of an azimuthally varying field index, $n(\phi)$, was artificially created. Using the damping condition (14 *a*) with $\gamma_1 = -\pi/2$, it follows that $\eta \simeq 0$. From (1), (4), and (6 *a*), $n(\phi) = \frac{1}{4} - \alpha_1 \sin\phi$; $\langle n \rangle_{av} = \frac{1}{4}$.

These are precisely the conditions found necessary by Jones *et al.* (1950) for successful injection into their machine.

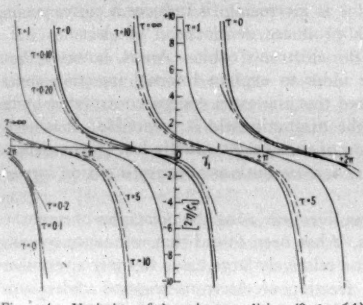

Figure 4. Variation of damping condition ($0 \leqslant \tau \ll 1$) and divergence condition ($\tau \geqslant 1$) with 'τ' and 'γ' for $a = 1$.

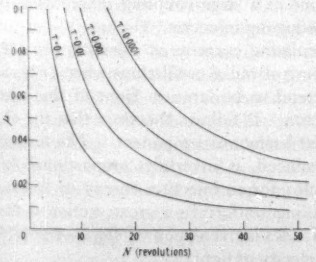

Figure 5. Number of revolutions after which minimum amplitude is reached; variation with 'μ' and 'τ'.

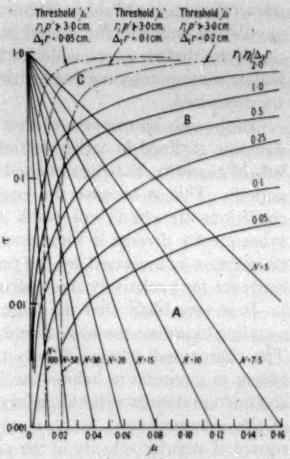

Figure 6.

It is perhaps worth noting that an alternative coupling could have been obtained from the creation of a first harmonic inhomogeneity $h_0(\phi)$ in the magnitude of the magnetic field given by $h_0(\phi) \propto +\alpha_1 \sin\phi$. This would give rise to first harmonic 'forced' oscillations in the median plane that, from (4) and (6 *b*), can be seen to perform the same function as that performed by azimuthally varying the field index.

§ 6. RESONANCE DAMPING OF RADIAL OSCILLATIONS WHEN $\langle n \rangle_{av} \simeq 3/4$

From the considerations of the previous sections it appears likely that resonance damping of radial oscillations could have been a contributory cause of the successful operation of a large number of betatrons and synchrotrons, as

most of these machines have been designed with a field index $\langle n \rangle_{av}$ approximately equal to 3/4 over a large fraction of doughnut space. In this section quantitative and qualitative treatment of this mechanism is provided.*

It has not yet been satisfactorily explained how an electron can be injected into betatrons or synchrotrons without hitting the injector structure on subsequent revolutions. Experimental work has shown (Westendorp and Elder 1949), however, that the presence of a large circulating current is essential for efficient injection, and a semi-quantitative theory has been developed by Kerst (1948) based on this fact. This theory is based on the assumption that while the circulating current in such a machine is increasing, it induces a corresponding change in orbit-linking flux, which produces deceleration of electrons and a consequent shrinkage in radius of the electron's orbit. Apart, however, from the fact that applications of these ideas to explain internal injection appear unconvincing, it should be mentioned that the extra energy contributed by the circulating currents and stored in the magnetic field is reversible; it is likely, therefore, that an appreciable fraction of the energy initially lost by the electron will be subsequently regained within a few revolutions as heavy injection currents are dissipated.

In the only known case of electron injection using the principles of resonance damping outlined in earlier sections, it has been found that resonance coupling has, of necessity, to be maintained at a relatively large value for only a very short period. This is because the large fraction of electrons trapped under initial conditions $0 < \tau \ll 1$ will reach a minimum oscillation amplitude, but will subsequently diverge if such resonance coupling persists. Thus the efficiency of injection is increased by the presence of a large coupling inhomogeneity, in existence for a relatively short period following injection.

It is very likely that the large circulating currents at injection provide the coupling to induce the resonance damping of radial oscillations when $\langle n \rangle_{av} = 3/4$. The charge and current density will tend to be large in front of the injector, falling to a minimum behind the injector. It follows therefore that the charge and current density will have a large first harmonic component. The magnitude of the inhomogeneity δn in n, so produced, is inversely proportional to the square of angular velocity of the particle; for an injection energy of 25 kv. and an emission of 500 ma. at injection filling uniformly a cross section 6 cm. in diameter the change in the effective field index is given by $\delta n \simeq 0{\cdot}08(1 - v^2/c^2) \simeq 0{\cdot}07$ where v is particle velocity, and c the velocity of light.

With the assumption that, to the first order, particle kinetic energy is conserved, the first harmonic component should therefore be characterized by a phase angle $\gamma_1 \simeq -\pi/2$ (cf. equations (3) and (6 *a*)), giving $n(\phi) \simeq \frac{3}{4} + \alpha_1 \sin\phi$; $\langle n \rangle_{av} = \frac{3}{4}$.

The damping conditions (15 *b*) are therefore satisfied, and the circulating space charge should initiate resonance damping.

For the case of an electron oscillating wholly in the median plane, ρ' represents the distance of the electron from its instantaneous circle at the instant of injection, and η is approximately the angle its trajectory makes with the tangent to the circle at the electron gun. It follows from (14 *a*) that there will be a series of instants of injection (corresponding to different values for ρ') to each of which there corresponds a certain angle of injection. An electron injected under such

* A preliminary account has already been published (Barden 1951).

conditions will perform oscillations about its instantaneous circle with an amplitude exponentially damped with time, at a rate depending on the coupling term q, and the proximity of a to unity, i.e. of $\langle n \rangle_{av}$ to $\frac{3}{4}$.

Consider, for example, $\mu = 0{\cdot}05$ when $a = 1$. The initial damping per revolution $\Delta_1 r$ is given by

$$\left| \frac{\Delta_1 r}{r_{inj} - r_i} \right| \simeq \mu\pi(1-\tau) \simeq 0{\cdot}15 \text{ for } \tau = 0. \qquad \ldots\ldots(18)$$

If $r_i\rho' = |r_{inj} - r_i| = 2$ cm., $\Delta_1 r \simeq 3$ mm., where r_{inj} represents the radius of the circle passing through the injector.

This damping is of the order of 500 times the damping of 'free' radial oscillations to be expected from Kerst–Serber (1941) theory. The original mechanism suggested by these authors can, however, be included in the solution (8) for the radial case, i.e. $\zeta = \rho$, by a modification of equation (3). For a constant κ very much less than 1, Serber damping per revolution can be written approximately $1 - e^{-\kappa\phi} = (\phi/2\pi)(\delta\rho/\rho') = (\Delta E/2E)(\phi/2\pi)$ where ΔE is the gain in energy by the electron per revolution, in ev., and E is their injection kinetic energy. Hence $\kappa \simeq \Delta E/4\pi E$.

Assuming that such damping is unaffected by the presence of inhomogeneities, the equation of motion becomes $d^2\rho/d\chi^2 + 2\kappa\, d\rho/d\chi + (a - 2q\cos 2\chi)\rho = 0$. The solution is written $\rho = Ae^{(\mu-\kappa)\chi}\sin(\chi - \sigma) + Be^{-(\mu+\kappa)\chi}\sin(\chi + \sigma)$. The boundary between the stable and unstable regions in Figure 1 is now formed by the iso-μ line $\mu = \kappa$. In the smaller accelerators $\Delta E \sim 100$ ev., $E \sim 5 \times 10^4$ ev. Hence $\kappa \simeq 10^{-4}$.

In the absence of resonance damping, such damping would be negligible, giving only about 0·007 mm. damping per revolution.

Up to now we have considered quantitatively only the case for $\tau = 0$. However as τ increases towards unity, the oscillation amplitude will not be damped indefinitely; it will reach a minimum only to diverge subsequently. The electron performing such an oscillation will therefore be lost if resonance persists sufficiently long. In such cases, the maximum amplitude will precess in phase, building up exponentially at $\phi \simeq \pi$. For a given period of non-zero coupling, it appears that there should be an optimum value for μ.

Consider quantitatively the case $a = 1$, $\gamma_1 = -\pi/2$. Combining (15*b*) and (18), eliminating ρ', we have

$$\tau/(1-\tau) = 2\pi\mu(\eta r_i/\Delta_1 r). \qquad \ldots\ldots(19)$$

This is plotted in curves B of Figure 6. The curves C define the threshold values for μ compatible with given values for $\rho' r_i$, and $\Delta_1 r$. Several interesting conclusions can be drawn from curves A, B, and C, which are based on equations (17), (19) and (18) respectively.

Consider first electrons injected at an angle η satisfying $r_i\eta/\Delta_1 r = 1$. The threshold coupling when the electron is injected towards the end of the acceptance time interval, e.g. $\rho' r_i \simeq 3$ cm. and $\Delta_1 r \simeq 0{\cdot}1$ cm., is $\mu = 0{\cdot}01$. Further increase in μ will result in the successful damping of electrons injected with smaller initial amplitudes, until the curve of family B intersects a relevant curve of family A. At larger emissions, electrons injected with successively smaller initial amplitudes at this angle will be successfully damped, only to be lost through subsequent undamping and consequent collision with the doughnut walls at

$\phi \simeq \pi$. Thus if the resonance coupling lasts for a period corresponding to about ten particle revolutions, the number of electrons accepted at this angle will be a maximum when $\mu \simeq 0{\cdot}05$. The numbers of accepted electrons injected at half this angle will, however, continue to increase, reaching a maximum when $\mu = 0{\cdot}07$. The values of τ at which such maxima occur represent the upper limit for the range of initial conditions defining trajectories of electrons that manage to avoid collision with the injector structure and the doughnut walls when μ falls to zero. It is assumed that μ is appreciable only during a period of the order of the acceptance time. Consequently as μ increases, injection efficiency rises from zero to a finite value at the threshold determined by $\rho' r_1$ and $\Delta_1 r$. The first accepted electrons are then those injected tangentially ($\eta = 0$) at the end of the acceptance time interval corresponding to largest $|\rho'|$. As μ increases further, electrons injected at larger angles are accepted, as a curve of family C successively intersects curves of family B corresponding to larger values for η. The maximum angle of the cone of accepted electrons is that corresponding to the intersection of a curve A with a curve C. While electrons injected at larger angles are being accepted, electrons injected at the smaller angles are accepted earlier (corresponding to smaller values of ρ' and larger values of τ).

Eventually, however, as μ increases still further, the angle of the cone of accepted electrons will decrease as a curve A intersects curves B corresponding to successively smaller values of η. However, electrons injected at sufficiently small angles will be accepted successively earlier, and for an optimum μ the injection efficiency should have a maximum value. The rate of loss of electrons due to undamping (reducing the vertical angle of the cone of accepted electrons) then equals the rate of gain of electrons due to the successful damping of electrons injected successively earlier, which increases the effective interval over which electrons are accepted. Ultimately, if μ is sufficiently increased, only electrons injected tangentially will be accepted and injection efficiency will tend to zero for a value of μ corresponding approximately with the intersection of a curve A with the μ-axis.

The coupling inhomogeneity, q, created by the presence of a large circulating current can be reduced by increasing the injector voltage. If it is assumed that the homogeneous component of h_1 is only slightly changed by increased emission, while the first harmonic component α_1 of h_1 is appreciably increased by such a change, the injection efficiency should increase with emission, output increasing very rapidly. At the value of μ corresponding to maximum injection efficiency, output should still increase with emission owing to the larger number of electrons available for acceleration. Larger emission should eventually result in fall in output; above this critical emission, an increase in the injection voltage will reduce μ, and thus increase output by restoring maximum injection efficiency. For values of μ below the critical value, injection efficiency should be reduced by an increase of the injector voltage. Thus the points at which output emission curves for different injection voltages intersect correspond to coupling inhomogeneities just larger than that at which injection efficiency is maximum. Experimental evidence is available (Westendorp and Elder 1949) in support of these arguments.

In general, increasing the injector voltage reduces the output of the machines for all values of emission up to a certain critical emission. Above this critical emission an increase in the injector voltage results in an increase in output.

Factors that need to be taken into consideration in comparing experimental results with this theory are the proximity of the factor $a=4(1-\langle n\rangle_{av})$, to unity, and the presence of quadrature fields.

A further important point to note is that such damping is *not* reversible. When the circulating current is largely dissipated, $q\to 0$ and the oscillation amplitude passes from a state of exponential amplitude modulation to a state of periodic amplitude modulation, and finally to one of zero modulation, as the point (a, q) enters well within the stable region. The typical path of such a representative point in (a, q) space is shown on the stability chart (Figure 1). It can be shown that the perturbation introduced by such a change over several particle revolutions is not large. For a given μ injection efficiency should also increase with the distance of the injector from the centre of the doughnut. This is because an increase in $\rho' r_1$ results in a larger acceptance angle η, given $r_1\eta/\Delta_1 r$. Thus it should generally be found that output increases the further the injector from the centre of the doughnut, and the threshold emission should be reduced. There could, of course, be exceptions to this rule under particular conditions.

As a consequence of these considerations it is suggested that the mechanism of resonance damping plays a part in the successful injection, both internal and external, of electrons into most betatrons and synchrotrons.

§8. CONCLUSIONS

It appears that the mechanism of resonance damping contributes, in some measure, to the successful operation of a large number of betatrons and synchrotrons, through the creation of favourable inhomogeneities by the large currents circulating at injection. An outstanding difference between this damping and Kerst's contraction mechanism is the sensitivity of the former to $\langle n\rangle_{av}$. In this connection it should be noted that currents through a pair of single-turn coils above and below the stable orbit do *not* alter the field index uniformly over the annular field region; this introduces second and higher order terms in the equations of motion which should be taken into account if the radial variation is sufficiently large. Under normal circumstances these terms are usually negligible.

From this work it should now be possible to achieve successful injection and increased outputs by means other than that used by Adams (1948). Thus, from (1), (6), (14 *a*) and (15 *b*) it can be seen that a first harmonic quadrature field of the form $h_0\simeq -[\alpha_1/(2-n)]\sin\phi$ could provide sufficient coupling inhomogeneity for resonance damping, without producing forced oscillations of intolerable magnitude.

ACKNOWLEDGMENTS

The author is indebted to his colleagues for much stimulating criticism, in particular to Mr. E. A. Finlay who introduced him to the problem, and to Messrs. C. A. Ambasankaran and D. Major who assisted him with the calculations. Thanks are also due to Dr. D. Gabor and Mr. F. R. Perry for the interest shown in this work, and for numerous contributions to clarity of style and notation. Finally, thanks are due to Sir Arthur P. M. Fleming, Director of Research and Education, and Mr. B. G. Churcher, Manager of Research Department, Metropolitan-Vickers Electrical Company Limited, for permission to publish this paper.

REFERENCES

ADAMS, G. D., 1948, *Rev. Sci. Instrum.*, **19**, 607.
BARDEN, S. E., 1951, *Proc. Phys. Soc.* B, **64**, 85.
BOHM, D., and FOLDY, L., 1946, *Phys. Rev.*, **70**, 249.
COURANT, E. D., 1949, *J. Appl. Phys.*, **20**, 611.
DAVIS, L., Jr., and LANGMUIR, R. V., 1949, *Phys. Rev.*, **75**, 1457.
DENNISON, D. M., and BERLIN, T. H., 1946, *Phys. Rev.*, **69**, 542.
JONES, W. B., *et al.*, 1950, *Phys. Rev.*, **78**, 60.
KERST, D. W., 1941, *Phys. Rev.*, **60**, 47; 1948, *Ibid.*, **74**, 503.
KERST, D. W., and SERBER, R., 1941, *Phys. Rev.*, **60**, 53.
SEWELL, D. C., HENRICH, L. R., and VALE, J., 1947, *Phys. Rev.* **72**, 739.
WESTENDORP, W. F., and ELDER, F. R., 1949, *Phys. Rev.*, **76**, 445.
WHITTAKER, E. T., and WATSON, G. N., 1950, *A Course of Modern Analysis* (Cambridge: University Press), p. 404.

Multiple Traversal of Cyclotron Targets

BY J. M. CASSELS, J. M. DICKSON AND J. HOWLETT
Atomic Energy Research Establishment, Harwell, Didcot, Berks.

Communicated by D. W. Fry; MS. received 29th January 1951

ABSTRACT. In high energy cyclotrons the accelerated particles may pass through the target more than once. The average number of traversals is calculated theoretically and compared with experimental results. Good agreement is found.

§ 1. INTRODUCTION

In high energy cyclotrons it is possible for the accelerated particles to pass through an internal target several times, since the rate of loss of energy by ionization is so low that the range of the particles is usually long compared with the target thickness. The process which limits the number of traversals is multiple Coulomb scattering (Helmholz, McMillan and Sewell 1947); particles which have been deflected vertically beyond a certain amount cannot be focused by the cyclotron magnetic field, and so do not return again to the target. Horizontal deflections do not lead to a loss of particles unless the beam is circulating very near to the edge of the magnetic field.

A theoretical treatment of the problem is given below, and this is followed by a comparison with some experimental results obtained with the 110-inch Harwell cyclotron.

§ 2. THEORY

If the protons are initially all travelling along the median plane of the cyclotron, their angular distribution function before the first traversal of the target is

$$f(\theta, 0) = \delta(\theta) \qquad \ldots\ldots(1)$$

where θ is the angle to the median plane made by the direction of motion of the various protons at the target. On leaving the target the angular distribution function becomes

$$f(\theta, 1) = \frac{1}{2\pi^{1/2}} \frac{w}{t^{1/2}} \exp\left(-\frac{w^2\theta^2}{4t}\right), \qquad \ldots\ldots(2)$$

with $w = 2E(E+2\mu)/E_s(E+\mu)$ where E is the kinetic and μ the rest energy of the proton, E_s is a constant equal to 21 MEV. and t is the thickness of the target in radiation lengths (Rossi and Greisen 1941). The radiation length X_0 in an element of atomic weight A and atomic number Z is defined by $X_0 = 716A/(Z^2 \ln [183Z^{-1/3}])$ gm. cm^{-2}.

As a result of the focusing action of the cyclotron magnetic field, particles which leave the target at an angle smaller than a limiting angle θ_{max} will execute simple harmonic oscillations about the median plane. If the target does not extend very far above or below this plane, then a proton which left at an angle θ will return at an angle $\pm\theta$, depending on whether an even or odd number of half cycles of oscillation has intervened. Since, however, the distribution of protons is symmetrical about the median plane it is possible to say that for every proton which leaves at an angle θ there is another which returns at the same angle, provided that $\theta < \theta_{max}$.

The value of θ_{max} will now be derived. The vertical displacement of the particle is given by $z = Z \sin(\nu_v \phi/\nu_0)$ where ν_v and ν_0 are the frequencies of the vertical oscillation and of the radio-frequency accelerating voltage respectively, and ϕ is the angular distance around the cyclotron orbit covered by the proton after leaving the target. As usual $\nu_v = n^{1/2}\nu_0$ with $n = -(r_0/H)(dH/dr)_{r=r_0}$ where $H(r)$ is the vertical magnetic field in the cyclotron at a radius r from the centre; the target is placed at the radius r_0. The angle at which the proton leaves the target is $\theta = (1/r_0)(dy/d\phi)_{\phi=0} = n^{1/2}Z/r_0$ and, if d is the height above and below the median plane of the obstacle which intercepts the protons, $Z_{max} = d$ and $\theta_{max} = n^{1/2}d/r_0$.

Returning now to the angular distribution of the protons leaving the target after the $(m+1)$th traversal, it is clear that

$$f(\theta, m+1) = \frac{1}{2\pi^{1/2}} \frac{w}{t^{1/2}} \int_{-\theta_{max}-\theta}^{\theta_{max}-\theta} f(\theta+\psi, m) \exp\left(-\frac{w^2\psi^2}{4t}\right) d\psi, \quad \ldots\ldots(3)$$

where ψ is the angle of deflection of the protons at the last traversal. Using (1) it is easily checked that (2) is a special case of this general equation. It is convenient to introduce $x = \theta/\theta_{max}$, $y = \psi/\theta_{max}$, $\lambda = w^2\theta^2_{max}/4t = w^2nd^2/4r_0^2$, so that equation (3) now reads,

$$f(x, m+1) = \left(\frac{\lambda}{\pi}\right)^{1/2} \int_{-1-x}^{1-x} f(x+y, m) \exp(-\lambda y^2)\, dy, \quad \ldots\ldots(4)$$

and the effective thickness T of the target is

$$T = t \sum_{m=0}^{\infty} \int_{-1}^{1} f(x, m)\, dx.$$

Equation (4) takes a more convenient form after making the substitution $u = x + y$. Then

$$f(x, m+1) = \left(\frac{\lambda}{\pi}\right)^{1/2} \int_{-1}^{1} f(u, m) \exp\{-\lambda(u-x)^2\}\, du.$$

Let $f(x) = \sum_{m=1}^{\infty} f(x, m)$,

then $$f(x)=\sum_{m=0}^{\infty} f(x,m+1)=\left(\frac{\lambda}{\pi}\right)^{1/2}\int_{-1}^{1}\exp\{-\lambda(u-x)^2\}\sum_{m=0}^{\infty} f(u,m)\,du$$
$$=\left(\frac{\lambda}{\pi}\right)^{1/2}\int_{-1}^{1}\exp\{-\lambda(u-x)^2\}[f(u,0)+f(u)]\,du$$
$$=\left(\frac{\lambda}{\pi}\right)^{1/2}\exp(-\lambda x^2)+\left(\frac{\lambda}{\pi}\right)^{1/2}\int_{-1}^{1} f(u)\exp\{-\lambda(u-x)^2\}\,du \quad \ldots\ldots(5)$$

since $f(u,0)=\delta(u)$.

This is now an integral equation for $f(x)$. If it can be solved then T can be found from

$$T=t\int_{-1}^{1}[f(x,0)+f(x)]\,dx=t[1+\int_{-1}^{1} f(x)\,dx].$$

There seems to be no reasonably simple analytical method for solving (5), so the following numerical process was devised. Let $g(x)=\exp(\lambda x^2)f(x)$. Then

$$g(x)=\left(\frac{\lambda}{\pi}\right)^{1/2}+\left(\frac{\lambda}{\pi}\right)^{1/2}\int_{-1}^{1} g(u)\exp(-2\lambda u^2)\exp(2\lambda xu)\,du.$$

Clearly $f(x)$, and therefore $g(x)$, is an even function of x; this must be so on physical grounds alone. So, with $g(-u)=g(u)$,

$$\left(\frac{\pi}{\lambda}\right)^{1/2} g(x)=1+2\int_{0}^{1} g(u)\exp(-2\lambda u^2)\cosh(2\lambda xu)\,du. \quad \ldots\ldots(6)$$

Now let $g(x)$ be expanded in a power series:

$$g(x)=\sum_{n=0}^{\infty}\left(\frac{g_{2n}}{(2n)!}\right)x^{2n} \qquad \text{where} \qquad g_{2n}=\left[\frac{d^{2n}}{dx^{2n}}g(x)\right]_{x=0}.$$

Putting $x=0$ in (6),

$$\left(\frac{\pi}{\lambda}\right)^{1/2} g_0=1+2\int_{0}^{1}\exp(-2\lambda u^2)\sum_{n=0}^{\infty}\left(\frac{g_{2n}}{(2n)!}\right)u^{2n}\,du$$

and differentiating $2r$ times, and then putting $x=0$,

$$\left(\frac{\pi}{\lambda}\right)^{1/2} g_{2r}=2(2\lambda)^{2r}\int_{0}^{1}\exp(-2\lambda u^2).u^{2r}\sum_{n=0}^{\infty}\left(\frac{g_{2n}}{(2n)!}\right)u^{2n}\,du.$$

Writing $I_p=\int_{0}^{1} u^p\exp(-2\lambda u^2)\,du$, these equations become

$$\left.\begin{aligned}\left(\frac{\pi}{\lambda}\right)^{1/2} g_0 &=1+2\sum_{n=0}^{\infty}\left(\frac{I_{2n}}{(2n)!}\right)g_{2n}\\ \left(\frac{\pi}{\lambda}\right)^{1/2} g_{2r}&=2(2\lambda)^{2r}\sum_{n=0}^{\infty}\left(\frac{I_{2n+2r}}{(2n)!}\right)g_{2n} \qquad (r=1,2,\ldots.)\end{aligned}\right\} \quad \ldots\ldots(7)$$

The problem is now reduced to the solution of the infinite set of equations (7). It was hoped that only a small number of coefficients would need to be determined, so that a good approximation could be found from only a small number of equations. This was in fact true, and for values of λ up to four not more than six equations (i.e. up to g_{10}) had to be taken.

Having found the g's,

$$\int_{-1}^{1} f(x)\,dx=\sum_{n=0}^{\infty}\left(\frac{g_{2n}}{(2n)!}\right)x^{2n}\exp(-\lambda x^2)\,dx=2\sum_{n=0}^{\infty}\frac{g_{2n}}{(2n)!}I_{2n}(\tfrac{1}{2}\lambda)$$

where the integral defined as I_p is in fact $I_p(\lambda)$.

The integrals I_n are easily computed from the recurrence relation

$$I_{2n} = \left(\frac{2n-1}{4\lambda}\right) I_{2n-2} - \left(\frac{e^{-2\lambda}}{4\lambda}\right)$$

with $I_0 = \frac{1}{2}(\pi/2\lambda)^{1/2} \operatorname{erf}(2\lambda)^{1/2}$. If λ is less than about $\frac{1}{2}$, however, accuracy is lost at each step; so for small values of λ an approximate value of the integral for large n (actually $n=10$) was obtained by integrating the power-series expansion of the integrand, and calculating backwards to I_0: the known value for I_0 was then a useful check.

The results are plotted in Figures 1 and 2. For small values of λ (i.e. thick target, say $\lambda<0{\cdot}2$), at most two terms of the series for $g(x)$ need be included;

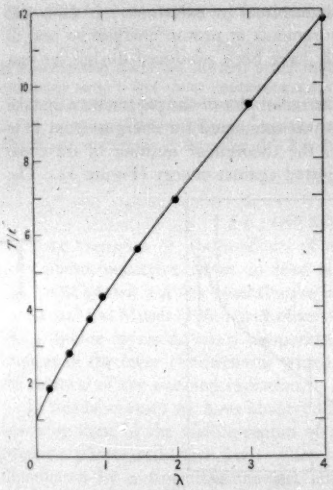

Figure 1. The average number of target traversals T/t as a function of the parameter λ.

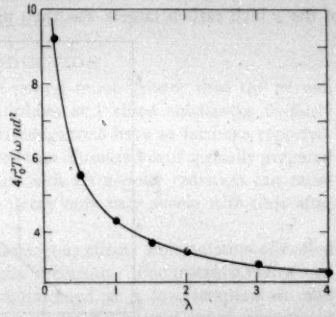

Figure 2. The effective target thickness, multiplied by $4r_0^2/w^2nd^2$, as a function of the parameter λ, which is inversely proportional to the actual target thickness t.

the final result can be written explicitly in terms of λ, and values correct to at least two significant figures are given by the expressions:

$$g_0 = \left[\left(\frac{\pi}{\lambda}\right)^{1/2} - 2 + \frac{4\lambda}{3} - \frac{4\lambda^2}{5} - \frac{8}{3}\lambda^2\left(\frac{\lambda}{\pi}\right)^{1/2}\right]^{-1},$$

$$g_2 = \frac{8}{3}\lambda^2\left(\frac{\lambda}{\pi}\right)^{1/2}, \quad \int_{-1}^{1} f(x)\,dx = 2(1-\tfrac{1}{3}\lambda)g_0 + \tfrac{1}{3}g_2.$$

When λ is very small the result is

$$g_0 = \left[\left(\frac{\pi}{\lambda}\right)^{1/2} - 2\right]^{-1} = \frac{(\lambda/\pi)^{1/2}}{1-2(\lambda/\pi)^{1/2}}; \quad \int_{-1}^{1} f(x)\,dx = 2g_0.$$

In accordance with the remarks made in the introduction, it has been assumed throughout that the slowing down of the protons in the target can be neglected. For this to be true the fractional energy loss in passing through the effective target thickness T must be suitably small.

§ 3. EXPERIMENTAL RESULTS

To test the theory, measurements were made of the effective thickness of $\frac{1}{8}$ inch carbon targets placed at various radii in the 110-inch Harwell cyclotron. The vertical height of the targets was about a quarter of the dee depth and the loss of energy by ionization in the effective thicknesses T was about 15 MEV., almost independent of the bombarding energy. The calibrating reaction was $^{12}C(p, pn)^{11}C$, for which the cross section has been determined (Peterson, private communication). The annihilation quanta from the ^{11}C positrons were counted in a calibrated Geiger counter.

The effective number of traversals T/t could be found from the observed activities of the targets, knowing that the true proton current accelerated by the cyclotron was $1{\cdot}0 \pm 0{\cdot}05\,\mu$a. This was determined by calorimetry (Adams and Edmunds 1950), and by activation measurements at proton energies so near to the reaction threshold that ^{11}C could only have been produced during the first traversal.

From the geometry of the cyclotron, the radial plot of the parameter n and the energy–radius relationship, the value of λ was calculated for energies from 40 to 170 MEV. Using the curve of Figure 1, the theoretical number of traversals of the $\frac{1}{8}$ inch carbon targets was then plotted against energy (Figure 3). The

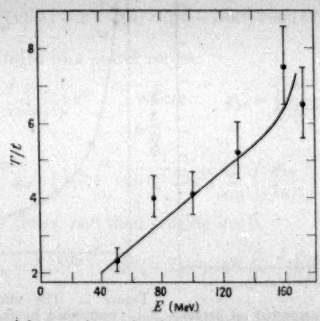

Figure 3. A comparison of the experimental and theoretical number of target traversals of an $\frac{1}{8}$ in. carbon target as a function of the proton energy E.

experimental points also plotted on this graph show gratifying agreement with theory. The irradiations were carried out over a period of several months and there was no attempt at beam current standardization, beyond maximizing the beam on a target at small radius before each irradiation. A variation of $\pm 15\%$ in beam current has therefore been allowed in computing the standard deviations on the experimental points.

ACKNOWLEDGMENTS

We should like to thank Mr. J. W. Flegg and Miss P. M. Dyson for computational work. This paper is published by permission of the Director, Atomic Energy Research Establishment, Harwell.

REFERENCES

ADAMS, J. B., and EDMUNDS, A. O., 1950, *A.E.R.E. Report* G/R 568.
HELMHOLZ, A. C., MCMILLAN, E. M., and SEWELL, D. C., 1947, *Phys. Rev.*, **72**, 1003.
ROSSI, B., and GREISEN, K., 1941, *Rev. Mod. Phys.*, **13**, 240.

The Characteristics of Long Period Photo-Effects in Lead Sulphide

By R. P. CHASMAR and A. F. GIBSON
Telecommunications Research Establishment, Great Malvern, Worcs.

Communicated by R. A. Smith; MS. received 11th January 1951

ABSTRACT. A photoconductive effect having a decay time of several hours has been observed in specially prepared layers of lead sulphide when maintained at low temperatures. These effects are characteristic of layers that have been treated in a certain manner with sulphur or with oxygen.

The general properties of the layers showing this photo-effect have been investigated. It is found that there are no first order differences between the properties of the layers containing oxygen and those containing sulphur. It is suggested that the phenomena are associated with the excitation of electrons from the upper filled band of the lead sulphide and the trapping of these electrons probably on the surface of crystallites. The depth of the traps is estimated to be of the order of 0·3 ev. below the bottom of the conduction band.

§ 1. INTRODUCTION

The existence of photo-effects of a period much greater than the normal photoconductive effect in lead sulphide and allied substances is fairly well known but few quantitative investigations have so far been reported. Genzel and Muser (1950) have observed that illumination of specially prepared lead sulphide layers at room temperature with ultra-violet radiation can cause changes in the layer conductivity which decay only very slowly with time after the removal of the exciting radiation.

In this laboratory we have observed analogous effects on irradiation of cooled layers by light in the visible region of the spectrum. For instance many lead sulphide photoconductive cells when maintained at a low temperature and illuminated by a tungsten filament lamp show the normal rapid increase in conductivity followed by a slow increase in conductivity that persists as long as the layer is illuminated. On extinction of the light however the conductivity returns rapidly to a value slightly higher than the original value of the conductivity in the dark. The final decay back to the original conductivity value may take many minutes or even hours. A rise in the magnitude of the normal rapid photo-effect accompanies the rise in conductivity due to prolonged illumination by the tungsten lamp. It was found and reported by one of us (Gibson 1949) that such long period photo-effects are exhibited to a marked degree by lead sulphide layers containing an excess of sulphur. We have since found that either excess of sulphur or strong oxidation of a layer deficient in sulphur will produce these properties. So far as first order properties are concerned there is no essential difference between the cells containing an excess of sulphur and those containing an excess of oxygen. Thus sulphur and oxygen seem to play identical roles in producing these slow photo-effects.

For simplicity we shall describe these two types of cell as 'excess sulphur' and 'excess oxygen' cells. The main properties of these cells have been determined and are described in the following experiments.

Similar slow photo-effects have been observed qualitatively in lead selenide and lead telluride but have not been exhaustively investigated. It is likely that the general behaviour for these materials is the same as for the sulphide.

§ 2. METHODS OF MANUFACTURE OF CELLS SHOWING LONG PERIOD PHOTO-EFFECTS

The cells used for the experiments described in this paper were all made in a standard Dewar type envelope (Figure 1). This form of construction permits simple direct cooling of the layer by the introduction of liquid oxygen or other coolant into the Dewar cavity. The cell blank is made from hard (Pyrex) type glass.

A conventional evacuation plant was used to pump out the cell blank to a pressure of 10^{-6} mm. Hg. Sublimation of the lead sulphide was achieved by heating the blank in an oven to about 580° c. and cooling by means of an air jet

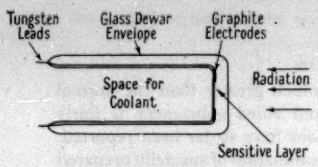

Figure 1. Section through photoconductive lead sulphide cell.

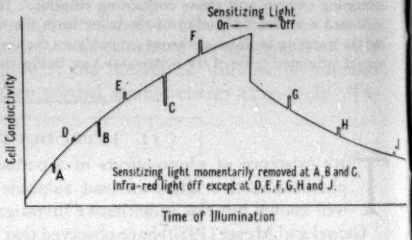

Figure 2. General behaviour of 'excess sulphur' and 'excess oxygen' cells.

that portion of the blank on which it was desired to deposit the layer. The methods of manufacture of the two types of cell were as follows:

(*a*) *Excess sulphur cells.* One milligram of PbS plus one milligram of S was introduced into the cell blank which was then evacuated to a pressure of 10^{-6} mm. Hg. With the pump sealed off the layer was collected on the electrodes. The layer was then transferred to the front window and back to the electrode, all processes taking place in the sulphur vapour. The cell was then cooled to room temperature, re-evacuated and sealed off.

(*b*) *Excess oxygen cells.* One milligram of PbS was introduced into the cell blank and the cell evacuated as before. The layer was formed on the electrode surface and then transferred from the electrode surface to the front window and back again until a layer of a few hundred ohms resistance and showing electronic conduction was obtained. Pumping continued during the whole of this process.

Air or oxygen at a few millimetres pressure was then introduced into the system and the layer baked at 200° c. for a period of the order of five to ten minutes. The time of baking and the pressure were not critical as the cell was cooled to room temperature at intervals and its properties checked until marked long period photo-effects were established. The cell was then evacuated at room temperature and sealed off. If the cell was evacuated at 200° c. the oxygen introduced into the layer was pumped out and the required cell properties were lost.

§ 3. GENERAL PROPERTIES OF 'EXCESS SULPHUR AND 'EXCESS OXYGEN' CELLS

As made, the cells showed only a small, or in exceptional cases zero, photoconductive sensitivity to infra-red illumination either at room temperature or when cooled. When however the cells were cooled in the dark to a low temperature such as liquid air temperature (90° K.) and then irradiated with light of less than a critical wavelength they acquired characteristics very similar to those of normal permanently sensitive lead sulphide cells at this temperature. As the illumination by the sensitizing light continued the cells acquired steadily increasing photoconductive properties over the whole band of wavelengths to which the PbS photoconductive cell normally responds. This includes the sensitizing band itself. At the same time the conductivity of the layer steadily increased with time of illumination by the sensitizing light, the conductivity being always 'hole' type as determined by measurements of thermo-electric power. These properties decayed very slowly with time after the removal of the sensitizing light while the layer remained cooled, this decay constituting the so-called 'slow' photo-effect. If the layer was allowed to warm up to room temperature however these properties rapidly disappeared and on recooling the layer in the dark the original non-sensitive condition was obtained. A simple diagrammatic indication of the behaviour of these cells is given in Figure 2.

The general behaviour suggested that the sensitizing light was removing electrons from the upper filled band of the semiconductor and placing them in empty traps situated below the conduction band. The free mobile holes remaining in the filled band carried the layer current which increased as more electrons were trapped. The trapped electrons would be stable only at low temperatures and warming the layer would return it to its original condition. It was with such a mechanism in mind that the following measurements were carried out. However, as will be seen, this model can at best be only partly true.

§ 4. EXPERIMENTAL PROCEDURE

Exhaustive measurements were made on four cells. These will be designated S_1 and S_2 excess sulphur cells, O_1 and O_2 excess oxygen cells.

4.1. *Conductivity and Time of Illumination*

The cells were cooled in complete darkness* to 90° K. by the introduction of liquid air into the Dewar envelope. They were then illuminated by a 24-volt 36-watt D.C. lamp placed at a distance of about 20 cm. from the layer. After measured intervals of time the lamp was switched off and the conductivity of the cell measured.

The results for two of the cells, S_2 and O_1, are given in Figure 3. Although measurements were continued in some cases for several hours with a very high intensity of illumination no saturation was obtained.

4.2. *Sensitivity and Time of Illumination*

The sensitivity of the cell to 800 c/s. pulses of monochromatic radiation was measured after various periods of illumination with sensitizing light. Measurements at wavelengths of $0{\cdot}8\,\mu$, $1{\cdot}6\,\mu$ and $2{\cdot}2\,\mu$ for the chopped radiation showed no essential difference in the shape of the curve obtained and so a wavelength of $1{\cdot}6\,\mu$ was in general used.

* This was complete visual darkness; room temperature radiation was still present. However this did not affect the experiment as is shown in § 4.5.

The sensitivity was calculated in terms of $\Delta\sigma$ where σ was the cell conductivity and $\Delta\sigma$ was the change in σ produced by the interrupted signal radiation. Care was necessary in calculating $\Delta\sigma$ to apply the right circuit corrections since the cell resistance was changing rapidly and thus $\Delta\sigma$ could not be measured simply as proportional to the A.C. voltage developed across the cell. Results

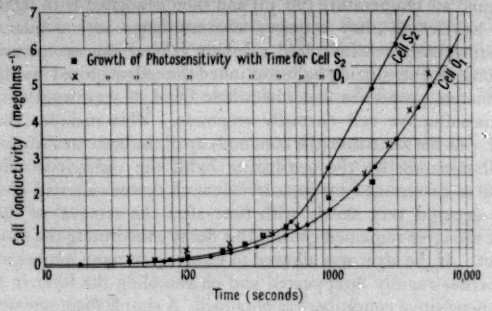

Figure 3. Conductivity against time of illumination, cells O_1 and S_2.

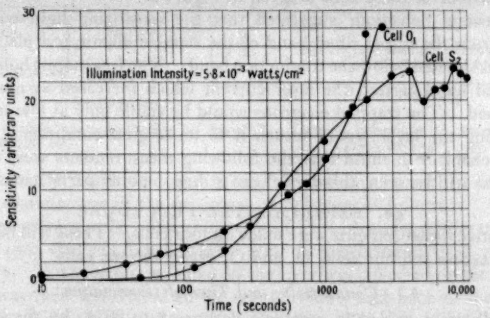

Figure 4. Sensitivity against time of illumination, cells O_1 and S_2 (cf. Figure 3.).

obtained for two of the cells, S_2 and O_1, are given in Figure 4. It was found that the time required to reach a particular cell sensitivity was inversely proportional to the intensity of the sensitizing light over a range of intensities of 1,000:1. Similar results were obtained from conductivity measurements during sensitization. The conductivity was given approximately by the empirical formula $n \propto \log(It+1)$ where n was the number of current carriers. As this should equal the number of electrons trapped the experiment is analogous to the print-out effect in photographic emulsions (Mott and Gurney 1940).

4.3. *Spectral Sensitivity*

Using 800 c/s. pulses of radiation from the monochromator the sensitivity of the cell was measured for wavelengths between 0·8 μ and cut-off. The cut-off wavelength was in the region 3·0 to 3·6 μ and three out of the four cells measured showed a small shift to longer wavelengths on illumination with the sensitizing

light. In the remaining cell the shift was towards the shorter wavelengths. The results for a typical cell, S_2, containing excess sulphur are given in Figure 5.

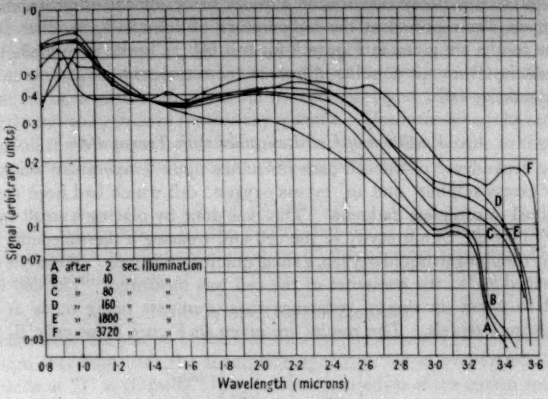

Figure 5. Spectral response of cell S_2 for different times of illumination. (Normalized to common value at 1·4 μ.)

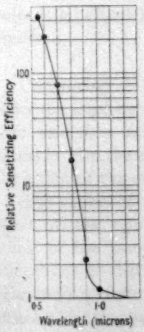

Figure 6. Sensitization spectrum for cell S_1.

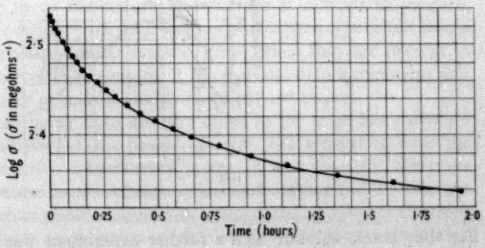

Figure 7. Decay of conductivity cell O_2 at 194·5° K. (CO_2 + ether).

4.4. *Sensitization Spectrum*

The relative efficiency of various wavelengths in producing sensitivity in an unsensitized layer was measured. This was done by replacing the sensitizing source by a monochromator and measuring the amount of sensitization produced by a known wavelength of known intensity in a given time. The sensitization spectrum is given in arbitrary units in Figure 6 for cell S_1.

4.5. *Decay of Conductivity*

The rate of decay of cell conductivity with time at a given temperature was measured by cooling the cell in darkness and then illuminating the layer until the conductivity had risen to some convenient value. The sensitizing light was

then switched off and the cell maintained at a constant temperature. Conductivity measurements were then made at definite time intervals.

At 90° K. this decay rate was so slow as to be almost unmeasurable. The experiment was repeated at the temperature of solid CO_2 in ether (194·5° K.) and the results are given in Figure 7 for cell O_2. Checks were made to ensure that radiation from surrounding objects at room temperature did not in any way affect the decay rate.

4.6. *Variation of Cell Resistance with Temperature*

The dependence of the cell dark resistance upon temperature was measured for an 'excess sulphur' and an 'excess oxygen' cell which had been cooled and maintained in complete darkness. This was done by placing a small amount of mercury into the Dewar cavity of the cell and freezing a thermocouple junction into it by dropping in liquid oxygen, a small quantity at a time. When the mercury had reached 90° K. the resistance of the cell was measured. The cell was then allowed to warm up slowly, resistance measurements being made at suitable temperature intervals. The results are given in Figure 8 for cells S_1 and O_2.

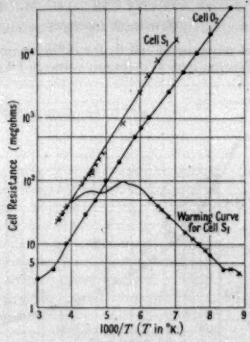

Figure 8. Resistance–temperature curves, cells S_1 and O_2.

For the 'excess sulphur' cell a further experiment was carried out. The cell was re-cooled in darkness to 90° K., and then partly sensitized by light. The cell was again allowed to warm up in darkness and the results are also given in Figure 8. Assuming, as already suggested, that an electron trapping mechanism is operating, the latter experiment indicates how the traps are emptied and how the cell returns to its unsensitized condition. From the wide range of temperatures over which trap emptying takes place it is concluded that their depth is not single valued but distributed in value.

4.7. *Time Constant*

The time taken for the signal produced by infra-red irradiation to decay to $1/e$ of its original value was measured during sensitization. Only a small variation in time constant during sensitization was observed, its value (about 1 millisecond) being about that found for many photoconductive cells at this temperature (90° K.).

4.8. *Effect on the Decay Rate of Infra-red Radiation beyond the Sensitization Limit*

A further experiment was carried out in order to examine the effect upon the decay rate of those wavelengths which produce photoconductivity but which lie outside the long wave limit of the sensitization spectrum.

Careful measurements on an 'excess sulphur' cell showed that the long-wave limit of the sensitization spectrum for this cell lay at $1{\cdot}2\mu$. Consequently $2{\cdot}0\mu$ was the wavelength used for this experiment. The intensity of the radiation corresponded to 10^{16} quanta/cm^2 falling on the layer. *No increase* in the decay rate was observed within the accuracy of the experiment.

§ 5. DISCUSSION

As already mentioned in § 3 the general behaviour of cells exhibiting long period photo-effects is strongly indicative of mechanisms involving electrons trapped in metastable levels.

5.1. *Source of the Trapped Electrons*

Evidence as to the source of the electrons can be obtained by comparing the sensitization spectrum with the absorption spectrum for an evaporated layer of lead sulphide at 77° K. (Gibson 1950). The steep edges of the curves are found to be almost coincident. Thus it would seem that the source of the electrons is the highest filled band of the lead sulphide lattice, the free and mobile positive holes left behind giving rise to the steadily increasing 'hole' current that is observed.

5 2. *Nature of the Traps*

Convincing evidence as to the nature of the traps is difficult to procure. Since the same behaviour occurs with both sulphur and oxygen type cells it would seem that they either produce similar types of traps when they are present in excess or else the traps are already present in the material before treatment and the action of the sulphur or oxygen is simply to empty the traps.

The action of the sensitizing light and the filling of the traps has a twofold effect on the photosensitivity of the layer. Firstly, the sensitivity over the whole of the photoconductive spectrum is increased and secondly, there are indications of the creation of a new photoconductive band around 3·5 microns (Figure 5). If the growth of photoconductivity is due to the trapping of electrons and if these trapped electrons are the source of the new photoconductive absorption band then the quantum efficiency of the photo-effect would be a function of the number of electrons trapped. The number of vacant mobile holes left in the filled band equals the number of electrons trapped and therefore the growth of the photo-effect with time of sensitization should follow the growth of conductivity until sufficient electrons are trapped for the quantum efficiency to approach unity. In Figure 3 it can be seen that the growth of the photo-current does indeed follow the growth of the conductivity and in the case of cell S_3 does appear to begin to flatten out for long periods of illumination. Some cells have been recorded that show a fall in sensitivity for long times of illumination (Gibson 1949). This might be due to a fall in the time constant which has also been observed or due to some fundamental inadequacy in the model under discussion.

Perhaps the most surprising phenomenon associated with the traps is the failure of all attempts to empty them by infra-red radiation (see § 4.8), although they can be easily emptied by thermal energy. If the photo-effect for wavelengths

outside the sensitization spectrum arises from excitation of trapped electrons then it would be expected that strong irradiation by wavelengths in this region would enhance the rate of decay of conductivity. No such effect was detected. This observation together with the fact that trapped electrons can exist in equilibrium in the presence of free mobile holes suggests that some spatial factor is responsible for keeping holes and electrons apart and this mechanism can only be overcome by strong thermal excitation, i.e. by heating up the layer to room temperature. A probable mechanism is the existence of surface traps on the crystallites which are maintained in a stable condition due to a space charge layer. Such a mechanism is consistent with other observations on photoconductive phenomena in lead sulphide made in this laboratory (Gibson 1950).

5.3. *Depth of the Traps*

On the model discussed above the dominant source of thermal electrons in the region between 90° K. and 300° K. would be the filled electron traps, assuming that a certain number of filled traps exist even before sensitization for a layer cooled in the dark. This is a reasonable assumption since almost all cells show a small amount of initial sensitivity. Then the relation between cell resistance and temperature in this region should give a value for the thermal trap depth. From Figure 8 an activation energy of 0·16 ev. is obtained giving a trap depth of 0·32 ev. If polarization effects can be neglected this is just the correct value to fit the observed position of the new photo peak in Figure 5.

5.4. *Growth of Conductivity with Time of Sensitization*

The analysis of a simple semiconductor model containing a single level of empty traps before sensitization leads to equations which cannot be accurately fitted to the observed curves. For this reason the calculations applying to this obviously over-simplified model are not given here. It is interesting to note however that for even a qualitative degree of correspondence to exist it can be shown that the probability of an electron being captured in a trap must be several orders less than the probability of its recapture in a mobile hole in the filled band. This conclusion arises from the observation that the conductivity is still rising after several thousand seconds of illumination by a very intense light source. Assuming a reasonable value of quantum efficiency the total number of electrons excited by the light in this time is so large that it is only possible for a minute fraction of these to be captured by the traps, even assuming the highest possible concentration of traps.

This conclusion lends support to the postulate of surface traps since a free electron in the body of the crystal would have much less likelihood of being trapped on the surface than of being caught by a mobile hole in the crystal itself.

ACKNOWLEDGMENTS

We are indebted to our colleagues at Telecommunications Research Establishment for much valuable discussion, and in particular to Miss L. M. Skinner who carried out many of the measurements described, also to the Chief Scientist, Ministry of Supply and the Controller, H.M. Stationery Office, for permission to publish this work.

REFERENCES

Genzel, L., and Muser, H., 1950, *Z. Phys.*, **127**, 194.

Gibson, A. F., 1949, *Nature, Lond.*, **163**, 121; 1950, *Proc. Phys. Soc.* B, **63**, 756.

Mott, N. F., and Gurney, R. W., 1940, *Electronic Processes in Ionic Crystals* (Oxford : Clarendon Press).

The Sensitivity and Response Time of Lead Sulphide Photoconductive Cells

By A. F. GIBSON

Telecommunications Research Establishment, Malvern, Worcs.

Communicated by R. A. Smith; MS. received 11th January 1951

ABSTRACT. Measurements of the response time and photosensitivity of lead sulphide photoconductive cells have been made with a view to establishing a theoretical working model for photoconductors of this type. The measurements include the variation in response time and photosensitivity with temperature, background illumination, applied electric field and other parameters. The results support, at least qualitatively, a theory of photoconductivity which postulates the existence of space-charge barriers at intercrystalline contacts. The height of such barriers is reduced on illumination and conduction facilitated.

§1. INTRODUCTION

THE photoconductivity of lead sulphide and similar compounds may arise from one of two processes. Either electrons are raised on illumination from bound states to conduction levels and thus increase the number of current carriers or, alternatively, the mobility of electrons already present in conduction levels is increased on illumination. One purpose of the experiments to be described is to distinguish between these two possibilities.

The general features of a theory relying upon an increase in the number of current carriers are well known (e.g. Mott and Gurney 1940, Pick 1948) and do not require further description. It is therefore proposed to give first an analysis of the mobility theory to be employed in discussing the experimental results and subsequently to describe the experiments. It must be admitted immediately that the theory given here is over-simplified, but more precise theoretical treatment does not seem to be warranted at this stage.

§2. THE BARRIER THEORY OF PHOTOCONDUCTIVITY

It is well known that a photosensitive layer of lead sulphide probably consists of a large number of micro-crystals separated by potential barriers which are the chief source of resistance (Chasmar 1948). It is assumed that the sensitization of PbS layers by baking in low pressures of oxygen is responsible for barrier formation, thus accounting for the large increase in layer resistance on oxidation (Schwarz 1948, 1949). It is postulated that the oxidation process results in the formation of a surface oxide film around each crystallite and the creation of surface states of the type envisaged by Bardeen (1947). Such states capture electrons from the interior of the crystallite (which is n-type before oxidation) and a Schottky type space-charge barrier is set up. The contact between two crystallites can then be represented by two Schottky barriers back to back. A similar model has been suggested for the contact between like crystals of silicon carbide (Mitchell and Sillars 1949), and has been briefly discussed for the present application by Smith (1951).

Photoconductivity is assumed to arise as follows: By some unspecified process (the actual process may be one of many and is immaterial in calculations

of response time or sensitivity) electrons are ejected from the surface states on illumination, thus reducing the surface negative charge. This results in a decrease in the height of the potential barrier at the surface and conduction is facilitated. Inasmuch as modulation of the barrier height is envisaged, the model is similar to those suggested qualitatively for CdS by Rose, Weimer and Forgue (1949) and for PbS by Rittner (1950) and Schwarz (1949). A decrease in barrier height on illumination has been observed in germanium by Brattain (1947) in measurements of work function. The general importance of intercrystalline barriers in PbS has been shown by the work of Sosnowski *et al.* (1947).

§ 3. THE CALCULATION OF RESPONSE TIME ON BARRIER THEORY

The type of intercrystalline barrier envisaged is sketched in Figure 1, where ϕ is the height of the barrier in electron volts and E the depth of the surface states below the conduction band. Let n_0 be the number of surface states per square

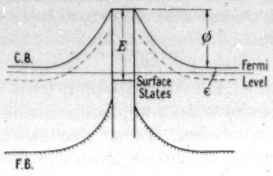

Figure 1.

metre; at any temperature above absolute zero Δn_0 surface states are empty, electrons having been ejected by thermal energy. Then, to a good approximation,

$$\Delta n_0 = n_0 \exp\{(\phi + \epsilon - E)/\boldsymbol{k}T\}, \qquad \ldots\ldots(1)$$

where $(\phi + \epsilon - E)$ is the energy depth of the surface states below the Fermi level (Figure 1). It is assumed throughout that $(\phi + \epsilon - E)$ is large compared with $\boldsymbol{k}T$ and that ϵ is approximately the same for all crystals.

Let M be the density of impurities per cubic metre in the semiconductor. It is assumed that these impurities lie close to the conduction band, and hence the number of electrons in the conduction band in the interior of each crystal is largely independent of temperature. This assumption is supported by measurements of Hall constant carried out in this laboratory (Putley and Chasmar 1951) and elsewhere (Dunaev 1947).

Following Bardeen (1947) the height of the barrier is then given by

$$\phi = \frac{M\boldsymbol{e}^2 l^2}{2K} = \frac{(n_0 - \Delta n_0)^2}{2KM}\boldsymbol{e}^2, \qquad \ldots\ldots(2)$$

where l is the depth of the space-charge penetration in metres and K the dielectric constant in farads per metre. The surface charge σ is given by

$$\sigma^2 = (\boldsymbol{e}Ml)^2 = 2KM\phi = (n_0 - \Delta n_0)^2\boldsymbol{e}^2. \qquad \ldots\ldots(3)$$

Suppose that on illumination the barrier height is reduced to $(\phi - \Delta\phi)$ and $(\Delta n_0 + \Delta n)$ surface states are empty, Δn having been emptied by illumination, then $\sigma\Delta\sigma = KM\Delta\phi$ and also $\Delta\sigma = \boldsymbol{e}\Delta n$; hence

$$\Delta n = \frac{KM}{\boldsymbol{e}\sigma}\Delta\phi = \frac{KM}{\boldsymbol{e}^2(n_0 - \Delta n_0)}\Delta\phi \simeq \frac{KM}{\boldsymbol{e}^2 n_0}\Delta\phi. \qquad \ldots\ldots(4)$$

For simplicity we shall put

$$N = KM/e^2 n_0 = (KM/2e^2\phi)^{1/2}. \qquad \ldots\ldots(5)$$

Now if Q is the total number of electrons flowing both ways across unit area of the barrier per second, then

$$Q = \text{constant} \cdot \exp(-\phi/kT). \qquad \ldots\ldots(6)$$

The incremental change in Q when Δn surface states are emptied by illumination is given by substituting equations (4) and (5) into equation (6) and is

$$\Delta Q = (Q/NkT)\Delta n \qquad \ldots\ldots(7)$$

provided that $\Delta Q \ll Q$, a condition which is always maintained experimentally. Q is, of course, approximately proportional to the observed current through the barrier and exactly proportional to it at high applied field strengths. The current i and the quantity Q are given by equations (8) and (9):

$$i = \text{constant} \cdot \exp(-e\phi/kT) \exp(-eF_2/kT)[\exp\{e(F_1+F_2)/kT\}-1] \qquad \ldots\ldots(8)$$

and

$$Q = \text{constant} \cdot \exp(-e\phi/kT) \exp(-eF_2/kT)[\exp\{e(F_1+F_2)/kT\}+1], \qquad \ldots\ldots(9)$$

where F_1 and F_2 are the voltage drops across each side of the barrier respectively (cf. Mott and Gurney 1940, p. 184).

Under steady-state conditions two further equations may be written down. In the dark we have

$$pQ\Delta n_0 = \nu n_0 \exp(-E/kT), \qquad \ldots\ldots(10)$$

where p is the capture cross section of an empty surface state and ν a constant having the dimensions of a frequency (Mott and Gurney 1940, p. 130). The quantity ν is determined in terms of p by equations (1) and (10).

When the layer is illuminated by a small intensity of infra-red radiation which ejects I electrons per second per square metre from surface states, then, in equilibrium,

$$I + \nu n_0 \exp(-E/kT) = p(Q+\Delta Q)(\Delta n_0 + \Delta n). \qquad \ldots\ldots(11)$$

Substituting equations (7) and (10) into equation (11) gives

$$I = \Delta Q\left\{\frac{\nu \exp(-E/kT)}{Q} + pNkT\right\} \qquad \ldots\ldots(12)$$

and thus ΔQ and hence the incremental change in current is proportional to the intensity of illumination for small signals, a well-known experimental result.

As I in equation (12) represents the rate of emptying of surface states, the right-hand side of the equation represents the rate of filling of holes. Hence

$$-\frac{d(\Delta n)}{dt} = \Delta Q\left\{\frac{\nu \exp(-E/kT)}{Q} + pNkT\right\}$$

$$= \Delta n \frac{Q}{NkT}\left\{\frac{\nu \exp(-E/kT)}{Q} + pNkT\right\}. \qquad \ldots\ldots(13)$$

Clearly equation (13) represents an exponential decay the time constant of which is given by

$$\tau_0 = \frac{NkT}{pQNkT + n_0\nu \exp(-E/kT)}. \qquad \ldots\ldots(14)$$

For the purpose of the experiments to be described it is also necessary to know the time constant of a photoconductive layer as measured by illuminating the layer with short pulses of low intensity in the presence of a steady background illumination of high intensity A. The background illumination A can be considered as acting in parallel with the thermal emptying of surface states, and then it can easily be shown that

$$\tau_A = \frac{NkT}{pQ_A NkT + n_0 \nu \exp(-E/kT) + A}, \qquad \ldots\ldots(15)$$

where τ_A and Q_A are respectively the time constant and current in the presence of the background illumination.

§4. THE CALCULATION OF PHOTOSENSITIVITY ON BARRIER THEORY

The photosensitivity of a photoconductive layer is usually defined as the fractional change in conductivity for unit incident intensity. Following this definition, the sensitivity is here defined as $S = d(\Delta Q/Q)/dI$. By differentiation of equation (12) and substitution from equation (14) it may be shown that

$$S = \tau/NkT. \qquad \ldots\ldots(16)$$

It is of interest to obtain equation (16) by another method which demonstrates its general nature. For small signals, on any theory, $\Delta Q = CI\tau$ in equilibrium. If I is defined, as above, as the number of electrons raised per second then C is a constant relating the number of holes produced to the number of electrons set in motion. For any theory relying solely upon an increase in the number of current carriers the numbers of holes and electrons produced are equal, that is, C equals unity. Hence

$$S = \tau/Q. \qquad \ldots\ldots(17)$$

This equation is perfectly general and applies to any numbers theory. It is obtained, for example, by Pick (1948) in a typical numbers theory.

For any barrier theory, however, the number of electrons set in motion per hole produced (and hence C) must be proportional to Q and hence Q cannot appear in the sensitivity equation. In the particular barrier model considered C is given by equation (7) and is equal to Q/NkT or $S = \tau/NkT$ as before. Thus the relation between sensitivity and response time is markedly different for the two types of theory, and the theories may be distinguished experimentally. In view of their general nature these relations are of some importance.

§5. EXPERIMENTAL METHODS

The lead sulphide cell under test was wired in series with a load resistance and the junction connected to a wide band A.C. amplifier designed by Mr. T. S. Moss of this laboratory. Care was taken to ensure that the electrical time constant of the input circuit was much less than that of the PbS cell.

The cell was illuminated either by a neon bulb driven with square pulses from a multivibrator or by means of a monochromator, the radiation from which was periodically interrupted by a sectored disc. The resulting voltage pulse at the output of the amplifier was displayed on a cathode-ray tube. The time base, the frequency of which could be altered in steps, was triggered by the illuminating pulse. The resulting display was then photographed and subsequently projected on to graph paper to be traced out. In view, however, of the very tedious nature of this method the signal at various decay times was sometimes read off directly from the display and immediately plotted on the appropriate coordinates.

It is well known that a sensitive PbS cell will detect room temperature radiation when the layer is cooled (Watts 1949), and this effect can reduce the cell resistance at 90° K. by as much as 100 times. A similar reduction in time constant takes place. If, therefore, the cell was to be examined at low temperatures, the cell and illuminating neon were totally immersed in a large Dewar of liquid oxygen and all possible light excluded. The PbS cells being of the normal Dewar-type construction, the layer temperature was measured by a thermocouple frozen into mercury in the inner tube.

It was found experimentally that the rate of decay of photoconductivity was dependent on the time duration of the initial light pulse if this was short. For this reason care was taken to ensure that the photocurrent saturated within the available pulse length. This condition was also essential for sensitivity measurements which relied upon measurements of pulse magnitude.

Finally, care had to be taken to ensure that the condition $\Delta Q \ll Q$ was maintained throughout. This proved very difficult at low temperatures, due to the high absolute sensitivity of the cell and the increased electrical noise due to the high cell resistance. In addition, some commercial chemical PbS cells proved very unstable at 90° K. The required condition was therefore not always adequately achieved.

§ 6. EXPERIMENTAL RESULTS

(i) *The Temperature Dependence of the Decay of Photoconductivity*

Typical sets of decay curves at various temperatures are given for two PbS cells in Figures 2 and 3. The cells were manufactured by chemical

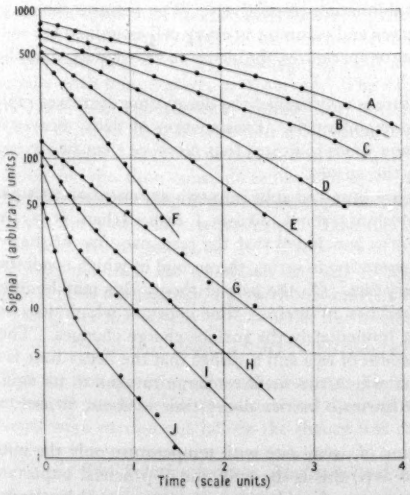

Curve	Temp(°K)	τ (μ sec)
A	77	1180
B	98	1020
C	133	790
D	159	585
E	183	407
F	205	230
G	224	70
H	243	44
I	263	26
J	282	16

Figure 2. Chemical cell decay curves.
Time base: curves A to F, 1 scale unit = 400 μsec.; curves G to J, 1 scale unit = 90 μsec.
Note. Curves have been displaced for clarity.

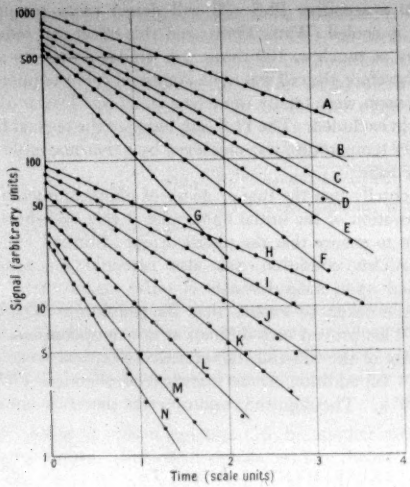

Curve	Temp(°K)	τ(μsec)
A	77	780
B	98	640
C	133	585
D	183	540
E	205	460
F	224	390
G	243	300
H	263	153
I	273	126
J	282	96
K	292	78
L	306	62
M	320	45
N	332	34·5

Figure 3. Evaporated cell decay curves.
Time base: curve A, 1 scale unit = 400 μsec.; curves B to G, 1 scale unit = 440 μsec.; curves H to N, 1 scale unit = 90 μsec.
Note. Curves have been displaced for clarity.

deposition and vacuum sublimation respectively. The features which are clear from inspection of the curves and common to every cell examined are as follows:

(*a*) At sufficiently low temperatures the decay is adequately described by a single exponential.

(*b*) As room temperature is approached the decay time decreases rapidly and the decay splits into two exponentials. Examination of decay curves at these temperatures over very long times indicates that no more than two exponentials are required to describe the curves.

(*c*) The decay curves are found to split into two exponentials at a particular value of initial time constant (about 50 μsec.) rather than at a particular temperature. From this it is concluded that the response time of the system is limited by two processes operating in series, the second of which is not important until the first becomes very fast. On the barrier theory this may be interpreted as follows: the barrier itself has an intrinsic time constant which does not allow the barrier height to alter immediately the surface charge changes. The theory already given takes no account of this and assumes that the decay time is entirely determined by the rate at which the surface charge returns to its equilibrium value. On this view the intrinsic barrier decay time is about 50 μsec. at room temperature.

In plotting the variation of decay rate with temperature only the initial time constant has been plotted as (i) this is the only one of practical importance, and (ii) it can be measured over a much wider temperature range than the final time constant which is masked by it at low temperatures. Figures 4 and 5 give the variation of time constant of two typical chemical PbS cells together with the

variation of the cell resistance in the dark. Eight cells (four chemical and four evaporated) have been examined in this way, and in all cases the results are qualitatively the same. At high temperatures the time constant falls rapidly (exponentially) with increasing temperature, but at low temperatures the rate of change of time constant with temperature is much less.

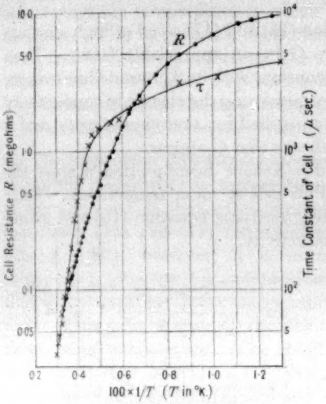

Figure 4. Chemical cell.

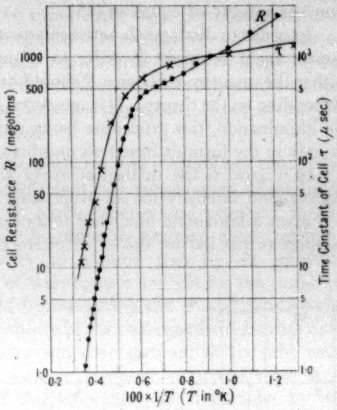

Figure 5. Chemical cell.

To compare these experiments with theory, equation (14) can be written in two parts. At high temperatures the exponential term is the most important and the time constant τ_0 is given by $N\boldsymbol{k}T/n_0\nu \exp(-E/\boldsymbol{k}T)$ and hence τ decreases exponentially with temperature, as observed. The values of E in electron volts obtained from the experimental results are, for the four chemical cells, 0·23, 0·20, 0·27, 0·16 and, for the four evaporated cells, 0·16, 0·19, 0·23, 0·15.

At low temperatures the exponential term in equation (14) is very small and the equation for the time constant reduces to $\tau_0 = 1/pQ$. Hence, unless p is a temperature-dependent quantity, we expect τ_0 to be proportional to the resistance in the dark in the same temperature region. That this is only very approximately so can be seen from inspection of Figures 4 and 5. Possibly the inability adequately to maintain the condition $\Delta Q \ll Q$ in this temperature region is responsible for this discrepancy, and further, it must be remembered that observed current and Q are not strictly proportional but related by

$$i/Q = \text{const.}\ \{\exp(\boldsymbol{e}F/\boldsymbol{k}T) - 1\}/\{\exp(\boldsymbol{e}F/\boldsymbol{k}T) + 1\},$$

where F is the voltage drop across the barrier. Unfortunately the values of F were not exactly the same for resistance and time-constant measurements as the experiments were carried out before the theory was devised.

(ii) *The Relation between Sensitivity and Time Constant*

(*a*) *Background illumination.*

The steady background illumination was provided by a battery-driven tungsten lamp at various distances from the cell. Tests with filters indicated that the

wavelength of the background illumination was immaterial provided it came within the special range of the cell.

The variation in time constant and sensitivity with background illumination can be used to distinguish between equations (16) and (17) (and hence between barrier theory and numbers theory) as Q, which is a function of illumination, appears in one of the equations. In addition, the experiment may be used to test the validity of equation (15).

In order to distinguish between equation (16) and (17) a cell of high absolute sensitivity is required in order to change Q by an appreciable factor. Then either the quantity τ/SQ or τ/S should be constant with background illumination, depending on the theory. Q is measured by measuring the change in conductivity on illumination, this procedure being quite justified for a numbers theory, and it is only in the formula based on numbers theory that Q appears.

In Figure 6 the quantities τ/SQ and τ/S have been plotted against the background intensity for an evaporated PbS cell at room temperature. Only τ/S gives a horizontal line, thus immediately verifying equation (16) and giving support to the barrier theory of photoconductivity.

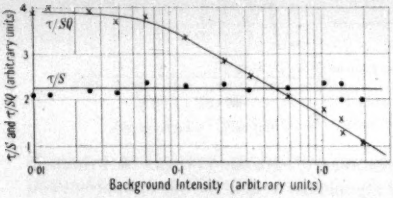

Figure 6. Evaporated cell at room temperature.

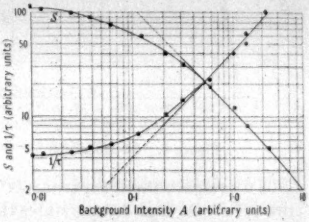

Figure 7. Evaporated cell at room temperature.

Observations on the variation of time constant with background illumination allow equation (15) to be checked. In Figure 7 the logarithm of $1/\tau$ and of S have been plotted against the logarithm of the background intensity. From equation (15) both S and τ will be largely independent of background intensity for small values of A, and subsequently S will decrease and $1/\tau$ increase proportionately with increasing A. On logarithmic coordinates this implies a slope of unity. For each curve of Figure 7 the appropriate 45° slope has been drawn in to lie upon the experimental points. Over the range of background intensities used the agreement between theory and experiment is quite adequate. A further feature of equation (15) which differs from that of any numbers theory is that, depending on the relative magnitude of A and the other terms, it is possible to obtain a change in time constant and sensitivity without a comparable change in conductivity. This situation is impossible on a numbers theory as τ, and hence S, only change with background illumination because the background increases the number of electrons and holes available for recombination. Experiments indicate that the change in τ and S is always more marked than the change in Q for PbS cells. In one case a change in τ and S of a factor of 34 was observed for a 28% change in conductivity. A large change in τ with A implies that the other terms are small and hence τ large. The time constant of this particular cell when in the dark was about 400 μsec., an unusually large value at room temperature.

The variation of time constant with temperature in the presence of background illumination has been measured by Lashkarev, Potapenko and Fedorus (1949), the results being given in Figure 11 of their paper. From equation (15) it will be seen that in the presence of background illumination τ should be largely independent of temperature at low temperatures, though at higher temperatures the exponential term will again become important. As the background intensity is increased the temperature at which the exponential term becomes important increases. This is precisely what these experimenters observe. The value of the quantity E may be obtained from their results both from the slope of the relation between τ and temperature at high temperatures and from the actual temperature at which the exponential term becomes important. Good agreement is obtained between these two determinations.

(*b*) *The temperature dependence of the relation between time constant and sensitivity.*

As the quantity Q is temperature dependent the temperature dependence of the ratio τ/S is markedly different in barrier theory and numbers theory (equations (16) and (17) respectively). In order to examine these relations experimentally, however, it is necessary to assume that (i) the effective illumination intensity I is independent of temperature and (ii) for the numbers theory the quantity Q can be measured by measuring the conductivity of the layer. That is, it is assumed that the mobility of the current carriers varies only slowly with temperature. The sensitivity and time constant of six cells were determined over as wide a temperature range as possible, two of these cells being examined by Mr. V. Roberts of this laboratory, the remainder by the writer. The experimental results were best expressed by plotting $\log(\tau/S)$ against either $\log T$ (barrier theory) or $\log Q$ (numbers theory). A slope of unity would then indicate agreement between theory and experiment. The results are given in the following Table:

Cell	Numbers theory plot	Barrier theory plot
Evaporated	2·7	1·24
Evaporated	5·6	1·29
Chemical	3·1	1·7
Chemical	2·5	1·3
Evaporated	3·2	1·48
Evaporated	2·4	1·34

Clearly, neither theory is in exact agreement with the experimental results, though the barrier theory is considerably better than the numbers theory. Perhaps this result is better illustrated as follows. We expect theoretically that (i) on barrier theory the quantity $\tau T/S$ should be constant with temperature: in fact it changes by a factor of about 1·4 between 90° K. and 290° K. (equivalent to a 1·3 power law); (ii) on numbers theory the quantity $\tau Q/S$ should be constant with temperature: in fact it changes by a factor of about 22·0 between 90° K. and 290° K. (equivalent to a 3·0 power law).

In spite of the fairly good agreement between barrier theory and experiment the discrepancy is too large and too consistent to be dismissed as experimental error. The discrepancy could be explained by assuming that the effective intensity increased on cooling from room temperature to 90° K. by a factor of about 1·4, due to a change in quantum efficiency. A more likely explanation

has, however, been suggested by recent measurements now in progress on the photoconductivity of single contacts. It is found experimentally, and predicted theoretically, that the height of the barrier ϕ decreases on increasing the temperature. Hence from equation (5) the constant N increases with increasing temperature and the change in N is found to be of the correct magnitude to explain the above discrepancy.

(iii) *The Effect of the Applied Electric Field*

Almost any theory of the time constant of photoconductive materials must involve the quantity Q or some related quantity. In a numbers type of theory, however, the increase in current on increasing the applied field arises from the increased drift velocity of the Q electrons in the conduction levels of the crystal. In a barrier theory this is not so. The applied field modifies the height of the barrier and hence the number of electrons moving across it. It is, of course, on this basis that barrier conductivity equations (for example equations (8) and (9)) are calculated. Thus the quantity Q is voltage dependent on barrier theory and independent of voltage on a numbers theory. Hence any variation of time constant or sensitivity with applied field is evidence in favour of a barrier theory. From equation (14) we expect that at temperatures around room temperature the time constant and sensitivity will be largely independent of applied field for low field strengths and will fall off at high fields so that S or τ are inversely proportional to Q and hence to the cell current.

In Figure 8 the sensitivity of a typical evaporated cell is plotted on logarithmic coordinates against the cell current. Qualitatively the expected behaviour is obtained. The application of high fields to PbS cells often produces permanent changes in the characteristics of the cells, and for this reason the sensitivity is given as the field was increased and subsequently decreased.

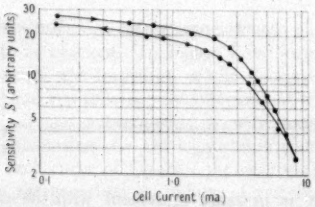

Figure 8. Evaporated cell at room temperature.

The quantities Q and i should be proportional at high voltages, and hence the sensitivity should fall off on a 45° slope at high currents. In fact the sensitivity falls off more rapidly than this. This feature was common to most cells examined, and only one gave a 45° slope in this region. This effect may be due to local heating at the intercrystalline contacts due to the large currents passed.

The existence of an effect due to the applied field having been established, which in itself gives support for the barrier theory, the variation in sensitivity and time constant with applied field was measured at various fixed temperatures. From equation (14) the condition that the sensitivity or time constant shall a ll to one-half of its original value is $pQM\boldsymbol{k}T = \nu n_0 e^{-E/\boldsymbol{k}T}$. Hence the current

at the above condition should be exponentially dependent on temperature and E may be determined for comparison with the value obtained from the variation of time constant with temperature. Experimentally it is found that the cell current when the sensitivity has fallen to half its original value does vary exponentially with temperature, and initial measurements were very encouraging. For the first cell examined the value of E from the variation of time constant with temperature was 0·164 ev. and from the voltage curves 0·161 ev. In no other case was the agreement as good as this, however, and in one cell the values obtained were 0·23 ev. and 0·15 ev. respectively, representing a very considerable discrepancy. The extent to which this was due to the lack of proportionality between i and Q could not be determined.

(iv) *The Effect of the Duration of the Illuminating Pulse*

The decay of the photocurrent after cessation of illumination has been found to be a function of the length of the exciting light pulse if its duration is comparable with the time taken to rise to equilibrium. This effect is most easily measured at low temperatures where the time of rise is long. At these temperatures the time constant increases as the pulse length decreases. This result is illustrated by the following figures for a typical chemical PbS cell at temperature 90° K.:

Pulse length (μsec.)	1400	820	153	80	39
Time to decay to half of original value (μsec.)	680	710	890	1000	1030

Similar results have been obtained for other chemical and evaporated cells. The experiment may be performed in two ways: either (*a*) the illumination intensity is not varied simultaneously with the pulse length and the decay commences from a different current value each time, or (*b*) the intensity is adjusted for each pulse length so that the decay commences from the same current value each time. In either case the result is qualitatively the same.

An explanation of these effects is not easy. A variation in decay rate with pulse length has been observed in phosphors by Garlick and Wilkins (1945), but it is in the opposite direction to the above and is due to an electron trapping phenomenon.

A possible qualitative explanation of the effect on barrier theory assumes that the barrier has an intrinsic response time, as suggested before. If then the exciting light pulse is cut short before equilibrium is attained the barrier will not have fallen as much as it should have done for a given number of emptied surface states. The decay will then commence with a higher barrier and the rate of recombination with surface states will be reduced. Hence the time constant will increase as the pulse length decreases, which is observed.

(v) *The Variation in Response Time with Exciting Pulse Intensity*

For very high exciting intensities, such that $\Delta Q \gtrsim Q$, the time constant falls rapidly with increasing excitation intensity. This would be expected on almost any theory. But the time constant is also slightly intensity-dependent when $\Delta Q \ll Q$, as illustrated by the following figures for a PbS evaporated cell at room temperature:

Excitation pulse intensity (arbitrary units)	5	10	40	160	490	1550
Time constant (μsec.)	220	235	247	240	210	178

This behaviour, which shows a maximum in τ, seems to be common to all PbS cells. It will be appreciated that the effect is very small, and a large change in intensity is required to produce any observable change in τ. At the highest intensity quoted in the above table $\Delta Q/Q$ was about 1·5%, so the condition $\Delta Q \ll Q$ is maintained throughout.

(vi) *The Variation of Decay Rate with Excitation Wavelength*

In the wavelength range from 0·4μ to 2·6μ there is no significant change in time constant with excitation wavelength. This result was first obtained by Mr. V. Roberts of this laboratory and later confirmed by the writer.

(vii) *The Time of Rise of Photoconductivity*

The time constant discussed here refers, of course, to the time of decay. The rise of the photocurrent on illumination follows the usual relation $i=i_0(1-e^{-t/\tau})$ where τ has two values when the decay involves two time constants. It is found, however, that τ_{rise} is always less than τ_{decay} under all conditions of excitation intensity, temperature, applied field, etc. The ratio $\tau_{\text{decay}}/\tau_{\text{rise}}$ is usually just under 2·0. It may fall as low as 1·2 at very low exciting intensities and is occasionally as high as 2·5.

It was originally thought that measurements of rise time would give information on the process by which electrons are ejected from the surface states, but in view of the relative constancy of the ratio $\tau_{\text{decay}}/\tau_{\text{rise}}$ a likely explanation of the difference between rise and decay time is as follows: In a real photoconductive cell there are a very large number of intercrystalline barriers, and values of τ are not likely to be single-valued but distributed in value. As the decay is given by $i=i_0e^{-t/\tau}$, those barriers with the largest values of τ will contribute the most current at any time t. During rise, however, $i=i_0(1-e^{-t/\tau})$, and those barriers with the smallest values of τ will contribute the most current at any time t. Hence, on the average, τ_{decay} will be slightly greater than τ_{rise}, as observed.

§7. CONCLUSIONS

From the experiments carried out and the theory given it is concluded that a model involving intercrystalline space-charge barriers whose height may be reduced on illumination gives a fairly good explanation of the experimental results. The equations obtained sometimes give only a qualitative description of the experimental results, but the success of the sensitivity equation (16) and the variation in time constant and sensitivity with applied electric field would appear to necessitate a barrier theory.

It will be appreciated that the theoretical equations developed here do not apply uniquely to the type of barrier envisaged. Any modulated barrier will lead to approximately the same results, and the generality of equation (16) has already been stressed.

One feature of the experimental methods which might be expected to lead to qualitative rather than to quantitative agreement with theory is the use of multi-contact photocells. Recently work has begun on the photoconductivity of single contacts to PbS or PbTe crystals; so far photosensitivity has been observed only at such contacts, illumination of the bulk of the crystal being entirely ineffective. It is hoped by these measurements to determine more accurately the properties of photosensitive contacts.

ACKNOWLEDGMENTS

The author is indebted to his colleagues at Telecommunications Research Establishment for much help, advice and criticism, and particularly to those to whom reference has been made in the text. He is indebted to the Chief Scientist, Ministry of Supply, and to the Controller, H.M. Stationery Office, for permission to publish this work.

REFERENCES

BARDEEN, J., 1947, *Phys. Rev.*, **71**, 717.
BRATTAIN, W., 1947, *Phys. Rev.*, **72**, 345.
CHASMAR, R. P., 1948, *Nature, Lond.*, **161**, 281.
DUNAEV, J. A., 1947, *C. R. Acad. Sci. U.S.S.R.*, **55** (No. 1), 21.
GARLICK, G. F. J., and WILKINS, M. H. F., 1945, *Proc. Roy. Soc.* A, **184**, 408.
LASHKAREV, V. E., POTAPENKO, I. R., and FEDORUS, G. A., 1949, *J. Exp. Theor. Phys., U.S.S.R.*, **19**, 887.
MITCHELL, E. W. J., and SILLARS, R. W., 1949, *Proc. Phys. Soc.* B, **62**, 509.
MOTT, N. F., and GURNEY, R. W., 1940, *Electronic Processes in Ionic Crystals* (Oxford : Clarendon Press).
PICK, H., 1948, *Ann. Phys., Lpz.*, **3**, 255.
PUTLEY, E. H., and CHASMAR, R. P., 1951, *Proceedings of International Conference on Semiconductors, University of Reading* (London : Butterworth's Scientific Publications), in the press.
RITTNER, E. S., 1950, *Science*, **111**, 685.
ROSE, A., WEIMER, P. K., and FORGUE, S. V., 1949, *Phys. Rev.*, **76**, 179.
SCHWARZ, E., 1948, *Nature, Lond.*, **162**, 614; 1949, *Proc. Phys. Soc.* A, **62**, 530.
SMITH, R. A., 1951, *Proceedings of International Conference on Semiconductors, University of Reading* (London : Butterworth's Scientific Publications), in the press.
SOSNOWSKI, A., *et al.*, 1947, *Nature, Lond.*, **159**, 818.
WATTS, B. N., 1949, *Proc. Phys. Soc.* A, **62**, 456.

LETTERS TO THE EDITOR

Multiple Traversal of Cyclotron Targets

A paper by Cassels, Dickson and Howlett (1951) gives the theoretical relation between the average number of traversals T/t of a cyclotron target and a parameter $\lambda = w^2nd^2/4tr_0^2$, where t is the actual thickness of the target and T the effective thickness. When the values of w, n, d and r_0 for the 110 in. Harwell cyclotron at 150 MeV. are substituted in this equation a curve of the average number of traversals against target thickness in radiation lengths can be drawn (see Figure). This curve is independent of the target material. The abscissae are also plotted in gm/cm² of carbon, for which the radiation length is 52 gm/cm².

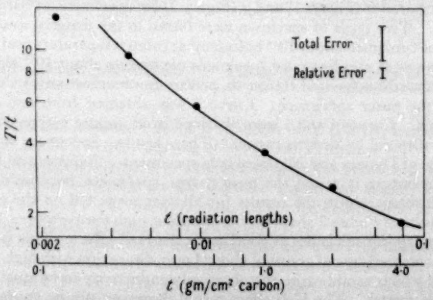

A comparison of the experimental and theoretical number of target traversals T/t as a function of the target thickness t, in radiation lengths and in gm/cm² of carbon.

Several carbon targets were irradiated in the cyclotron internal proton beam at 150 MeV. to verify this theoretical curve. The targets were all 1 in. in height and varied in thickness from 0·030 in. to 1·0 in. (i.e. 0·122 gm/cm^2 to 4·064 gm/cm^2). Each target was irradiated for 5 minutes. Since the cross section for the production of beryllium 7 from carbon is known for 150 MeV. and the excitation function is nearly constant in the range 150 MeV. to 100 MeV. (Dickson and Randle to be published), the effective number of traversals could be calculated for each target from the beryllium 7 counting rate in a calibrated γ-ray Geiger counter and the known true beam current. The chief uncertainties in these measurements were in the value of the true beam current and the efficiency of the Geiger counter. The total errors on each of the experimental points was estimated at 15% standard deviation, while the relative errors are less than 5%. The theoretical curve of T/t has been calculated up to $\lambda=4$; it therefore does not include the experimental point at $t=0{\cdot}0023$, which corresponds to $\lambda=6{\cdot}34$.

The author wishes to thank the cyclotron operating team for their co-operation during these experiments.

Atomic Energy Research Establishment,
Harwell, Didcot, Berks.
23rd February 1951.

J. M. DICKSON.

CASSELS, J. M., DICKSON, J. M., and HOWLETT, J., 1951, *Proc. Phys. Soc.* B, **64**, 590.

Lead Sulphide—An Intrinsic Semiconductor

Numerous measurements of the Hall coefficient R and conductivity σ of lead sulphide have been made at room temperature. These have indicated that it may be a p- or n-type semiconductor with carrier concentration ranging from 10^{16} to 10^{20}/cm^3, of either sign. Also it has been found that by suitable heat treatments p-type specimens may be converted to n-type and vice versa (Eisenmann 1940). Mott (1949) has pointed out that from these results one should expect to observe intrinsic conductivity in the purer samples of PbS.

Measurements of the variation of R and σ with temperature have been made by Dunaev and Maslakovitz (1947); but they did not find any evidence for intrinsic conductivity. The specimens they used contained not less than 10^{18} electrons/cm^3, and it will be seen from the results described here that specimens as impure as this do not show intrinsic conductivity below 1,000° K., while Dunaev and Maslakovitz did not make measurements at temperatures greater than 900° K.

We have measured R (Figure 1) and σ (Figure 2) for specimens of Sardinian galena from 290 to 1,100° K. Two types of specimen were found in the material available to us. The purest specimens contained about 10^{16} holes/cm^3 at room temperature and showed transistor effects, and there were also less pure specimens containing about 10^{17} electrons/cm^3 which did not show transistor behaviour (Hogarth, private communication). Curves 1 and 2 were obtained from the purer specimens. Curve 3 was obtained from one of the fairly pure n-type specimens. Curves 4 and 5 were obtained from impure n-type specimens prepared from the purer material by heat treatment. These last two specimens were of purity comparable with that of Dunaev and Maslakovitz's specimens. Referring to Figure 1, it is seen that as the temperature is raised the pure p-type specimens become n-type and that at sufficiently high temperatures the results for all specimens fall on the same curve. The conductivity results in Figure 2 show similar trends at high temperatures, but the agreement between different specimens is not as good as for the Hall effect. This is probably because the specimens contained crystal grains of about 1 mm. dimension with high resistance barriers separating them which would cause the observed conductivity to be smaller than would be found in a single crystal. The Hall effect would, however, not be appreciably affected by these barriers.

The criterion for intrinsic conductivity in a semiconductor is that the value at a given temperature should be independent of the specimen on which it is measured. The temperature at which a given specimen starts to exhibit intrinsic properties of course depends on its purity. Since we have observed values of the Hall coefficient of PbS above 650° K. which are the same for a number of specimens of different purity we believe these results represent the intrinsic region.

It will be noticed that the impure specimens 4 and 5 show a long transition region in which the Hall coefficient varies quite rapidly before finally reaching the intrinsic curve. Dunaev and Maslakovitz measured only this transition region. They concluded that it was not the intrinsic region, but they attributed the change in R to electrons from deep impurity levels. By fitting straight lines to their results between 700° and 900° K. they found an activation energy of about 0·3 ev. for their impurity centres. Similar values are obtained if straight lines are fitted to our results over this range.

From the results for the intrinsic region one expects to determine the distance ϵ between the full and empty bands. The intrinsic Hall coefficient should vary according to the formula $R=AT^{-3/2}e^{\epsilon/2kT}$, and for the elementary semiconductors silicon and germanium this has been substantiated. But for lead telluride the intrinsic results cannot be represented

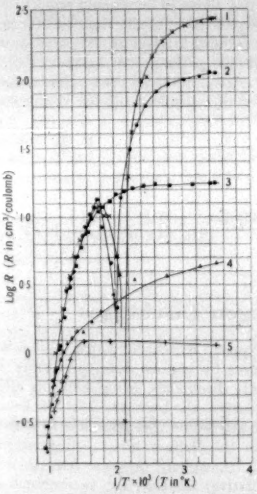

Figure 1. Hall coefficient of Sardinian galena.

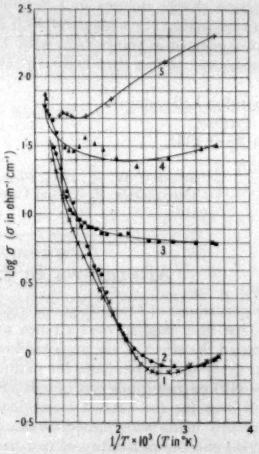

Figure 2. Conductivity of Sardinian galena.

by this formula unless one assumes ϵ to be a function of T (Putley, unpublished). The formula was checked for PbS by plotting $(\log R+(3/2)\log T)$ against $1/T$. The result was not a straight line, although it appeared to tend to a straight line above 900° K., and its slope gave $\epsilon=1{\cdot}17$ ev. Similar behaviour in the intrinsic region has already been found for PbTe. The limiting value of ϵ is of the order expected from measurements of the absorption edge in PbS (Gibson 1950). This also was found for PbTe.

The conclusions reached from these measurements are that PbS does exhibit intrinsic conductivity, and behaves qualitatively according to the accepted semiconductor model with an energy gap of about 1·2 ev. The theoretical formulae which have given such good agreement with experimental results for the elementary semiconductors Si and Ge do not fit the intrinsic curve for PbS so well; this behaves very similarly to PbTe.

We wish to thank Dr. C. A. Hogarth of Reading University for supplying us with samples of Sardinian galena. Acknowledgment is made to the Chief Scientist, Ministry of Supply, and the Controller of H.M. Stationery Office for permission to publish this letter.

Telecommunications Research Establishment,
Ministry of Supply, Great Malvern, Worcs.
12th April 1951.

E. H. Putley.
J. B. Arthur.

Dunaev, C. A., and Maslakovitz, J. P., 1947, *J. Exp. Theor. Phys.*, **10**, 901.
Eisenmann, L., 1940, *Ann. Phys., Lpz.*, **38**, 121.
Gibson, A. F., 1950, *Proc. Phys. Soc.* B, **63**, 756.
Mott, N. F., 1949, *Proc. Instn. Elect. Engrs.*, Part I, **96**, 253.

The Role of the Self Magnetic Field in High Current Gas Discharges

Since publication of the paper with title as given above (Thonemann and Cowhig 1951) the authors have found that Bennett (1934) has treated theoretically the case of magnetically self-focusing charge streams in a different manner and arrived at the same conclusions. Bennett's equation (11) is identical with equation (16) of the authors' paper except that T_2 has been neglected in comparison with T_1. The critical currents are in similar agreement. The authors regret that they had no knowledge of this important paper at an earlier date.

Clarendon Laboratory,
Oxford.
20th April 1951.

P. C. Thonemann.
W. T. Cowhig.

Bennett, W. H., 1934, *Phys. Rev.*, **45**, 890.
Thonemann, P. C., and Cowhig, W. T., 1951, *Proc. Phys. Soc.* B, **64**, 345.

Afterglows in Hydrogen Discharges

The persistence of luminosity in excited and ionized hydrogen, in the absence of a drift current, has been studied over a range of pressures by various authors. Thus, Rayleigh (1944) noted the effect in electrodeless low pressure discharges, using a special tube with a side arm in which, remote from the path of conduction, the persistence of the Balmer lines for some (10) microseconds was noted. Rayleigh attributed this afterglow to unexpectedly long half-lives for the excited states involved in the Balmer series. Experiments were independently made with pulsed discharges at 1 atmosphere pressure (Craggs and Meek 1945, 1946) and the possibility of two-body (radiative) electron–ion recombination being partly responsible for the afterglow was suggested. This work has been continued (Craggs and Hopwood 1947) since the above results were reported and further results are now available. Lee and Fowler (1951), who have recently extended Rayleigh's experiments, have suggested that a shock-wave mechanism may possibly be operative in producing the radiation, and state that no decision regarding the relevance of recombination processes could yet be made.

We have obtained direct evidence of recombination in pulsed discharges and their afterglows in hydrogen at 1 atmosphere where the electron concentration (10^{17} to 10^{18}/cm^3) will tend to be appreciably higher than in the work of Lee and Fowler (0·1 to 0·8 mm. Hg) so that recombination will become more probable. Our experiments have been made with photographic spectroscopy and with electron multiplier tubes (Meek and Craggs 1943, Craggs and Hopwood 1947). The latter are made with ultra-violet glass bulbs which are sensibly transparent to about 3000 A., and which are therefore suitable for studies of the Balmer series limit continuum, due to radiative recombination. This continuum has $\lambda = 3647$ A. as the long wavelength limit but the smearing of levels to the extent of about 0·3 ev. makes the effective limit at a longer wavelength.

Figure 1 (*a*) shows the current pulse (1200 amp. peak), Figures 1 (*b*) and (*c*) respectively show the temporal variations of the Balmer H_β and the continuous (λ=3500 A.) radiations, and it is clear from these records and their calibrations that the recombination radiation is appreciable both before and during the afterglow period. It is hoped that the data now obtained on the spectral variation of intensity in the continuum will enable electron temperatures, and possibly their temporal variations, to be determined using the theoretical

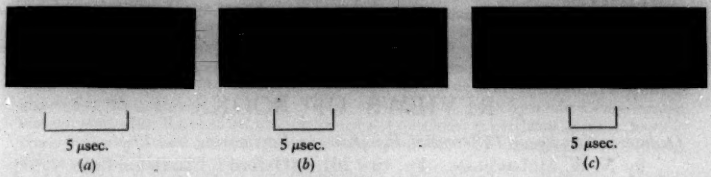

Figure 1.

treatment of hydrogen recombination spectra due to Cillié (1936) and others. These results will be published later in detail.

The Balmer series limit continuum has been previously observed with various discharges in hydrogen (Herzberg 1927, Chalonge and Ny Tsi Ze 1930) (no quantitative data were obtained, and no afterglow studies were made since temporal resolution was not used) and with hydrogen arcs at 1 atmosphere pressure (Edels and Craggs 1951). Further work is being carried on.

One of us (P.R.) is indebted to the Electrical Research Association for financial support and for permission to publish this note.

Department of Electrical Engineering,
The University of Liverpool.
16th May 1951.

P. Ravenhill.
J. D. Craggs.

Chalonge, D., and Ny Tsi Ze, 1930, *J. Phys. Radium*, **1**, 416.
Cillié, G. G., 1936, *Mon. Not. Roy. Astr. Soc.*, **96**, 771.
Craggs, J. D., and Hopwood, W., 1947, *Proc. Phys. Soc.*, **59**, 755, 771.
Craggs, J. D., and Meek, J. M., 1945, *Nature, Lond.*, **156**, 21; *Proc. Roy. Soc.* A, **186**, 241.
Edels, H., and Craggs, J. D., 1951, *Proc. Phys. Soc.* A, **64**, 562.
Herzberg, G., 1927, *Ann. Phys., Lpz*, **84**, 565.
Lee, R. J., and Fowler, R. G., 1951, *Phys. Rev.*, **81**, 457.
Meek, J. M., and Craggs, J. D., 1943, *Nature, Lond.*, **152**, 538.
Rayleigh, Lord, 1944, *Proc. Roy. Soc.* A, **183**, 26.

Solvent Effects in Dipole Moment Measurements

Since publication of the paper with title as given above (Ross and Sack 1950) the authors' attention has been drawn to the fact that the 'internal field functions' ξ used throughout the paper are identical with the 'demagnetizing factors of the general ellipsoid' evaluated by Osborn (1945) and Stoner (1945), in whose papers some tables of the functions are given.

University College, London W.C.1.
National Standards Laboratory, Sydney, N.S.W.
20th April 1951.

I. G. Ross.
R. A. Sack.

Osborn, J. A., 1945, *Phys. Rev.*, **67**, 351.
Ross, I. G., and Sack, R. A., 1950, *Proc. Phys. Soc.* B, **63**, 893.
Stoner, E. C., 1945, *Phil. Mag.* (7), **36**, 803.

Corrigenda

"Solvent Effects in Dipole Moment Measurements", by I. G. Ross and R. A. Sack. *Proc. Phys. Soc.* B, 1950, **63**, 893.

P. 899, equation (20). Numerator on right hand side *should read* $3\epsilon[1+(n^2-1)\xi]$.

P. 900, Table. ϵ for benzene should be 2·273. Values of S_{RS} *should be diminished* by from 0·004 to 0·006, except for acetone (S_{RS}=0·946, 0·919). Values of S_{II} are substantially correct.

REVIEWS OF BOOKS

Ordinary Non-linear Differential Equations in Engineering and Physical Sciences, by N. W. McLachlan. Pp. vii+201. (Oxford: Clarendon Press, 1950.) 21*s*.

Those branches of mathematical physics in which the physical systems under consideration are adequately described in terms of linear differential equations form the subject matter of classical expositions in which the general theory is systematically developed and used to solve problems which, besides being of interest in themselves, serve as illustrations of the theory. It is not to be expected that a work on non-linear differential equations should conform to this pattern. Indeed, the author states, in his preface to this book, that it is "... not an analytical treatise with technical applications". It is, rather, a book on how to get the answer: exactly in the simpler cases, by analytical approximation in others, and graphically or numerically where these methods prove unsuitable.

Ordinary non-linear differential equations only are discussed. After an introductory review of the subject, examples are given of non-linear equations which are solved exactly by simple transformation into equations which are either linear or of the separable variable type. An account of equations which are integrable in terms of elliptic integrals and functions contains instructive treatments of the simple pendulum, mass-spring systems and the elastica. There is extensive discussion, covering several chapters, of equations having periodic solutions, such as those occurring in the theory of thermionic valve circuits, and in the analysis of the behaviour of oscillatory mechanical devices. The methods used include the perturbation method of Poincaré, successive approximation and a method which involves determining the coefficients of a Fourier series. A chapter is devoted to the consideration of periodic solutions in which the amplitude and phase are slowly varying functions of time, and another to the fact that approximate solutions obtained on this basis satisfy linear differential equations. The theory and application of Mathieu functions are dealt with in another work by the author, but are briefly mentioned in this book as a basis for the discussion of non-linear equations with periodic coefficients. Graphical and numerical methods of solution are described in a final chapter. The two graphical constructions which are used (the isocline method and the Liénard method) involve the drawing of $y-v\,(=dy/dt)$ graphs which indicate periodic solutions by approaching closed curves. The book concludes with a useful and extensive list of references.

There are many mechanical, electrical and acoustical problems in which the non-linearity is the essential feature, and the engineering mathematician who encounters them in the course of his work will find this book of great interest. M. R. HOPKINS.

The Friction and Lubrication of Solids, by F. P. Bowden and D. Tabor. Pp. xii+337. 1st Edition. (Oxford: Clarendon Press, 1950.) 35*s*.

A new textbook of experimental physics or chemistry can generally be read with interest and profit because the author, having himself carried out the described experiments, knows what he is talking about. This is not always the case with new books devoted to more specialized subjects. Too often the writer's own experience of the field he has chosen to discuss

is restricted to some narrow section, and his book, filled out with an uncritical survey of the literature, both relevant and otherwise, affords dreary and unprofitable reading. In this respect the present monograph, which deals with the important, though much neglected, subject of friction and lubrication, is a notable exception. It does not attempt to cover every aspect of this broad field, but is confined mainly to an account and discussion of the outstanding work of the authors and their collaborators. The story therefore is developed and told with the verve of first-hand experience and makes fascinating reading, fresh and stimulating from beginning to end.

Man's first use of sliding mechanisms and friction-reducing agents dates back to antiquity. Since then there has accumulated a vast fund of empirical knowledge which has in the past served the engineer well enough. This success, added to the astonishingly complex nature of the sliding system, has done much to discourage, until comparatively recently, a scientific approach to the problems of sliding. The severe demands made by modern engineering, however, make clear the need for placing the subject on a more generalized scientific footing. This is the task which the authors have set themselves, and their monograph is a testimony of their success.

Taking Amonton's law as a starting point, the authors examine the physical and chemical processes which occur during sliding and relate these to the friction experienced. They then consider in detail the role of the lubricant, particularly under the boundary conditions so often encountered nowadays in engineering practice. The reader may differ with some of the conclusions and wish that some aspects had been examined in greater detail, but I have no doubt that a young and vigorous school which has contributed so much to the subject in so short a lifetime (barely fifteen years) is also aware of the gaps and will fill many of them in time for the next edition.

The volume is well produced and illumined with excellent and well-chosen illustrations. It should be in the library of every practical physicist and engineer. G. INGLE FINCH.

Theory of Flow and Fracture of Solids, Vol. I, by A. NADAI. Pp. xxii+572. (Engineering Societies' Monographs.) 2nd Edition. (New York: McGraw-Hill Book Co., 1950.) 85*s*.

Dr. Nadai is revising his earlier work on Plasticity (English publication, 1931) in two volumes, of which this is the first. It is not his purpose to make more than a passing reference to the interpretation of the mechanical properties of solids in terms of their atomic structure. On the other hand, he writes for those interested primarily in the results of the field theories and not in the problems of mathematical technique involved in their formulation and application. He is particularly concerned to bring out those features of deformation and fracture common to very different types of solids, and to compare their behaviour with that predicted for certain ideal solids obeying simple mechanical laws. A number of important applications, including those to the metallurgical processes of rolling, drawing and the forging of thin shells, and to geology, are reserved for his second volume. A wide range of subjects is however included. While much of the book deals with the behaviour of ductile metals, experiments on ceramics, paraffin-wax, plastics and minerals are reported; this broad sweep even encompasses the creep of candles and the slow bending of tombstones!

The book is divided into three parts. After some introductory remarks, the author deals with the structure of solids and its relation to deformation and fracture. Here, in the limited space available, some of the detailed description of pioneering work could be replaced with advantage by a more general account of recent developments, particularly in dislocation theory. After a chapter on the theory of the tensile test, the remaining six chapters of Part I deal with the analysis of stress and strain. Mohr's method of representation is used extensively and the notation is that recommended by the American Engineering Societies. Dr. Nadai is opposed to the use of a tensor notation in works of this kind, but he includes a final chapter on the analysis of stress and strain using dyadics. Part II is concerned with the yielding of solids. Theories of fracture and yielding are reviewed, and experimental tests under combined stresses, compression, bending, buckling and torsion are then reported. The author has here performed a valuable service in assembling some recent results. Many references are given, and a number of interesting photographs of flow figures and lines of

fracture are included. Part III is largely theoretical. The behaviour of ideal solids, including those simulating work hardening, is analysed and applications made to the deformation of cylinders, discs and rings under static and centrifugal stresses. Experimental methods, using sand-heaps and rubber membranes, for determining the plastic regions in torsion are described and comparison made with observed flow layers in twisted mild steel bars. In a final chapter on plane strain and plane stress a brief discussion of the partial differential equation for the stress function and of the determination of lines of slip is given.

Lengthy footnotes occur frequently throughout the book. This, combined with a style which is not always as clear as it might be, does not make it an easy book to read. A number of pictures of famous men of science enlivens the work. B. A. B.

Les théories de la turbulence, par L. AGOSTINI et J. BASS. Pp. 118. (Paris: Publications scientifiques et techniques du Ministère de l'Air, 1950.) 750 fr.

The theory of turbulence has made enough progress to warrant a review of the results acquired and the hypotheses on which they are based. This book, which is founded on lectures given by the authors at the Sorbonne in 1949, is doubly welcome for its summary of work on turbulence up to the recent past, and for its ordered logical account of the theory. Indeed, apart from the appendix, which gives curves, due to A. Favre, from wind-tunnel measurements, the work is entirely theoretical. The contents are as follows: I—Generalities on turbulence; Statistical methods; Applications of random functions, leading to the equations of hydrodynamics. II—Correlations and spectra functions; A discussion of the functions and their modification by special hypotheses such as incompressibility or isotropy. III—Dynamics of turbulence. This chapter is a mathematical study of the application of the Stokes–Navier equation, the derivation of the fundamental equation of turbulence and its transformation and solution under different hypotheses. IV—Theory of local isotropy and statistical equilibrium. This chapter is concerned with the work of Kolmogoroff and that of Weizsäcker and Heisenberg. V—Decay of turbulence behind a grid, an account of the work of Batchelor and Townsend. L. M. MILNE-THOMSON.

Lehrbuch der theoretischen Physik: I—Physik der Vorgänge, by W. WEIZEL. Pp. xiv+771. (Berlin: Springer-Verlag, 1949.) In paper, 53 DM.; in cloth, 56.90 DM.

The first volume of this textbook deals with phenomenological physics, i.e. essentially with classical physics. It does not contain, however, classical statistical mechanics, which is to be treated in the second volume. It is divided into six parts. The first section contains particle mechanics and mechanics of rigid bodies, leading up to a detailed treatment of Lagrangian and Hamiltonian theories. It concludes with the transition to wave mechanics following Schrödinger's original treatment. The next section deals with hydrodynamics and elasticity. It also contains a detailed treatment of the theory of vibrations and a chapter on capillarity in addition to the fundamental principles and simple applications. The chapter on electrodynamics is subdivided in the usual way into static, stationary, quasi-stationary etc. fields. The Maxwell equations are introduced at a fairly early stage. Optics, in addition to a fair treatment of questions of interference and diffraction, contains crystal optics at an advanced level. This is followed by a short chapter on relativity, and the book is concluded with a chapter on thermodynamics.

The book has a high standard. The presentation is clear and thorough and it follows nearly always the conventional methods of treatment. The chapter on thermodynamics should in my opinion be much longer. It also would be profitable to have a greater number of examples illustrating how to apply general principles to the solution of particular problems. The book should be very useful to the advanced student. H. F.

CONTENTS FOR SECTION A

PAGE

Dr. B. Bleaney, Dr. D. J. E. Ingram and Mr. H. E. D. Scovil. Paramagnetic Resonance in Vanadous Ammonium Sulphate 601

Dr. J. M. Cowley, Dr. A. L. G. Rees and Mr. J. A. Spink. Secondary Elastic Scattering in Electron Diffraction 609

Dr. R. Huby and Mr. H. C. Newns. Nuclear Excitation by Electric Interaction with Charged Particles 619

Dr. L. M. Yang. Nuclear Shell Structure and Nuclear Density 632

Mr. D. J. Littler. A Method of Calibrating Neutron Sources Absolutely . . 638

Dr. L. Pincherle. Energy Levels of F-Centres 648

Letters to the Editor :

Prof. J. Rayski. On the Reciprocal Field Theory 657

Mr. Vachaspati. Some Remarks on the Use of β-Formalism of the Meson Field for Nuclear Interactions 659

Mr. A. V. Crewe. The Multiple Scattering of μ-Mesons 660

Mr. E. G. Michaelis and Dr. E. P. George. Measurements of the Star-Producing Radiation with a Scintillation Counter 662

Dr. L. Pincherle. Change of Activation Energy with Impurity Concentration in Semiconductors 663

Mr. R. Cade. On Mechanical Action in Dielectrics 665

Dr. G. Stephenson. Calculation of the Oscillator Strength for the $^2\Pi - ^2\Delta$ Transition in the CH Molecule 666

Dr. J. Hatton, Dr. B. V. Rollin and Mr. E. F. W. Seymour. Superconductivity of Lead Sulphide 667

Dr. R. H. Dalitz. On an Alternative Decay Process for the Neutral π-Meson 667

Reviews of Books 669

Contents for Section B 679

Abstracts for Section B 679

ABSTRACTS FOR SECTION A

Paramagnetic Resonance in Vanadous Ammonium Sulphate, by B. Bleaney, D. J. E. Ingram and H. E. D. Scovil.

ABSTRACT. In the solid state the orbital momentum of the divalent vanadium ion $3d^3$ is quenched by the cubic crystalline field, leaving a spin quadruplet as the ground state. Paramagnetic resonance measurements show that in $V(NH_4)_2(SO_4)_2.6H_2O$ this is split into two doublets with a separation of $0{\cdot}36\ cm^{-1}$ by a component of the crystalline field with rhombic symmetry. An extensive and isotropic hyperfine structure is observed, from which the value of 7/2 for the nuclear spin of ^{51}V is confirmed. The contribution from the observed splittings to the tail of the magnetic specific heat curve is evaluated.

Secondary Elastic Scattering in Electron Diffraction, by J. M. COWLEY, A. L. G. REES and J. A. SPINK.

ABSTRACT. Electron diffraction patterns from films of long-chain paraffins show the effects of secondary elastic scattering of electrons in the form of extra spots, groups of spots, arcs of circles, diffuse bands with sharp edges, and forbidden reflections in single-crystal patterns. Examples of such effects are given and analysed to demonstrate their origin in the successive diffraction of electrons from two different single-crystal regions. It is pointed out that many effects recorded in the literature on electron diffraction may be explained in the same way. The modification of the intensities in single-crystal patterns and the appearance of forbidden reflections are treated quantitatively on the basis of secondary diffraction by parallel but non-coherent regions of crystal. Expressions are derived whereby observed intensities may be corrected for secondary scattering when once the scattering efficiency of the crystal has been deduced from the observed intensities of forbidden reflections. The importance of such corrections for purposes of structure analysis is demonstrated in the comparison of two Fourier projections made from a cross-grating pattern of dicetyl ($C_{32}H_{66}$), one using observed intensities and the other using corrected intensities. Both show clearly the general arrangement of the molecules, but that based on corrected intensities contains much less spurious detail than the other, and gives greater accuracy and a much clearer indication of the positions of the hydrogen atoms.

Nuclear Excitation by Electric Interaction with Charged Particles, by R. HUBY and H. C. NEWNS.

ABSTRACT. Inelastic scattering of charged particles can take place through the electrostatic interaction between the particles and the nucleus. Expressions for the total cross section of the process have been derived using several methods and are found to be in close agreement. The angular distributions are less reliable. Questions of more practical interest are discussed and conditions given for the best observation of the effect. The total cross sections are not negligible and certain experimental results can be explained. Inelastic nuclear scattering has been extensively used hitherto to obtain the positions of nuclear energy levels. It is suggested that more information about nuclear states might be provided by experiments exploiting the electrostatic interaction.

Nuclear Shell Structure and Nuclear Density, by L. M. YANG.

ABSTRACT. Correlations between the nuclear shell structure and the density distribution are analysed on the assumption that the former is associated with the successive appearance of particles of higher angular momentum. General requirements for the possible form of the nuclear density distribution are derived. It is shown that a reasonable density distribution conforming with the above requirements and other known facts reproduces unmistakably the ' magic numbers '.

A Method of Calibrating Neutron Sources Absolutely, by D. J. LITTLER.

ABSTRACT. A method has been developed for calibrating neutron sources absolutely, using the Graphite Low Energy Experimental Pile. The method used is to convert the measurement of the number of neutrons emitted by a source to a determination of the absolute beta activity of an irradiated sodium or phosphorus sample.

One source calibrated by this method, which contained 1,290 mg. of radium in the form of sulphate, mixed with 12 gm. of beryllium, was found to have a neutron strength of $9{\cdot}3\times10^6$ n/second ($\pm 4\frac{1}{2}\%$).

Energy Levels of F-Centres, by L. PINCHERLE.

ABSTRACT. The energy levels of F- and F′-centres are calculated on a very simple model. The ground state of F-centres is found to be determined mainly by the radius of the hole that represents the missing ion in Jost's model, and to vary only slightly with the dielectric constant.

In thallium and silver halides the long-wave photoconductivity is probably due to F-centres. In PbS the energy levels of F- and F′-centres are much too deep to be responsible for photoconductivity. D-centres consisting of a pair of adjacent missing ions are also investigated : they may act as shallow traps, thereby reducing electron mobilities.